

Satbayev University

UDC: 66:622.276.34(043)

Manuscript copyright

NURBATYR MUKHAMETGAZY

**"Synthesis and characterization of acrylamide-based polyampholytes
for EOR, drilling of wells and tracer applications"**

Specialty - 6D073900 Petrochemistry

A thesis submitted for the scientific degree of
Doctor of Philosophy (Ph.D.)

Scientific supervisors:

Dr. Chem. Sci., Professor,
Kudaibergenov S.E.
Institute of Polymer Materials
and Technology

PhD, Iskander Gussenov.
Satbayev University

Professor, Heikki Tenhu
University of Helsinki, Finland

The Republic of Kazakhstan
Almaty, 2024

CONTENT

NORMATIVE REFERENCES		5
LIST OF ABBREVIATIONS		6
INTRODUCTION		7
CHAPTER 1. LITERATURE REVIEW		14
1.1	Chemical flooding for enhanced oil recovery (EOR)	14
1.2	Polymer flooding technology	18
1.3	Types of EOR polymers	22
1.3.1	Partially hydrolyzed polyacrylamide (HPAM)	22
1.3.2	Polyampholytes	23
1.3.2.1	Annealed polyampholytes	28
1.3.2.2	Quenched and/or zwitterionic polyampholytes	29
1.4	Application of polyampholytes in oil industry	31
1.4.1	Acrylamides based polyampholytes for EOR	33
1.4.2	Polyampholytes as rheology enhancer and fluid loss control agents for salt tolerant water-based drilling fluids (WBDFs)	35
1.4.3	Application of polymers as tracer agents for monitoring of oil reservoirs	37
CHAPTER 2. EXPERIMENTAL PART		39
2.1	Materials	39
2.1.1	Chemicals	39
2.1.2	Sand pack models and core samples	40
2.1.3	Brine	41
2.1.4	Crude oil	41
2.1.5	Bentonite clay	42
2.2	Research methods	42
2.2.1	FTIR spectroscopy	42
2.2.2	¹ H and ¹³ C-NMR spectroscopy	43
2.2.3	UV-Vis and fluorescence spectroscopy	43
2.2.4	Dynamic light scattering (DLS) and zeta-potential measurements	43
2.2.5	Gel-permeable chromatography (GPC)	43
2.2.6	Differential scanning calorimetry (DSC) and thermogravimetric analysis (TGA)	43
2.2.7	Scanning electron microscopy (SEM) and transmission electron microscopy (TEM)	44
2.2.8	Chemical analysis	44
2.2.9	Elemental analysis	44
2.2.10	Rheological study	44

2.2.11	Permeability and porosity measurements of sand pack and core samples	45
2.2.12	Core/sand pack flooding experiments	45
2.2.13	Preparation of bentonite/water and bentonite/polymer dispersion	46
2.2.14	Fluid loss tests	47
2.2.15	Permeability of filter cake and SEM analysis	47
CHAPTER 3. RESULTS AND DISCUSSION		48
3.1	Synthesis of acrylamide-based ternary polyampholytes (AAm-co-AMPS-co-APTAC) derived from acrylamide (AAm), 2-acrylamido-2-methyl propane sulfonic acid sodium salt (AMPS) and 3-acrylamidopropyl trimethylammonium chloride (APTAC)	48
3.1.1	Synthesis and characterization of AAm-co-AMPS-co-APTAC (80:10:10 mol. %)	49
3.1.2	Determination of molecular weights of the AAm-co-AMPS-co-APTAC (80:10:10 mol. %)	52
3.1.3	TGA and DTA analysis of AAm-co-AMPS-co-APTAC (80:10:10 mol. %)	53
3.1.4	DLS measurement of AAm-co-AMPS-co-APTAC (80:10:10 mol. %) in pure water and brine solution	54
3.1.5	SEM and TEM results of AAm-co-AMPS-co-APTAC (80:10:10 mol. %)	55
3.1.6	Zeta potential measurements of AAm-co-AMPS-co-APTAC (80:10:10 mol. %) and bentonite clay	55
3.2	Rheological study	56
3.2.1	Viscosity of ternary polyampholyte in aqueous solution	56
3.2.2	Salt- and temperature-dependent viscosity of AAm-co-AMPS-co-APTAC	57
3.2.3	Salt- and concentration dependent dynamic viscosities of ATP and HPAM in synthetic brine	58
3.2.4	Comparative viscosity measurements of TPA and HPAM in high salinity brine	59
CHAPTER 4. Results of core/sand pack flooding experiments		62
4.1	Oil displacement ability of amphoteric terpolymers in reservoir water	62
4.2	Core flooding experiment using TPA	63
4.3	Sand pack flooding experiments using TPA	65
4.3.1	Oil saturation	65
4.3.2	Water and polymer flooding	66
4.3.3	Oil recovery factor	67
4.4	Comparison of oil recovery efficiency with TPA and HPAM	67
4.4.1	Sand pack flooding tests with TPA and HPAM	67

4.4.2	Core flooding tests with TPA and HPAM	68
4.4.3	Comparative oil displacement experiments of TPA and HPAM	71
4.4.4	Issuing recommendations for the use of heat- and salt-resistant amphoteric terpolymers as reagents to enhance the thickening and leveling of injectivity profiles	72
CHAPTER 5. Development of water-based drilling fluids based on the ternary polyampholyte AAm-co-AMPS-co-APTAC (80:10:10 mol.%) and bentonite clay		75
5.1	Rheological properties of TPA and PAC-LV solutions without bentonite	75
5.1.1	The intrinsic viscosities $[\eta]$ of polymer solutions	75
5.1.2	The apparent viscosities of polymer solutions	75
5.2	Rheological properties of bentonite/polyampholyte dispersions	78
5.3	Comparative rheological behavior of different drilling fluids at a high salinity (35 wt. %) of brine	81
5.4	Fluid loss tests	82
5.4.1	Permeability of filter cake and SEM analysis	83
5.5	On the mechanism of stabilization drilling fluids by ternary polyampholyte	85
CHAPTER 6. Application of AMPS-co-APTAC-co-ANB (50:49:1 mol.%) terpolymer as tracer agent		87
6.1	Synthesis and identification of AMPS-co-APTAC-co-ANB terpolymer	87
6.2	Identification of AMPS-co-APTAC-co-ANB terpolymer from FTIR spectrum	87
6.3	The average hydrodynamic size and zeta potential of AMPS-co-APTAC-co-ANB terpolymer	88
6.4	UV-Vis spectra of AMPS-co-APTAC-co-ANB in aqueous solution	88
6.5	Core flooding experiment with AMPS-co-APTAC-co-ANB solution	89
6.6	The absorption tests of amphoteric terpolymer AMPS-co-APTAC-co-ANB aqueous solution on the rock	91
CONCLUSIONS		92
ACKNOWLEDGEMENTS		93
REFERENCES		94

NORMATIVE REFERENCES

In this dissertation, references are made to the following standards:

GOST 7.32-2001. Report on research work. Structure and design rules.

GOST 7.1-2003. Bibliographic record. Bibliographic description. General requirements and compilation rules.

GOST 4517-87 Reagents. Methods for the preparation of auxiliary reagents and solutions used in the analysis.

GOST 23932-90 E. laboratory glassware and equipment.

GOST 25336-82. Laboratory glassware and equipment. Types, basic parameters, and sizes.

GOST 29252-91. Laboratory glassware. Burettes. Part 1. General requirements.

GOST 1770-74. Measuring laboratory glassware. Cylinders, beakers, flasks, test tubes.

General specifications.

GOST 2922-91. Laboratory glassware. Graduated pipettes.

GOST 9147-80. Porcelain laboratory glassware and equipment. Technical conditions

GOST 20292-74. Volumetric flasks with a capacity of 100, 200, 500, 1000 ml. Technical conditions

GOST 12.1.008-76. Occupational safety standards system. Biosafety. General requirements.

LIST OF ABBREVIATIONS

The following designations and abbreviations were used in the given dissertation:

AAm –	Acrylamide
AMPS –	2-Acrylamido-2-methyl propane sulfonic acid sodium salt
ANB –	Acrylamide Nile Blue
APS –	Ammonium persulfate
APTAC –	3-acrylamidopropyl trimethylammonium chloride
API –	American Petroleum Institute
BT–	Bontonite
CMC–	Carboxymethyl cellulose
DLS –	Dynamic light scattering device
EOR–	Enhanced oil recovery
FTIR-spectroscopy –	Fourier Transform Infrared spectroscopy
GPC –	Gel permeation chromatography
HPAM –	Hydrolyzed polyacrylamide
IEP –	Isoelectric point
IAPV–	Inaccessible pore volume
IOR –	Improved oil recovery
M –	Mobility ratio
M_n –	The average-number molecular weight
M_w –	The weight-average molecular weight
NMR-spectroscopy –	Nuclear magnetic resonance spectroscopy
ORF –	Oil recovery factor
PVs –	Pore volumes
PAC–	Polyanionic cellulose
QPA –	Quenched polyampholytes
SEM	Scanning electron microscopy
TPA –	Ternary polyampholytes
TEM	Transmission electron microscopy
TGA –	Thermogravimetric analysis
TMEDA –	N, N, N', N'-Tetramethylethylenediamine
UV-Vis-spectroscopy–	Ultra violet and visible spectroscopy
UIC-C(2) –	Special core flooding setup
WBDFs –	Water based drilling fluids
λ –	Wavelength
ϕ –	Porosity
ξ –	Zeta potential
η_{app} –	Apparent viscosity

INTRODUCTION

Assessment of the current state of the scientific or technological problems to be solved. According to a survey of the applicable literature, strongly charged, or so-called 'quenched' polyampholytes, are a less studied subject in comparison with annealed polyampholytes [1, 3]. The present study focuses on a series of amphoteric ternary polyampholytes with different molar ratios of linear acrylamide-based polyampholytes, consisting of a nonionic monomer – acrylamide (AAM), an anionic monomer – 2-acrylamido-2-methyl-1-propanesulfonic acid (AMPS), and a cationic monomer – (3-acrylamidopropyl) trimethylammonium chloride (APTAC), which were synthesized and characterized.

The obtained results are promising for the development of novel salt- and temperature-tolerant amphoteric terpolymers for EOR, well drilling, and tracer applications. Further study was conducted on the structure, morphology, physicochemical, and rheological properties of the amphoteric polyampholytes. The sweep efficiency of strongly charged ternary polyampholytes concerning EOR, wells drilling and tracer applications. The key studies were conducted to evaluate the structure, morphology, physico-chemical, and rheological properties of the ternary polyampholytes AAm-co-AMPS-co-APTAC. The sweep efficiency of strongly charged polyampholytes with respect to enhanced oil recovery and their role as tracer agents is demonstrated.

The rheological and self-thickening ability of polyampholyte terpolymers in elevated high salinity of brine using a sand pack model and artificial high-porous core samples were improved by increasing the molecular weight through altered polymerization conditions.

Basis and initial data. Newly synthesized polyampholytes with a linear structure, based on anionic and cationic monomers, undergo conformational and volume-phase transitions. They exhibit stimuli-responsive behavior with respect to temperature, ionic strength, and the thermodynamic quality of the solvent. The isoelectric effect of salt-tolerant TPA has been proposed for application in oil recovery (EOR), well drilling, and as tracer agents in the oil industry.

The general methodology for conducting research included synthetic and physico-chemical components. The methods utilized include free radical polymerization, visible and infrared spectroscopy, scanning and transmission electron microscopy, differential scanning calorimetry and thermogravimetry, viscometric method, gel-permeable chromatography, and dynamic laser light scattering, as well as viscosity-rheological measurements, filtration experiments, adsorption and API fluid loss tests .

The relevance of the work. Water is usually used to displace oil from matrix rocks. However, because of the unstable displacement front due to the differences in oil and water viscosities and heterogeneous nature of matrix rocks the oil production rates are often decline accompanied by the increase of water production.

Injection of polymer solutions into wells is one of the most efficient processes in oil production. In world practice the HPAM found the widest application due to its low cost and commercial availability. However, the main disadvantage of HPAM is

its intolerance with respect to high salinity of oil reservoir. With an increase in salinity, the HPAM chains tend to coil, because the electrostatic repulsion between negatively charged carboxylic groups is screened by the added salts. Moreover, the bivalent cations (Ca^{2+} and Mg^{2+}) present in saline water can bridge the carboxylic ions in the HPAM, effectively shrinking the macromolecules leading sometimes to precipitation. In fact, relatively high oil viscosity and brine salinity are common phenomena for Kazakhstani oil reservoirs. For example, the viscosity of Karazhanbas field oil may be higher than 350 cp, while brine salinity of Zhetibay and Moldabek fields may exceed 150 g/L. In this connection, the oil industry of Kazakhstan needs the salt tolerant polymers that are able to viscosify the brine solution.

The ability of amphoteric polyelectrolytes to swell and be effective viscosity enhancers in high salinity and high-temperature reservoirs plays a crucial role in enhanced oil recovery (EOR) processes. Strongly charged (or quenched) polyampholytes due to salt- and temperature resistance can serve as viscosifying agents in EOR where thickeners are required in brine solution. In this regard, amphoteric polyelectrolytes – polymers that have both positively and negatively charged monomers, are promising, because in high saline water the anions and cations of salts screen the electrostatic attraction between positively and negatively charged groups of the polymer chain and increases the viscosity of the brine solution. The present thesis is devoted to synthesis and characterization of specially designed polyampholyte terpolymers possessing antipolyelectrolyte effect that can increase the viscosity of reservoir brine water.

Water-based drilling fluids (WBDF) play an important role in oil well drilling operations, including cleaning of the wellbore, carrying and suspending cuttings, cooling and lubricating drilling tools, and maintaining stability of the wellbore and formation. Conventional polymer additives, such as HPAM, polyanionic cellulose and carboxymethyl (or ethyl) cellulose work badly in saline environment due to the polyelectrolyte effect. Expanded (or swollen) in pure water polyelectrolyte chains shrink in salt solution due to the screened electrostatic repulsion between uniformly charged macroions (polyelectrolyte effect) and adopt coil conformation. In its turn this leads to worse keeping the hydration dispersion becoming poorer in performance and even to insolubility. To overcome this problem WBDFs containing salt-tolerant polyampholyte, bentonite and inorganic salt was developed for wells with high salinity.

Many inter-well tracers have been widely used to obtain information on the interaction between producer and injector, evaluation of interwell and interlayer connections, as well as heterogeneities of oil reservoirs. The fluorescence-detection technology attracts considerable interest in oilfield operations due to many advantages over radioactive isotopes, ionic and organic tracers. For evaluation of interwell permeability and porosity the fluorescent polyacrylamide microspheres, which fluoresce under ultraviolet irradiation, were applied. However, some parts of polymer-based fluorescent tracers, including microspheres, are absorbed onto the surface of rocks in the stratum, and it is difficult to detect them precisely. In the frame of this Thesis the trace amount of fluorescent monomer – ANB (1 mol.%) was introduced into the composition of previously developed quenched polyampholyte to

prepare globular and fully electroneutral macromolecular chains to minimize or exclude its adsorption to the rock. The advantage of proposed approach is that the quenched polyampholyte of equimolar composition containing fluorescent dye – Nile Blue is insoluble in oil, but water-soluble, salt tolerant, detectable in very low concentrations, and does not adsorb on the rock or clay minerals. In the present Thesis, the passing of fluorescently labeled ternary polyampholyte based on acrylamide derivatives through the core sample was showed for monitoring of well-to-well connections.

The aim of the study: The research work aims to improve the synthesis and characterization of acrylamide-based ternary polyampholytes and determine their potential applications in the oil industry, such as enhanced oil recovery, drilling fluids, and the development of as tracer agents. To achieve this goal, we have outlined the following main tasks:

1. Synthesize, characterize and optimize the composition of high molecular weight water-soluble ternary polyampholytes that can achieve high viscosity in high salinity brine (200-300 g.L⁻¹).

2. Investigate the rheological characteristics of the selected polyampholyte in high salinity brine at 25°C and 60°C.

3. Conduct laboratory oil displacement experiments using TPA aqueous solutions through the sand pack model and core samples, with the goal of evaluating the potential application of polymer flooding technology in EOR.

4. Compare the enhanced oil recovery efficiency of the high molecular weight TPA with HPAM, a commonly used polymer-flooding agent in Kazakhstan.

5. Study the use of TPA as a rheology enhancer and fluid-loss additive for the preparation of salt-tolerant WBDFs.

6. Synthesize and characterize fluorescently labeled novel ternary polyampholyte (AMPS-*co*-APTAC-*co*-ANB=50:49:1 mol%) containing a fluorescent dye ANB and test it as a tracer agent in core flooding experiments.

Objects of the study: improvement of synthesis and characterization of acrylamide-based polyampholytes for EOR, well drilling and tracer applications.

The subjects of the research: selection of optimal molar composition of acrylamide-based polyampholytes with the highest viscosity value in a wide range of salt water and temperature for use in oil recovery and drilling fluids

The methods of the research

The research presented in this dissertation employed a multi-faceted approach to synthesize and characterize novel high molecular weight TPA intended for application in the oil industry. The following subsections outline the various methods and techniques utilized in this study:

The novel TPA was characterized using various techniques, including Fourier transform infrared (FTIR) spectroscopy, nuclear magnetic resonance spectroscopy (¹H and ¹³C-NMR), Fluorescence spectroscopy and elemental analysis (C, H, N, S) were used for identification of functional groups and confirmation of copolymer structure, and thermogravimetric analysis (TGA), dynamic light scattering (DLS), gel permeation chromatography (GPC), zeta-potential measurements, scanning and

transmission electron microscopy (SEM and TEM), rheology measurements including the apparent viscosity, yield stress and gel strength, sand pack and core flooding experiments by UIC-C2, aging time, and UV-Vis spectrometric adsorption, and fluid-loss tests.

The main research results

1. The dynamic viscosity of ternary polyampholytes (AAm-*co*-AMPS-*co*-APTAC) in water depends on the composition of the terpolymers and increases in the following series: 80:10:10 > 60:20:20 > 70:15:15 > 50:25:25 > 90:5:5 mol%. In this regard, for the comprehensive study of the behavior of TPA in saline solutions, the optimal composition [AAm]:[AMPS]:[APTACH] = 80:10:10 mol% was chosen. Initially, injecting the low-molecular weight TPA solution during the core flooding tests resulted in a 4.8-5% increase in the oil recovery factor (ORF).

2. Rheological studies of high-molecular-weight TPA (AAm-*co*-AMPS-*co*-APTAC in an 80:10:10 ratio) solutions showed improved viscosifying behavior in high-salinity brine (200-300 g·L⁻¹) at both 24 and 60 °C.

3. Injection of 0.25-0.5 wt.% of amphoteric terpolymer dissolved in 200-300 g·L⁻¹ synthetic brine into high permeable sand pack model exhibited that the oil recovery factor (ORF) increases up to 23-28% in comparison with water flooding. The TPA allowed the production of 2 times more oil at its maximum than did HPAM.

4. The addition of TPA not only improved rheological properties and reduced fluid loss of WBDFs but also increased salt resistance of the drilling fluids and gel strength, providing excellent performance in a wide range of high salinity brine and shear rate under room temperature geothermal conditions.

5. A novel ternary polyampholyte (AMPS-*co*-APTAC-*co*-ANB=50:49:1) in both water and saline solutions effectively reduces rock adsorption, resulting in a 90% recovery factor when injecting a 0.1 wt.% solution into the core. This suggests potential use as a polymer tracer for monitoring oil wells.

The novelty of the Thesis.

The novelty of the PhD Thesis is that the high molecular weight ternary polyampholytes (TPA) based on AAm-*co*-AMPS-*co*-APTAC were synthesized for the first time and they have a superior oil displacement capability in high-saline reservoirs compared to hydrolyzed polyacrylamide (HPAM) traditionally used in EOR. The injection of 0.25% amphoteric terpolymer and HPAM solutions prepared in 200 g/L brine into the 0.62 and 1.77 Darcy sand packs resulted in the increase of the oil recovery factor by 28 and 18%, respectively. Incremental 10% oil recovery by AAm-*co*-AMPS-*co*-APTAC confirms that the amphoteric terpolymer has a higher oil displacement capacity than HPAM.

Moreover, the salt-tolerant ternary polyampholyte AAm-*co*-AMPS-*co*-APTAC was applied for preparation of water-based drilling fluid. The novel amphoteric terpolymer possessed not only to boost its salt tolerance but also to enhance drilling mud performance (viscosity and filtration properties) under lower temperature geothermal conditions.

For the first time the trace amount of fluorescent monomer – acrylamide Nile Blue (ANB) was introduced into the composition of AMPS-*co*-APTAC copolymer.

As a result, the novel ternary polyampholyte [AMPS]:[APTAC]:[ANB] = 50:49:1 mol.% with globular structure and fully electroneutral macromolecular chains to minimize or exclude its adsorption to the rock was obtained. The ternary polyampholyte containing the fluorescent marker was characterized by physico-chemical methods and core flooding tests as tracer agent for fluorescence-detection technology in oil industry for monitoring of well-to-well connections, (or interwell tracer test)..

The practical significance of the thesis

TPA emerges as a novel alternative to HPAM for application in enhanced oil recovery under high salinity conditions. It also serves as a crucial polymeric additive, enhancing the rheological properties of salt-tolerant WBDF while minimizing fluid loss. Additionally, its application extends to interwell connections via core analysis, leveraging fluorescence detection technology within oil well monitoring. Its important role as a tracer agent in polymer flooding tests further underscores the significance and practical relevance of this study.

The validity and reliability of the results the obtained data were confirmed using selective, accurate, and modern analysis methods, as well as the scientific methods. To ensure reliability and reproducibility, all experiments were conducted in several parallels.

Relation of the thesis with research and government programs

The work was carried out as part of projects funded by the Ministry of Education and Science of the Republic of Kazakhstan. The first project, titled "Synthesis and Study of Thermo- and Salt-Sensitive Polyampholyte Nano- and Microgels" for the period 2020-2022 (AP08855552), aimed to develop new materials. The second project, ongoing from 2021 to 2023 (AP09260574), focused on the "Development of New Thermal and Salt-Resistant Amphoteric Terpolymers for Enhanced Oil Recovery." Moreover, the Science Committee of the Ministry of Science and Higher Education of the Republic of Kazakhstan provided funding to support the research under the project "Zhas Galym" for the period 2022-2024 (AP14972771), focusing on the "Synthesis and Study of New Modified Complexes Based on Synthetic and Natural Polyampholytes for Water-Based Drilling Fluids." Therefore, the author of the dissertation deserves the degree of Doctor of Philosophy (Ph.D.) in the specialty 6D073900 Petrochemistry.

Main provisions to be defended:

1. Novel high molecular weight TPA were successfully synthesized and characterized, comprising 50-90 mol.% acrylamide (AAm) as a nonionic monomer, 5-25 mol. % 2-acrylamido-2-methyl-1-propanesulfonic acid sodium salt (AMPS) as an anionic monomer, and 5-25 mol. % (3-acrylamidopropyl) trimethylammonium chloride (APTAC) as a cationic monomer. The sample AAm-co-AMPS-co-APTAC=80:10:10 mol. % was chosen for the further sand pack and core flooding tests due to its highest viscosifying ability in high salinity (200-300 g.L⁻¹) brine.

2. The injection of 0.25 % TPA and HPAM solutions, prepared in 200 g.L⁻¹ brine, into the 0.62 and 1.77 Darcy sand pack models saturated with viscous Karazhanbas oil (420 cp) at 30 , resulted in an increase of the IOR by 28 % and 18 %,

respectively. These results show that the TPA has a higher oil displacement capacity than HPAM in high salinity conditions.

3. Adding 2 wt.% of a novel ternary polyampholyte (AAm-co-AMPS-co-APTAC=80:10:10 mol. %) to a high salinity (35 wt.%) NaCl brine with bentonite (4 wt.%) drilling fluid formulation significantly reduced the filter cake thickness to 0.09 cm. This reduction in filter cake thickness surpassed the thickness achieved with BT/PAC-LV (0.18 cm) and bentonite alone (0.41 cm). Additionally, the BT/TPA drilling fluid showed the lowest permeability/thickness ratio at 13 mD/cm, indicating its potential as a rheology enhancer and fluid loss additive for salt-resistant WBDF. Furthermore, the BT/TPA drilling fluid exhibited remarkably low fluid loss, measuring only 3.5 ml, well below the API standard limit of 12 ml.

4. A novel ternary polyampholyte composition (AMPS-co-APTAC-co-ANB = 50:49:1 mol. %) was synthesized and found to be efficient at minimizing adsorption on rock surfaces. When injected a 0.1 wt.% (or $1.3 \times 10^{-3} \text{ mol} \cdot \text{L}^{-1}$) aqueous solution into a core, it achieved a 90% recovery factor, making it a promising polymer tracer for monitoring oil wells in oil industry.

Approval of practical results of the work. The main results of the work were presented at the following international conferences and symposia: 8th International Symposium on Specialty Polymers (Karaganda, Kazakhstan, August 23-25, 2019); AIP Conference Proceedings, (Conference paper, Scopus/WoS CiteScore 0.7 Percentile 17%, Q4, Volume 2167, Page 020236-Pages 1-3, Nov 19, 2019); 8th All-Russian Conference "Recovery, Preparation, and Transportation of Oil and Gas" (Tomsk, Russia, October 1-3, 2019); VIII All-Russian Kargin Conference "Polymers in the Strategy of Scientific and Technological Development in the Russian Federation, Polymers-2020" (Tver, Russia, September 20-24, 2020); Uzbek-Kazakh Symposium "Modern Problems of Polymer Science" (Tashkent, Uzbekistan, November 24, 2020); and 13th International Symposium on Polyelectrolytes (Shanghai, China, June 21-25, 2021);

Publications

The results of the work are reflected in 12 publications: 1 article – in the Scientific Journal cited in the Scopus data base (Q1, 77 percentile), 1 article in AIP Conference Proceedings (Q4, 17 percentile), 4 articles – in the Scientific Journals listed in the recommended by the Committee for Quality Assurance in the Sphere of Education and Science of the Ministry of Science, and 1 publication in other (Kazakhstan Journal for the Oil & Gas Industry) scientific journals and publications. Scientific results were also reported at 5 International Conferences and Symposiums.

The personal contribution of the Ph.D. candidate to the preparation of each article was as follows:

In the article "Comparative Study of Oil Recovery Using Amphoteric Terpolymer and Hydrolyzed Polyacrylamide" (Polymers 2022, 14(15), 3095; ISSN: 2073-4360. Q1 Scopus/WoS CiteScore 5.7 Percentile 77%), Nurbatyr M. is the corresponding author. The Ph.D candidate participated in conducting all experiments, interpreting the results, and preparing the initial drafts of the article, including descriptions of the introduction, methodology, results, conclusion, and graphics.

Additionally, he was involved in formatting the article according to the journal's requirements and improving it after each stage of peer review.

In the article "Salt-Tolerant Acrylamide-Based Quenched Polyampholytes for Polymer Flooding" (Bulletin of Karaganda University, Chemistry Series, №4 (100)/2020, pages 119-127), and "Oil Recovery at High Brine Salinity Conditions Using Amphoteric Terpolymer" (Bulletin of the University of Karaganda – Chemistry Series. No. 3(107)/2022, pages 141-149), Nurbatyr .M is the first author. In "Synthesis and Characterization of a Novel Acrylamide-Based Ternary Polyampholyte as a Tracer Agent" (Chemical Bulletin of Kazakh National University, 100(1): 22-29, 2021), "Synthesis and Characterization of High Molecular Weight Amphoteric Terpolymer Based on Acrylamide, 2-Acrylamido-2-Methyl-1-Propanesulfonic Acid Sodium Salt, and (3-Acrylamidopropyl) Trimethylammonium Chloride for Oil Recovery" (Chem. Bull. Kazakh Natl. Univ. 2021, 103, 12-20), and "Synthetic Polyampholytes Based on Acrylamide Derivatives – A New Polymer for Enhanced Oil Recovery" (Kazakhstan Journal for Oil & Gas Industry, 4(4), 104-116), Nurbatyr M. is the corresponding author. Additionally, Nurbatyr M. participated in formatting the articles according to the journal's requirements, submitting the articles to the journals, and improving the articles after each stage of peer review.

Dissertation structure. The dissertation includes a review of applicable literature, an explanation of methodology, and a discussion of the results, a conclusion, and a list of available sources. The total volume is 109 pages, including 67 figures, 14 tables, and a bibliography of 206 titles.

CHAPTER 1. LITERATURE REVIEW

1.1 Chemical flooding for enhanced oil recovery (EOR)

Although polyampholytes have not been extensively used in commercial applications, their unusual solution properties present unique opportunities for formulation in the presence of electrolytes [4]. These include areas such as personal care, enhanced oil recovery, and flocculation. Water soluble and water-swelling polyampholytes could be used in desalination of water, sewage treatment, flocculation, and coagulation, drilling fluids and enhanced oil recovery [5].

The ability of polyampholytes to swell and be effective viscosity enhancers in high salinity media plays a crucial role in enhanced oil recovery (EOR) processes. In the recovery of oil from oil-bearing reservoirs, an important component is the formulation of drilling muds. A conventional water-based drilling mud formulation includes water, clay such as bentonite, lignosulfonate, a weighting agent such as BaSO_4 and a caustic material such as sodium hydroxide to adjust the pH between 10 and 10.5 Amphoteric terpolymers have been found to act as viscosity control additives for water-based drilling muds. They are chemically and thermally stable in high ionic strength environments. The solution viscosity remains essentially invariant to temperature changes. Terpolymers composed of acrylamide, metal styrenesulfonate and methacrylamidopropyltrimethylammonium chloride show improved drag reduction in water, while efficient drag reduction in a variety of organic solutions was exhibited by terpolymers of styrene, metal styrenesulfonate and 4-vinylpyridine [6].

Protein-polyelectrolyte complexes have found application for protein separation and enzyme immobilization [7]. The interaction of proteins with DNA is central to the control of gene expression and nucleic acid metabolism. One method for protein separation by water soluble polyampholytes that have random sequences is based on a selective complexation of a polyampholyte with a protein that has a net complementary charge. A prerequisite of the process is that the latter interaction is stronger than that between other proteins in the same solution. Thus, only one of the proteins will form a complex with the polyampholyte and phase separate, while the other proteins remain in the supernatant phase. The resultant protein/polyampholyte assembly can be removed from the system and redissolved at a different pH. Finally, the polyampholyte can be separated at its pH, when precipitation occurs. The phenomenon of adsorption of polyampholytes on a charged surface has great potential because many biological and technological processes are closely connected with the adsorption phenomenon [8, 9].

Oil and gas resources remain the world's major contributor to energy supply even with the recent energy generation from renewable sources [10, 11]. As global energy demand increases in juxtaposition to dwindling energy resources, maximizing oil recovery from previously under-exploited reserves becomes crucial to meet the ever increasing energy demand [11]. The processes of oil recovery are majorly in three stages namely: primary, secondary and tertiary (EOR) stage. After the application of primary and secondary oil recovery techniques, two-third of the original oil in place (OOIP) remains in the reservoir [12, 13]. This is either because

the oil is trapped by capillary forces (residual oil) or bypassed in some other way. The bypassed oil arises due to reservoir heterogeneities or because of unfavourable mobility ratio between the aqueous and oleic phase. On the other hand, the residual oil is made up of discrete ganglia that are produced when a finger like protrusion of the oleic mass forms a narrow neck by the combined effects of local pressure gradient and interfacial tension (IFT) [14].

To enhance the overall oil displacement efficiency, numerous EOR methods have been devised and utilized [13]. During oil recovery, the overall oil displacement efficiency is a combination of macroscopic (volumetric sweep) and microscopic (pore scale) displacement efficiency. Macroscopic displacement efficiency is a measure of the effectiveness of the injected fluids in contacting the oil zone volumetrically with respect to the total reservoir volume while microscopic displacement efficiency is the efficiency related to the ability of the displacing fluid(s) to mobilize oil trapped at the pore scale when it contacts the oil. Summarily, any mechanism that can increase oil recovery efficiency at either the micro or macro-scale or both is beneficial for EOR [15]. The devised and utilized EOR methods are majorly categorized into thermal and non-thermal EOR methods [16]. Unfortunately, thermal EOR methods are unsuitable for reservoirs with great depth and thin pay zone. Thus, non-thermal EOR has received prodigious attention for recovering oil bypassed or trapped in the reservoir [17].

Amongst all the EOR techniques, chemical EOR method, a non-thermal EOR method, has been adjudged as the most promising because of its higher efficiency, technical and economic feasibilities and reasonable capital cost [18]. The application of this EOR method became popular in the 1980 s due to higher oil prices and technological advancement that enables understanding their mechanism. Chemical EOR methods increase oil recovery by increasing the effectiveness of water injected into the reservoir to displace the oil. Dependent on the type of chemical EOR process, chemicals injected with the water slug alter the fluid-fluid and/or fluid-rock interaction in the reservoir. This includes lowering of the IFT between the imbibing fluid and oil or an increment in the viscosity of the injectant for improving mobility and conformance control. Besides, the injected chemical results in wettability alteration of the rock to increase oil permeability [19].

The well-known traditional chemical EOR methods are polymer flooding, surfactant and alkaline flooding [20]. However, the conventional chemical EOR methods have their limitations. Polymers, whose main recovery mechanism is to increase viscosity of injectants and consequently mobility, suffers viscosity loss in the presence of reservoir brines and elevated temperature conditions. Surfactant and alkali lose their efficiency during their flow in porous media due to adsorption phenomena. Subsequently, different modes of chemical flood injections were devised, studied and applied for EOR processes. These include the binary mix of alkali-surfactant (AS), surfactant/polymer (SP), alkaline/polymer (AP), and alkaline/surfactant/polymer (ASP) slug (see Fig.1.1). The synergy of the combined conventional chemicals recorded an improved efficiency during their applications in oil wells. Recently, the use of foam enhanced by surfactants and polymers, for

improved stability and mobility control have been studied to improve oil recovery [2, 21].

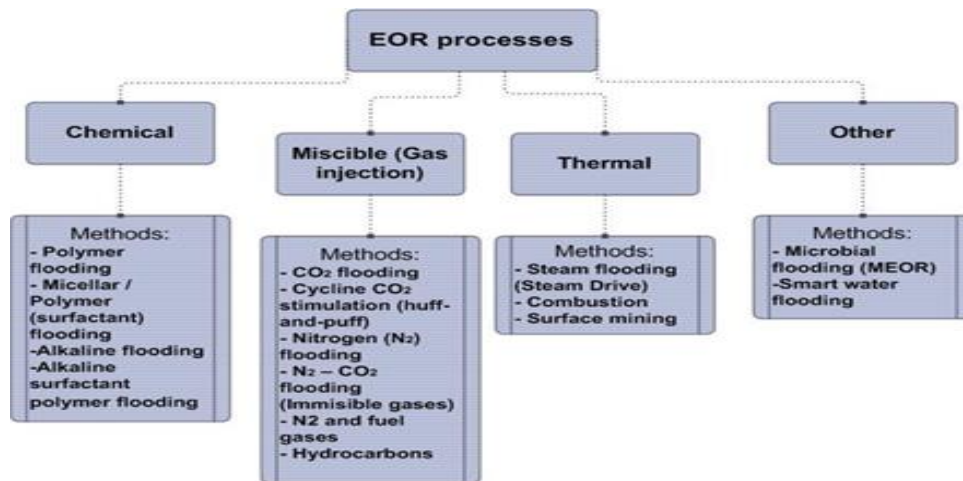


Figure 1.1- Simplified classification of EOR methods

More recently, the evolution of nanotechnology and their applications to improve the efficiency of various processes in the fields of metallurgy, electronics, medicine, aeronautics, catalysis, and fuel cells have prompted its use and application in the oil and gas industry [22,23]. The field of nanoscience and nanotechnology describes the creation and exploitation of materials with structural features having at least one of its dimensions in the nanometre range (1-100 nm). The “engineered nano-material” is called nanoparticle. The resultant improvement in the functional properties of a process generated due to addition of nanoparticles is attributable to their scalable and quantum effects. The application of this functional materials requires a base fluid such as gas, oil, water, or any other suitable liquid substance, hence, they are termed nanofluid. The application of nanotechnology has proffered solutions to various oil and gas problems ranging from drilling operations, petroleum exploration, inhibiting asphaltene depositions and gas hydrate formations, hydraulic fracturing jobs and EOR [24, 25].

For EOR processes, nanofluid flooding has been evaluated and explored as a chemical EOR process with field application reported in Colombia [26]. The mechanism of the IOR were identified as structural disjoining pressure, wettability alteration, IFT reduction and improved viscosity of injectant [27]. More recently, the addition of nanoparticles to conventional EOR chemicals have been studied and reported to yield novel materials with excellent and fascinating properties. For example, polymeric nanofluids, a synergistic combination of nanoparticle and polymers were found to possess improved rheological properties and stability for application in the presence of high-temperature and high-salinity conditions [28]. Furthermore, the synergistic application of nanoparticles with surfactant lowers their adsorption via competitive adsorption mechanism, while their applications with foams generate stable foams with longer half-life [29].

This overview is a fundamental study that presents the current scenario of

available research on chemical EOR. First, a survey of conventional chemical EOR method was carried out. The conventional EOR chemical types were identified and the mechanism of their EOR applications are discussed, and their limitations are highlighted. Thereafter, the binary application of conventional chemical EOR methods were also defined and analysed. Afterwards, the recent trend of incorporating nanotechnology for chemical EOR was also explored. The various nanofluid types, mechanism of their application and laboratory studies were outlined. Finally, the challenges associated with chemical EOR methods were enumerated and recommendations for future works were proffered.

The notable conventional EOR chemicals are polymers, alkali, and surfactants. The injection of polymers with waterfloods increases the viscosity of the aqueous phase, and consequently mobility as they move from the injection well towards the producer. Additionally, the polymer solution increases oil recovery by reducing permeability to water in the reservoir [30]. Surfactant solutions reduce the IFT between water and crude oil by reacting with certain crude oil constituents, thereby, solubilizing interfacial films, and causing emulsification [31]. The IFT reduction causes lowering of the capillary forces of trapped and residual oil. Besides, surfactant adsorb on reservoir rocks to change rock wettability, hence, an increased oil recovery. Alkali flooding operates with a mechanism in similitude to surfactant solutions though with a different injectant [32]. Foam flooding ensures diversion of injected fluid from thief zones to low permeable regions of the reservoir [33]. Meanwhile, AP, AS, and ASP flooding are borne out of the basis to incorporate the different strengths and efficiency of alkali, surfactant and/or polymer solutions to improve the pore scale and sweep efficiency of the OOIP [34].

1.2 Polymer flooding technology

Polymer flooding is an enhanced oil recovery method (EOR) which consists in the addition of water-soluble polymers in the injection water. This polymer addition results in an increase of the injected fluid viscosity, and thus, the mobility ratio between displacing (water) and displaced (oil) fluids is reduced [35]. Mobility ratio reduction improves the volumetric sweep efficiency by reducing viscous fingering [36] and channeling effects [35]. Thus, polymer flooding can be advantageous for heavy oil recovery or heterogeneous reservoirs [1] and was successfully applied in sandstone and carbonate reservoirs [37]. Polymer flow in porous media is subject to specific phenomena, such as non-Newtonian viscosity and inaccessible pore volume (IAPV).

Polymer IAPV is a phenomenon that results in the transport of polymer molecules through a smaller pore volume than the one available for small molecules (i.e., salts) [35]. That results in faster transport of polymer species through the porous medium than those small molecules [37].

There are two explanations for the IAPV: 1. IAPV is an effect of blocked pores and pores that are too small compared to the polymer molecular size [37], a concept

similar to that of gel permeation chromatography [5]. 2. IAPV is a consequence of the depleted layer, a thin layer of polymer-free liquid resulted from entropic (or steric) exclusion of large molecules from the pore walls [50,55]. Fig.1.3 shows the two interpretations for the polymer IAPV.

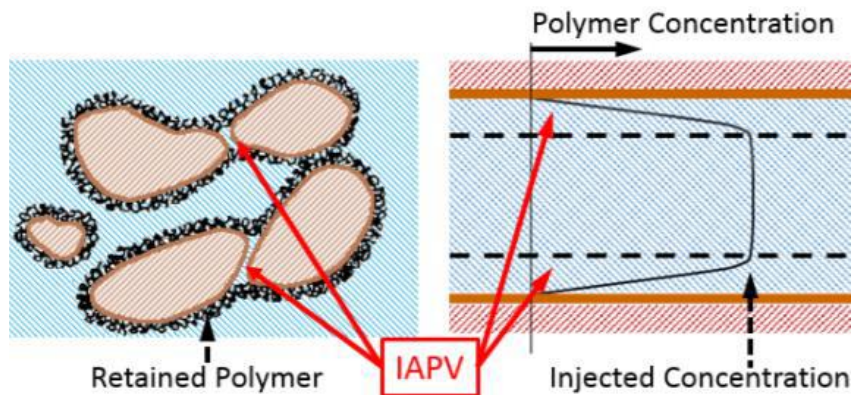


Figure 1.2 - The two interpretations for the polymer IAPV. Left: illustration of a porous medium with blocked pores; Right: polymer concentration profile illustrating the depleted layer near pore walls (adopted from [55])

Polymeric solutions for EOR applications are shear-thinning fluids, and their bulk rheology can be estimated through rheometers. However, polymer apparent viscosity when flowing through a porous medium (i.e., *in-situ* viscosity) differs from the bulk viscosity [38, 39]. There are four distinct *in-situ* viscosity regions for flexible polymers (e.g., HPAM) [38]:

1. Newtonian plateau at low shear rates;
 2. Shear-thinning region at medium shear rates;
 3. Shear-thickening region at high shear rates due to viscoelastic effects;
 4. Another shear-thinning region at very high shear rates due to mechanical degradation.
- For polymers with rigid structures (e.g., xanthan in its ordered state), the region 3 does not exist, since these polymers do not present viscoelastic behavior. Fig. 1.3 illustrates the bulk and *in-situ* viscosities for flexible polymers. The viscosity behavior of regions 1 and 2 are similar to bulk viscosity, however *in-situ* viscosity is lower than bulk viscosity due to an apparent slip effect caused by the depleted layer [39], and thus, linked to the IAPV.

The conventional method for estimating polymer IAPV is based on the core flooding in the presence of a polymer and an inert tracer. Effluent analysis to determine the polymer and tracer breakthrough instants are required to estimate the IAPV. Determination of polymer concentration may require complex methods and/or equipment, and often the presence of oil is a contaminant to those measurements [40, 41].

The objective of this paper is to develop a method for estimating IAPV based on the *in-situ* rheology of polymers. The method should require pressure drop measurements in core flooding and rheology experiments and could be used in both single- and two-phase experiments [42]. A total of ten samples were used in the

experiments. As early as the 1960 s, polymer flooding had been suggested as an oil recovery process to further increase oil recovery after water flooding; the main purpose of adding polymer was to increase the viscosity of the displacing fluid, which is commonly water [43-45]. This work was followed by wide research attention to recognize the benefits of polymer flooding in oil recovery applications [46-49].

For most oil reservoirs, especially heterogeneous formations, at least half of the reserved oil still leaves behind after extensive water flooding due to the unfavorable mobility ratio between water and oil. Once a preferential flow path is formed between injector and producer, the subsequently injected water would flow straight to the production well bypassing the oil bearing zones, which ultimately causes a low sweep efficiency and oil recovery. In order to cover the bypassed oil zones, polymer is usually used to thicken the injection water and makes the mobility of water and oil comparable. Through polymer flooding, the poor mobility ratio encountered in conventional water flooding is corrected, and consequently the volumetric sweep efficiency of the water-flooded reservoirs can be significantly improved. Among all the EOR methods, polymer flooding is considered as one of the most promising technologies because of its technical and commercial feasibility. The worldwide interests in polymer flooding applications were further stimulated recently by the exciting field reports from the scaled use in Daqing oilfield in China, with incremental oil productions of up to 300,000 barrels per day [50].

The overall oil recovery efficiency in oil production processes is generally governed by two sub efficiencies, i.e., macroscopic and microscopic recovery efficiency. The macroscopic recovery efficiency refers to the volume that the flooding agents are able to sweep; while microscopic recovery efficiency is a measure of the effectiveness of the displacing fluid(s) in mobilizing the oil trapped at pore scale by capillary forces. In other words, any mechanism that can improve either macroscale or microscale oil recovery efficiency is beneficial for increasing oil production [51]. The mechanisms of polymer flooding have been pursued since it incepted [52]. The well established relationship between capillary number and oil recovery indicates that a substantial increase in oil recovery at the pore level (microscale) can be obtained only when the capillary number is increased by several thousand times. However, for polymer flooding, the capillary number is normally increased less than 100 times [53, 54]. Therefore, it was previously suggested that polymer flooding can only improve the volumetric sweep efficiency without any effect on the microscopic displacement efficiency [55]. However, in Daqing oilfield, China, the oil recovery factor using polymer flooding was increased by up to 13% OOIP, and this value seemed unachieved only relying on sweep efficiency improvement. This fact made researchers to revisit the oil recovery mechanisms occurred in polymer flooding. After almost 15 years' efforts, it was demonstrated that the incremental oil recovery by polymer flooding could also be explained by the simultaneous increased microscopic displacement efficiency due to the distinctive flow characteristic of polymer solutions. Regarding EOR polymers, HPAMs are still the most widely used polymer to date in oilfields because of their availability in large quantity with customized properties (molecular weight, hydrolysis degree, etc.) and

low manufacturing cost [56,57]. However, it is known that polyacrylamides are very susceptible to chemical, mechanical, thermal, and microbial degradation, and this issue might affect its acceptance in type II and type III reservoirs having high temperature and salinity. As alternatives to HPAM, many novel polymers with tough properties have been proposed in the past several years, such as hydrophobically modified polymers and biopolymers [58].

Water is usually used to displace oil from matrix rocks. However, because of the unstable displacement front due to the differences in oil and water viscosities and heterogeneous nature of matrix rocks the oil production rates are often decline accompanied by the increase of water production [59].

Water-soluble polymers in brine water are widely used in a great many of oil fields. Their rheological properties in brine water are very important in order to use in high salinity reservoirs [60]. Such polymers are an important topic of modern research due to their practical application. Polyacrylamide is widely used in wastewater treatment, paper production and oil industry according to its thickening, flocculation and rheological properties [61].

HPAM is globally used to increase water viscosity. The expansion of the polymer molecule due to the repulsion between negatively charged groups on HPAM chains results in the increase of solution viscosity [62]. However, if cations are present in water, the negative charges on the polymer chain are screened and as a result, the hydrodynamic volume of the polymer molecule is reduced [63,64]. Thus, at higher salinities higher polymer concentrations of HPAM are required in order to achieve the target viscosity. At extremely high salinity and temperature, the HPAM chains will coil up and precipitate [65].

When water flooding of an oil reservoir proves inadequate due to viscous fingering phenomena culminating in early water breakthrough, polymer flooding may be introduced/incorporated. The process of polymer flooding involves the injection of high molecular weight water soluble polymers along with the water slug to increase the viscosity of the injectant [66,67]. The incremental viscosity of the injectant improves the mobility and conformance control of the injected slug and eradicates viscous fingering phenomena. Polymer flooding has been successfully implemented in many oilfields either on a pilot scale or on commercial scale for several decades. This includes the Daqing oilfield in China, East Bodo Reservoir and Pelican Lake field in Canada, Marmul field in Oman, and Tambaredjo field, Suriname, to mention just a few [68]. In addition, polymer flooding has maintained its increasing importance to the current energy market. The most notable contribution is the reported incremental oil production of up to 300,000 bbl/day from Daqing oil field in China [69].

Mobility control. Mobility ratio is defined as the ratio of the mobility of the injectant (water) to the mobility of the displaced fluid (oil). Primarily, water is used to displace oil from matrix rocks. However, because of an unstable displacement front due to the differences in oil and water viscosities and the heterogeneous nature of matrix rocks, oil production rates often decline along with an increase in water cut [70]. In order to prevent water from bypassing oil, the following actions are required:

- 1) Water permeability reduction;

- 2) Oil viscosity reduction;
- 3) Oil permeability increase; and,
- 4) Water viscosity increase.

Based on this concept, the mobility factor (M) was introduced in order to quantitatively assess oil displacement by water [71]:

$$M = \frac{k_w \cdot \mu_o}{k_o \cdot \mu_w} \quad (1.1)$$

where M - mobility factor; k_w - water permeability; μ_o - oil viscosity; k_o - oil permeability; μ_w -water viscosity.

Whereas, the first three above listed tasks are challenging in practice, the fourth task of increasing water viscosity can be achieved by using high molecular weight polymers [72]. The increase in the viscosity of the injected water as an oil displacing agent after the addition of high molecular weight polymers results in substantial acceleration of oil production [73]. This is explained by a reduction in the propagation velocity of water in matrix rocks in relation to that of the oil, and as a result, the injected water sweeps more oil. Indeed, polymer flooding has been shown to be an effective method of unlocking viscous oil resources [74].

Polymer viscoelasticity is the third mechanism posited to be responsible for improved macroscopic efficiency during polymer flooding. Unlike Newtonian fluids, polymers undergo a series of expansion and contraction (stretching and recoiling) during their flow in porous media [75].

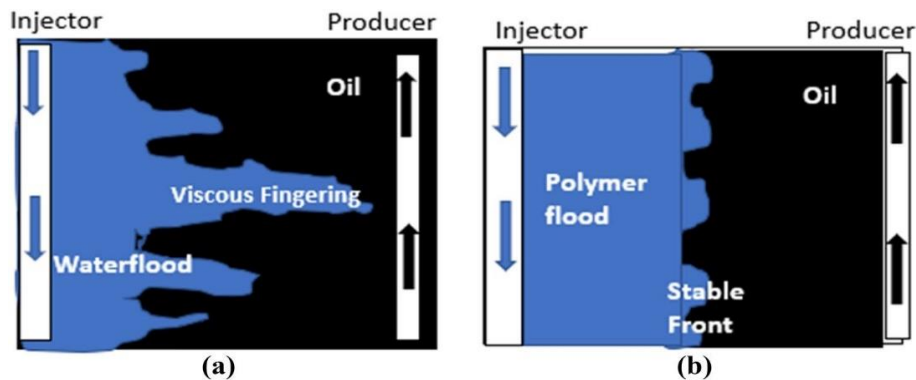


Figure 1.3 -Typical mobility ratio of (a) water flooding process ($M > 1.0$), (b) polymer flooding process ($M \leq 1.0$) (Adapted from [8])

This helps the polymeric molecules to generate additional “elastic viscosity” which improves macroscopic and microscopic displacement efficiency. Urbissinova et al. [76] and Veerabhadrapa [77] investigated the effect of viscoelastic properties of polymer on macroscopic sweep efficiency. The elastic difference of the polymer solution with the same shear viscosity was generated using polymer of similar average molecular weight but different molecular weight distribution (MWD). The result of

their individual experiment indicated that high elastic polymer solution exhibited a considerably higher resistance to flow through porous media and stability of the propagating front thereby minimizing fingers. This cumulated in a higher sweep efficiency, lower residual oil saturation and an improved oil recovery [78].

1.3 Types of EOR polymers

Generally, two major classifications exist for polymers used during polymer flooding recovery operations, namely, synthetic polymers and biopolymers. Typical examples of synthetic polymers are polyacrylamides and its derivatives such as partially hydrolysed polyacrylamide (HPAM), hydrophobically associating polyacrylamide (HAPAM), and copolymers of acrylamide. On the other hand, biopolymers include xanthan gum, scleroglucan, hydroxyethylcellulose, carboxymethylcellulose, welan gum, guar gum, schizophyllan, mushroom polysaccharide, cellulose, and lignin. It is noteworthy that field application of HPAM and xanthan gum are the most widely reported and will be discussed further. For additional information of other polymer types, Taylor et al. provided a comprehensive review of water-soluble HAPAM [79], and Kamal et al. [80] described the state of the art review of copolymers of acrylamide polymers for EOR. Additionally, Pu et al. [81] published a detailed review of polysaccharide biopolymer for EOR. Finally, Wever et al. [82] chronicled a general review of polymers for EOR.

1.3.1 Partially Hydrolyzed polyacrylamide (HPAM)

Hydrolyzed polyacrylamide is water-soluble, synthetic straight chain polymers used in EOR applications. It is a copolymer of polyacrylamide and polyacrylic acid obtained by the partial hydrolysis of PAM or by copolymerization of sodium acrylate with acrylamide [83]. They are widely regarded as the most used polymer for EOR [84]. HPAM is mostly preferred during field applications because it is resistant to bacterial attack, it has good water solubility, mobility control and it is a low-cost polymer [85, 86]. When used during polymer flooding, the polymer molecule undergoes partial hydrolysis which converts some of the amide groups ($-\text{CONH}_2$) to carboxyl groups ($-\text{COO}^-$). Typical degree of hydrolysis (DOH) for this polymer is 15–35% of the acrylamide (AM) monomers. Hence, they are negatively charged. The DOH accounts for many of the physical and rheological properties of the polymer solution such as adsorption, viscosity and water solubility. Nonetheless, HPAM is very sensitive to external factors such as pH, temperature, salinity, shear forces and hardness.

Hydrophobic interactions among the polymer chains result in either intra- or inter-molecular associations or their combination. An illustration of the concept of intra- or inter-molecular associations for a hydrophobically modified polyacrylamide is shown in Fig 1.4. The dominance of either association type depends on the polymer concentration and has a strong impact on the viscosity of the polymer solution. In the dilute regime, HMPAM forms more intra-molecular associations than intermolecular ones, twisting the macromolecular chains and reducing the hydrodynamic radius, thus

reducing the viscosity. At concentrations higher than the critical association concentration (CAC), inter-molecular associations become more dominant, which abruptly increases the hydrodynamic radius of the polyacrylamides [83].

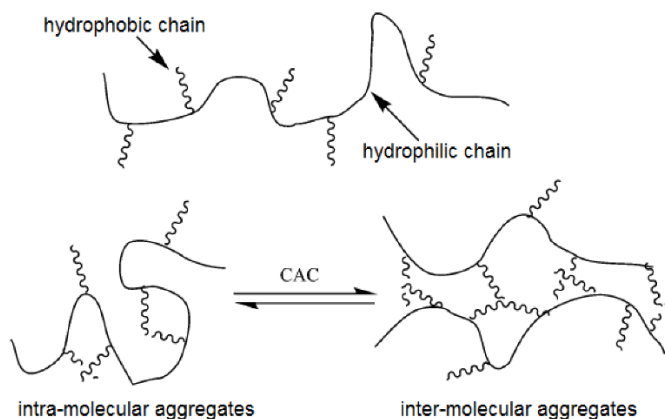


Figure 1.4 - Intra- and inter-molecular associations in a hydrophobically modified polyacrylamide. Adapted with permission from [95]

HPAM is widely used to increase water viscosity. The expansion of the polymer molecule, due to the repulsion between negatively charged groups on HPAM chains, results in an increase in the viscosity of the solution. However, if cations are present in water, the negative charges on the polymer chain are screened, so the hydrodynamic volume of the polymer molecule is reduced [82-84]. At higher salinities, greater concentrations of HPAM are therefore required in order to achieve the target viscosity. At extremely high salinity and temperature, HPAM chains coil up and precipitate [85].

The ability of amphoteric polyelectrolytes to swell and be effective viscosity enhancers in reservoirs with high salinity and temperatures plays a crucial role in the enhanced oil recovery (EOR) processes [86-87]. Due to their salt- and temperature resistance, strongly charged, or quenched, polyampholytes can serve as viscosifying agents in EOR when thickeners are required in brine solution [88-91]. In this regard, amphoteric polyelectrolytes, being polymers that have both cationic and anionic groups, are promising, because in high salinity water, the anions and cations screen the electrostatic attraction between the positively and negatively charged groups of the polymer chain, thus the chain expands, increasing the viscosity of the solution [92,93].

1.3.2 Polyampholytes

Polyampholytes have attracted much attention both theoretically and experimentally due to their unique properties and technological importance [94, 95]. They are the most important class of macromolecules due to their wide range of industrial applications [96]. These types of polymers range from naturally occurring biopolymers such as proteins and polynucleotides to synthetic viscosity modifiers and soaps. Ion containing polymers can be classified into two major categories, namely,

polyelectrolytes and polyzwitterions. Polyelectrolytes contain either anionic or cationic functional groups along the polymer chain, while polyzwitterions contain both anionic and cationic groups. Common polyelectrolytes include polyacrylic and polymethacrylic acids and their salts, sulfonated polystyrene, and other strong polymeric acids and bases [97].

The intra - primarily governs the aqueous solution properties such as viscosity and hydrodynamic volume of polyelectrolytes and polyzwitterions- and intermolecular electrostatic interactions [98] that occur among the cations and anions in aqueous media. In dilute, salt-free aqueous solutions, the coulombic repulsions between like charges along a polyelectrolyte chain lead to an expansion in the hydrodynamic volume of the polyelectrolyte coil; however, the addition of electrolytes like sodium chloride (NaCl) results in coulombic shielding and a decrease in hydrodynamic volume and thus solution viscosity. This solution behavior is termed the polyelectrolyte effect [99]. For polyzwitterions, the charges may be located either on the pendent side chains of different monomer units, or in the case of some polyesters, polyphosphazene, and polybetaines, one or both of the charges may be located along the polymer backbone [100]. The distinction between zwitterionic polyampholytes and polybetaines is not always clear from the literature. The term polyzwitterion includes all polymers that possess both cationic and anionic groups. Polyampholytes refers to those polymers that specifically possess charged groups on different monomer units, while polybetaines refer to those polymers with anionic and cationic groups on the same monomer unit. In contrast to polyelectrolytes, structure-property relationships of polyampholytes are governed by coulombic attractions between anionic and cationic polymer units [100].

The coulombic interactions between positively and negatively charged repeat units of polyampholytes reduce hydrodynamic volume, because of which the polymer adopts a collapsed or globular conformation in dilute, salt-free aqueous media [100]. In some cases, the electrostatic interactions are so strong that the polymer may become insoluble. On adding simple electrolytes like NaCl to a polyampholyte solution in the dilute regime, the hydrodynamic volume of the polymer coil increases due to the screening of the intramolecular charge-charge attractions, allowing the transition from a globule to a random coil conformation. Such a solution behavior is known as the anti-polyelectrolyte effect and is evidenced by increased polymer hydrodynamic volume and solution viscosity.

In addition to interactions with small molecule electrolytes, other factors such as charge density and distribution, charge balance, monomer sequence distribution (random, alternating, and block), and the nature of the ionizable groups along the polymer backbone plays an important role in determining polymer conformation and rheological behavior of polyzwitterions in aqueous solution [100]. For polyampholytes, the magnitude of the globule to coil transition, the extent of polymer solubility, and the hydrodynamic volume are typically governed by the charge density of the system. Larger concentrations of electrolytes are needed to elicit coil expansion as charge density is increased; however, the magnitude of hydrodynamic volume increase observed is greater with an increased number of zwitterionic interactions. As the degree of charge imbalance [101-102] on a

polyampholyte chain increases, the polymer tends to behave in a manner that is more characteristic of a conventional polyelectrolyte.

Typically, polymers that have random incorporation of charged species exhibit more profound antipolyelectrolyte behavior than polyampholytes with alternating incorporation of anionic and cationic groups. This is due to long-range electrostatic interactions in the random moieties versus the alternating ones, which are governed by short-range interactions. The solution properties of polyampholytes also depend on the chemical nature of the charged groups [100]. Polyampholytes bearing strong acids or salt-like functionalities such as sulfonic acids and quaternary ammonium ions are generally insensitive to changes in solution pH; thus, the charge balance and charge density are determined solely by the relative incorporation of the anionic and cationic monomers. However, in polyampholytes containing weak acid/base functionalities such as carboxylic acid and primary, secondary, or tertiary amine groups, the charge density and charge balance of the polymer are determined by the relative incorporation of the ionizable monomers. An example is that of a polyampholyte containing equimolar amounts of a carboxylic acid and quaternary ammonium functional groups. At low pH, this polymer behaves as a cationic polyelectrolyte due to an overall net charge that is a result of virtually no ionization of the acidic groups.

As the solution pH is raised, these groups are ionized, eventually establishing a charge balance, at which point the polymer exhibits polyampholyte behavior. For polyampholytes in which the amphoteric repeat units (for example, in monomers containing carboxylic acid units) are present more than permanently charged repeat units, polyampholyte behavior is observed at the isoelectric point (IEP). The isoelectric point (IEP) is defined as the pH at which the number of cationic and anionic groups are equal. As the solution behavior is adjusted from the IEP, polyelectrolyte behavior is observed due to the increase in the net charge [100]. Alfrey, Morawetz, Fitzgerald, and Fuoss reported the first study of synthetic polyampholytes in their 1950 article “Synthetic Electrical Analog of Proteins”.

Polyampholytes are interesting for several reasons, not the least of which is the fact that they are synthetic analogs of naturally occurring biological molecules such as proteins, and find applications in areas such as lithographic film, formulation of emulsions and drug reduction. Polyampholytes can be grouped into four subclasses, based on their responses to changes in pH, as shown in figure 1.1. Firstly; the polyampholyte may contain both anionic and cationic species that may be neutralized (1.5a). Secondly, the anionic group may be neutralized, but the cationic groups are insensitive to pH changes, for example, quaternary alkylammonium groups (1.5b). Thirdly, the cationic species may be neutralized, with the anionic groups showing no response to pH changes, for example, sulfonate groups – which called like highly charged polyampholytes (1.5c), and finally both the anionic and cationic species may be insensitive to changes in the pH of the solution throughout the useful range (1.5d).

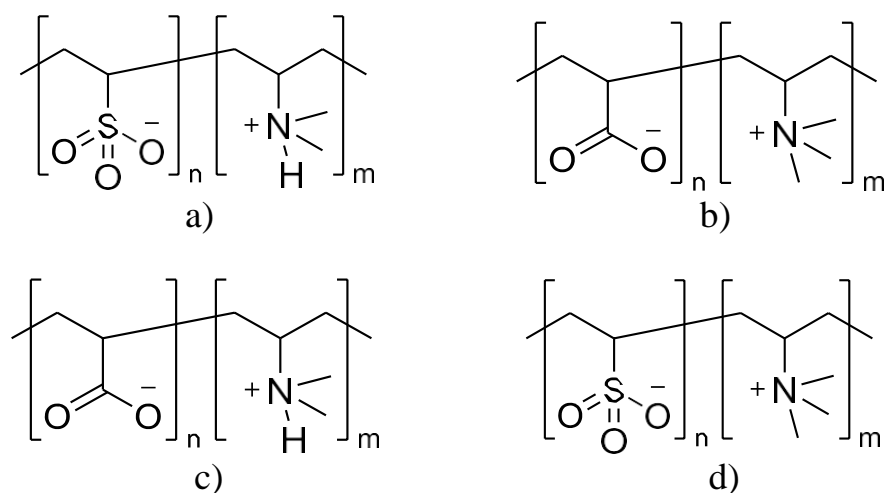


Figure 1.5 - Representative structures of the four subclasses of polyampholytes [100]

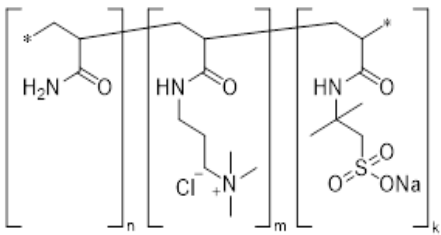
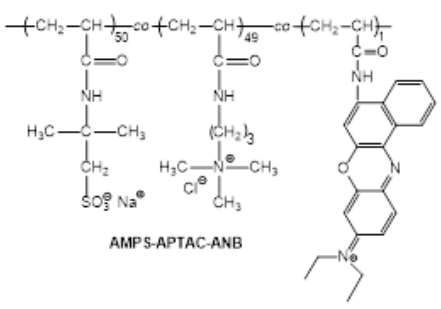
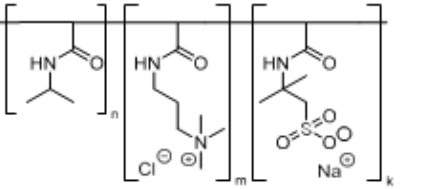
The anionic group may be neutralized (1.5a), but the cationic groups are insensitive to pH changes (1.5b). The cationic species may be neutralized, with the anionic groups are insensitive to pH changes (1.5c). Both the anionic and cationic species may be insensitive to changes in the pH of the solution (1.5d). The polyampholyte may contain both anionic and cationic species that may be neutralized.

More reports on the synthesis of polyampholytes first published in the 1950s. These polyampholytes synthesized via conventional free radical polymerization. Some examples include methacrylic acid-stat-2(dimethylamino)ethyl methacrylate copolymers, synthesized by Ehrlich and Doty, acrylic acid-stat-2-vinyl pyridine copolymers, synthesized by Alfrey and Morawetz, and acrylic acid-stat-2-(dimethyl amino)ethyl methacrylate copolymers reported by Alfrey and Pinner. Since then, numerous researchers have reported on the synthesis and properties of a variety of statistical polyampholytes.

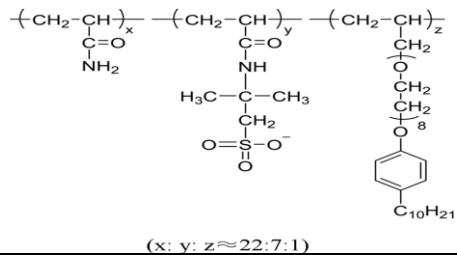
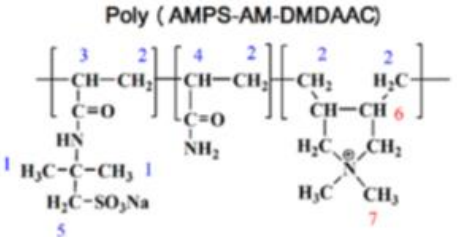
The block copolymers of 2-vinyl pyridine and trimethylsilyl methacrylate (TMSMA) were synthesized. Poly (TMSMA) was readily hydrolyzed to poly (methacrylic acid) using a water/methanol mixture. Subsequently, Varoqui and co-workers synthesized AB diblock polyampholytes from styrene sulfonate and 2-vinyl pyridine. Later, Morishima and co-workers reported the synthesis of block copolymers of TMSMA and p-N, N-dimethylaminostyrene [103]. Creutz and co-workers have developed the synthesis of block copolymers of methacrylic acid with co-monomers like dimethylaminoalkyl methacrylates [104]. These were synthesized by anionic polymerization using tert-butyl methacrylate (tBMA) as the protected precursor to poly (methacrylic acid) groups. Until recently, classical anionic polymerization was the most attractive route to the synthesis of block polyampholytes. Patrickios and co-workers, in 1994, reported on the synthesis of diblock, triblock, and statistical methacrylic polyampholytes by employing group transfer polymerization (GTP) [105, 106]. Similar to anionic polymerization, monomers with labile protons, namely methacrylic acid, could not be directly

polymerized, and protected acid monomers were required. Patrickios and co-workers selected TMSMA and 2-tetrahydropyranyl methacrylate (THPMA) as protected methacrylic acid (MAA) monomers. TMSMA was chosen because it is commercial and can easily be converted to MAA, and THPMA can be converted to MAA under very mild acidic conditions. They copolymerized the protected monomers with 2-(dimethylamino) ethyl methacrylate (DMAEMA), and in the synthesis of the triblock copolymers, methyl methacrylate (MMA) was introduced as the third hydrophobic comonomer. Subsequently, Lowe, Billingham, and Armes synthesized AB diblock copolymers of DMAEMA with MAA using THPMA as a protected precursor [107]. The recent developments in controlled free radical polymerization techniques, such as nitroxide-mediated polymerization (NMP) [110-114], atom-transfer radical polymerization (ATRP) [108], and reversible addition-fragmentation chain transfer (RAFT) polymerization [109]. McCormick and co-workers have prepared AB diblock copolymers of DMAEMA with acrylic acid (AA) via RAFT. They also accomplished the polymerization of sodium acrylate directly in aqueous solution via RAFT as well as the anionic acrylamido monomers, 2-acrylamido-2-methyl propane sulfonic acid (AMPS) and 3-acrylamido-3-methylbutanoic acid (AMBA). Some typical examples of polyampholyte terpolymers are shown in table 1.1.

Table 1.1-Typical examples of structures of Acrylamide based ternary polyampholytes

Chemical structure of ternary polyampholytes*	Name	Reference
	AAm-co-AMPS-co-APTAC	[110]
	AMPS-co-APTAC-co-ANB	[111]
	NIPAM-co-APTAC-co-AMPS	[112]

Continuation of the table 1.1

 <p>(x: y: z ≈ 22:7:1)</p>	<p>AAm-co-AMPS-co-1-2 (allyloxy)octethoxy)-4-decylbenzene</p>	<p>[113]</p>
 <p>Poly (AMPS-AM-DMDAAC)</p>	<p>AMPS-co-AM-co-DMDAAC</p>	<p>[114]</p>

1.3.2.1 Annealed polyampholytes

Annealed polyampholytes are copolymers consisting of weak acid/weak base, strong acid/weak base (or else weak acid/strong base), and strong acid/strong base monomers in which the net charge and the charge distribution along the chain are monitored mainly by changing pH of the solution [1, 2]. Annealed polyampholytes are a class of complex polymers that are characterized by containing both positively and negatively charged groups along their polymer chains. These charged groups can be in the form of cationic and anionic functional units. The term "annealed" in this context refers to the process of subjecting the polymer to a heat treatment, where the material is heated to a specific temperature and then slowly cooled down. This annealing process can lead to changes in physical and mechanical properties of polymer, including its conformation, crystallinity, and overall stability [3, 9].

The unique combination of charged groups in annealed polyampholytes leads to interesting and tunable properties, making them highly attractive for various applications. Some potential properties and applications of annealed polyampholytes include:

1. **Responsive Behavior:** Annealed polyampholytes can exhibit pH or temperature responsiveness due to changes in their charged interactions. This responsiveness can be exploited in drug delivery systems, where changes in the local environment trigger the release of drugs from the polymer.

2. **Biomaterials:** Annealed polyampholytes have been explored as biomaterials in tissue engineering and regenerative medicine due to their ability to mimic the charged nature of biological tissues and interact with cells.

3. **Coatings and Membranes:** Their charged nature makes annealed polyampholytes useful as coatings for surfaces or as components in membrane technology for selective ion transport.

4. **Biomedical Devices:** Annealed polyampholytes have shown promise in the design of biomedical devices, such as sensors and biosensors.

5. Self-Assembly: These polymers can self-assemble into various structures, including micelles and vesicles, which are valuable in drug delivery and nanotechnology applications.

It is important to note that the specific properties and applications of annealed polyampholytes can vary depending on their molecular structure, the nature of the charged groups, and the annealing conditions used during their synthesis.

Typically annealed polyampholytes consisting of the weak acid and weak base groups are copolymers of acrylic (or methacrylic) acid and vinyl pyridines, which were first synthesized in the 1950s by Alfrey and Katchalsky as have written before [116, 117]. While copolymers of vinyl or styrene sulfonic acid and N-substituted allylamine derivatives belong to strong acid/strong base polyampholytes. Usually, radical copolymerization of acidic and basic monomers results in statistical copolymers due to the difference in reactivity of monomers. A classic example is that of the copolymerization of 2-vinyl pyridine (a weak base) and methacrylic acid (weak acid), which leads to the formation of statistical copolymers. Kabanov et al. [118] have thoroughly discussed a significant influence of salt and hydrogen bonds form between acidic and basic monomers on the kinetics and mechanism of radical copolymerization. Most of the early studies concerned annealed polyampholytes [10,116].

1.3.2.2 Quenched and/or zwitterionic polyampholytes

McCormick et al. [120] synthesized a series of low- and high-charge-density ampholytic copolymers of AMPS and AMPDAC and thoroughly studied their solution properties. In studied systems, the sulfonate and quaternary ammonium groups are pH insensitive, and the composition of copolymers exclusively determines the charge balance of these terpolymers. Low-charge-density polyampholytes were derived from the polymerization of cationic and anionic monomers with acrylamide or N-isopropyl acrylamide [119]. For terpolymers, the relationships between the radius of gyration and molecular weight ($R_g - M$) and between the intrinsic viscosity and molecular weight ($[\eta] - M$) were found. Charge-balanced terpolymers exhibited antipolyelectrolyte behavior at the isoelectric point (IEP) pH 6.5 while unbalanced terpolymers exhibited typical polyelectrolyte character. The dilute solution behavior of the terpolymers is in good agreement with the theoretical predictions of authors [121]. In general, fully charged polyampholytes prepared in solution from charged cationic and anionic monomers tend alternation, as a result of the strong electrostatic attractive forces [22] acting between the opposite charges [122,123]. However, microemulsion polymerization leads to almost random polyampholytes, that is, to copolymers more homogeneous in composition than those prepared in solution. This result was accounted for by the marked differences in mechanism and microenvironment between the two processes.

Polyampholyte hydrogels based on cationic (quaternized N, N-dimethylaminoethylmethacrylate, 2-methacrylamido-2-propyl trimethyl ammonium chloride) and anionic (2-acrylamido-2-methyl propane sulfonic acid, the sodium salt of styrene sulfonic acid) monomers represent a new class of tough and viscoelastic

materials that can be tuned to change multiple mechanical properties over wide ranges. These polyampholyte hydrogels exhibit excellent biocompatibility and anti-biofouling properties, and due to excellent mechanical properties in physiological solutions, they have high potential as structural biomaterials in medicine [124].

Quenched polyampholytes can also be classified as semi-quenched when one of the monomer units bears permanent charge, while another contains ionizable acidic or basic group. Typical examples of self-quenched polyampholytes are copolymers of N, N'-dimethyl-N, N'-diallyl ammonium chloride (DMDAAC) with acrylic acid (AA) and maleic acid or alkyl (aryl) derivatives of maleamic acids, sodium styrene sulfonate (SSS)-4-vinyl pyridine (4VP) [125-126], etc. Such self-quenched polyampholytes are pH-responsive and adopt globular or collapsed confirmation at the IEP when the cationic and anionic charges are fully compensated, and the whole macromolecules are quasineutral [127]. According to the literature survey, the quenched polyampholytes are less considered in comparison with annealed polyampholytes and polymeric betaines [128].

Zwitterionic polyampholytes. Polymeric betaines or zwitterionic polyampholytes are polyampholytes those oppositely charged groups remote one from another are displaced on one-pendant substituents [129]. When the positive and negative charges are replaced on one pendant group and form inner salt without counterions they are classified as ampholytic ionomers. The synthetic strategy of polyampholytes with betaine structure has been outlined in detail in pioneering works of Salamone et. al. Polymeric betaines [130] can be synthesized directly by polymerization of betaine monomers or modification of functional polymers studied the kinetic features of the radical polymerization of the betaine type monomers [131]. The rate of polymerization R_p was found to be proportional to the square root of the initiator and monomer concentration, which is in good agreement with the general peculiarities of radical polymerization. There are several types of polymers with betaine structure: poly-carboxy betaines, polysulfobetaines, and polyphosphobetaines. Poly (N- ethyleneglycine) (1), poly [(N-3-sulfopropyl)-N-methacryloyloxyethyl-N, N- dimethylammonium betaine] (2) and poly (2-methacryloyloxyethylphosphorylcholine) (3) are typical examples of this kind of zwitterionic polyampholytes.

McCormick et al. [132] described the synthesis of a series of copolymers of acrylamide (AA) and with a novel carboxy betaine monomers_ The novel carboxy betaine monomers, 4-(2-acrylamido-2-methylpropyl dimethyl ammonio) butanoate (AMPDAB) and 6-(2-acrylamido-2 methylpropyldimethylammonio) hexanoate(AMPDAH) involve the quaternization of the monomeric tertiary amine by the reaction with ethyl 4-brombutyrate and 6-bromhexenoate. Free radical polymerization of vinylbenzyl chloride or block copolymerization of vinylbenzyl chloride and styrene resulted in reactive polymers with narrow molecular weight distribution and hydrophilic/hydrophobic balance [133]. The further modification of polymer precursors leads to corresponding amphiphilic polycarboxybetaines containing a hydrophobic styrene block. Kaladas et. al. [134] described the synthesis of a series of zwitterionic copolymers based on the copolymerization of N, N-diallyl-N, N-dimethylammonium chloride (DADMAC) (or N, N-diallyl-N-methylamine

(DAMA with 3-(N, N-diallyl-N-methylammonio) propane sulfonate (DAMAPS) (or 4- (N,N-diallyl-N-methyl ammonio)butanoate (DAMAB). A series of polycarboxybetaines and polysulfobetaines with varying distances between the positively and negatively charged groups were synthesized [135]. The synthesis of poly (ampholyte-electrolytes) via hydrolysis of the poly (N, N-diallyl quaternary ammonium salts), which were prepared from the nonzwitterionic monomer, has been described by authors [136]. The specific features of these polymers are that they exhibit both polyelectrolyte and polyampholyte character simultaneously.

By adding AA to a solution of polyiminoethylene or polyiminohexamethylene both, a protonation and a Michael addition reaction take place simultaneously. Carboxyethylation reaction proceeding in pure chloroform yields a poly ampholyte with more than 90% zwitterion structure. Ethyl ester of 3-amino-2-butenoic acid existing in enamino and imino tautomeric forms has been involved in the copolymerization process with unsaturated carboxylic acids. The reactivity of ethyl ester of 3-amino-2-butenoic acid is very low due to the formation of intramolecular hydrogen bonds that stabilize 1t-conjugated bonds [136].

1.4 Application of polyampholytes in oil industry

The acrylamide-based polyampholyte is also invented to a novel method for the treatment of oil or gas production wells. A microgel was obtained by dilution in water of a self-invertible inverse latex or a self-invertible inverse microlatex of a crosslinked polyelectrolyte, obtained by copolymerization, in the presence of a crosslinking agent of partially or totally salified free 2-methyl-2-[(1-oxo-2-propenyl) amino]-1-propane sulfonic acid, with at least one cationic monomer and with at least one neutral monomer chosen for example acrylamide [137].

Polyampholyte or polyelectrolyte solution behavior depends in solution pH, thus allowing the production of functional terpolymers with pH-triggerable solution properties. Such pH-responsive ampholytic systems are called annealed polyampholytes. These polyampholytes are well suited for a range of applications in which pH-triggerable changes in the solution viscosity might be useful, such as smart polymers for EOR or formulations for coatings and personal care products [138].

McCormick et al. prepared low charge density amphoteric copolymers and terpolymers composed of crylamide, the cationic comonomer (3 acrylamidopropyl) trimethylammonium chloride (APTAC), and amino acid-derived monomers (e.g., *N*-acryloyl valine, *N*-acryloyl alanine, and *N*-acryloyl aspartate) [139].

Then, terpolymers with random charge distributions have been compared to terpolymers of like compositions containing the anionic comonomer NaAMB. The results indicated the low charge density terpolymers had excellent solubility in deionized water with no phase separation. The experimental tests show that conformational restrictions of the NaAMB and *N*-acryloyl valine segments result in increased chain stiffness and higher solution viscosities in deionized water and brine solutions. However, the terpolymers with *N*-acryloyl alanine and *N*-acryloyl aspartate segments are more responsive to changes in the salt concentration [140].

The ability of polyampholytes to swell and be effective viscosity enhancers in high salinity media plays a crucial role in enhanced oil recovery (EOR) processes [141]. Suitable polymers have been investigated for the secondary recovery of oil from high-temperature reservoirs with high-density brine fluids. In the recovery of oil from oil-bearing reservoirs, an important component is the formulation of drilling muds [142]. A conventional water-based drilling mud formulation includes the following ingredients: water, a clay such as bentonite, lignosulfonate, a weighting agent such as BaSO₄ (barite), and a caustic material such as sodium hydroxide, or caustic barite, to adjust the pH of the drilling mud to a pH between 10 and 10.5. Amphoteric terpolymers have been found to act as viscosity control additives for water-based drilling muds [143]. They are chemically and thermally stable in high ionic strength environments. The solution viscosity remains essentially invariant to temperature changes [144].

Synthesized from acrylamide, sodium styrene sulfonate and methacrylamidopropyltrimethylammonium chloride, polyampholytes are stable to the presence of acids, bases, or salts. Terpolymers that consist of acrylamide, metal styrene sulfonate and methacrylamidopropylmethylammonium chloride showed improved drag reduction in water [145], while efficient drag reduction in a variety of organic solutions was exhibited by terpolymers of styrene, metal styrene sulfonate, and 4-vinylpyridine [146]. Graft copolymers of a polysaccharide with a zwitterionic monomer or cationic/anionic monomer pairs are effective thickening and stabilizing agents for aqueous and electrolyte-containing aqueous media [147]. An amphoteric polyelectrolyte that has both quaternary ammonium groups and sulfonate groups was employed to increase the viscosity of an organic liquid, wherein a polyampholyte solution in organic solvents has improved viscosity and exhibits shear thickening at increased shear rates [148]. The amphoteric polyelectrolyte employed for oil recovery was a copolymer of vinylpyridine with the appropriate alpha olefin or hydrogenated diene with subsequent sulfonation [149]. Patented a method for oil and/or gas recovery from a subterranean formation penetrated by a well bore, and for reducing the concomitant production of reservoir water [150]. Lightly crosslinked amphoteric gels tested as EOR agents were synthesized from the commercially available monomers N, N-dimethyl-N, N -diallylammonium chloride, diallylamine, and maleic acid. [151,152] Rheological and viscometric experiments revealed that the salient property of amphoteric gels is their ability to swell effectively in brine solution. Model experiments showed that amphoteric gels, dissolved in brine solution that contained up to 180 g.L⁻¹ of salt, recovered up to 75–95% oil from the sand's surface, depending upon gel concentration and oil type (Table 1.2).

Table 1.2 - Oil recovery from the sand surface by a saline water and amphoteric gel solution

Oil type and oil density	Amount of oil adsorbed on sand	Gel concentration	Desorbed oil amount	Oil recovery
kg.m ⁻³	ml (%)	%	ml	%

Continuation of the table 1.2

			Saline water	Gel solution	Saline water	Gel solution
Light,814	2.2(22)	0.5	0.22	1.1	10	50
		1		1.67		76
		1.5		1.8		82
		4		2.1		95
		5		2.1		95
Middle,877	3(30)	4	0.15	1.5	5	50
		5		2.3		76
Heavy, 917	5.2 (52)	4	0.15	1.9	3	36
		5		4		77

1.4.1 Acylamaide based polyampolytes for EOR

The rheology of polyelectrolyte solutions has been studied extensively due to the wide variety of practical applications of this type of polymer as viscosity control additives. Copolymers of the AMPSNa with acrylamide have potential in oil-field applications [153].

In the dilute regime, ampholytic terpolymers characteristically exhibit unique globule to coil transitions, with increasing electrolyte concentrations resulting in larger hydrodynamic volumes and subsequent increases in the solution viscosity. This phenomenon is often called the antipolyelectrolyte effect. To fully understand the solubility and solution properties of ampholytic terpolymers, a general understanding of the complex associations that govern these properties, such as polymer–solvent and polymer–polymer interactions, must be known [154]. Of fundamental importance are the electrostatic interactions that occur among the charged repeating units of the polyampholyte chain. Factors such as the charge density, charge asymmetry (e.g., degree of charge balance), charge spacing and distribution, and solution ionic strength are critical parameters. Even though the solution behavior of polyampholytes is typically dominated by electrostatic effects, other interactions along the polyampholyte backbone and with the solvent must be considered. Factors such as hydrophobic substitution, steric hindrance/chain stiffening due to bulky pendant groups, and hydrogen bonding along the backbone or with pendant groups must be taken into account when we examine polyampholyte behavior in aqueous solutions [155]. Of the previously mentioned polyampholyte characteristics, unique salt-responsive behavior is the focus of study in academic laboratories as well as industrial laboratories.

Synthetic polyampholytes based on acrylamide (PAM) are excellent prospects for electrolyte-tolerant rheology modifiers, drag-reducing agents, and flocculants because of their ability to sustain high solution viscosities under saline conditions and exhibit stimuli-responsive behavior. AM based polyampholytes that contain low charge densities and incorporate large concentrations of acrylamide (AM) are often preferred because long runs of hydrophilic AM repeat units increase the terpolymer solubility at low ionic strengths [152-156]. The overall performance of lowcharge-

density polyampholyte terpolymers as viscosifying agents is typically greater than that of highcharge-density ampholytic copolymers. Sulfonate anions and quaternary ammonium cations are the most commonly reported ionic functional groups for most AM-based polyampholyte systems, and these are known to be insensitive to changes in the solution pH [157,158].

Such non-pH-responsive systems are often called quenched polyampholytes, and their degree of exhibited polyampholyte or polyelectrolyte character is solely determined by the ratio of anionic-to-cationic monomer incorporation [159,160]. However, when polyampholytes are prepared with comonomers bearing weak acid and/or weak base functionality (e.g., carboxylic acids and tertiary amines), the degree of polyampholyte or polyelectrolyte behavior exhibited in aqueous solutions is governed not only by the ratio of anionic-to-cationic comonomer content but also by the solution pH [161]. Changes in solution pH can elicit either polyampholyte or polyelectrolyte solution behavior, thus allowing the production of functional terpolymers with pH-triggerable solution properties [162]. Such pH-responsive ampholytic systems are called annealed polyampholytes. These polyampholytes are well-suited for a range of applications in which pH-triggerable changes in the solution viscosity might be useful, such as smart polymers for enhanced oil recovery (EOR) or formulations for coatings and personal care products [163].

To date, our synthetic research efforts have been focused on the development of stimuli-responsive, water-soluble polymers designed for use in EOR applications [161-162]. These model systems are structurally tailored for potential applications as viscosifiers and/or mobility-control agents for secondary and tertiary EOR methods⁷.

The goal of previous synthetic work has been to design novel polymers that exhibit large dilute solution viscosities in the presence of the adverse conditions normally encountered in oil reservoirs (e.g., high salt concentrations, the presence of multivalent ions, and elevated temperatures) [162,163]. The polymers are also designed to have triggerable properties that can be elicited by external stimuli such as changes in the pH and/or salt concentration. Chemical processes, mainly polymer flooding and surfactant polymer injection, have been the focus of attention of longstanding research in the field of polymer science in relation to EOR. Polymer flooding is based on the principle of improving (decreasing) the mobility difference between injected and in-place reservoir fluids to reduce channeling effects. Mobility control must be maintained within the flood, and the displacing phase should have a mobility equal to or lower than the mobility of the oil phase [164].

In EOR processes, surfactants and water-soluble polymers are used together to mobilize crude oil trapped in underground reservoir formations [165]. The surfactants are necessary for reducing interfacial tension and solubilizing trapped oil, while the water-soluble polymers are required to viscosify the water flood that drives the solubilized oil from the porous rock media. Ideally, water-soluble polymers employed as viscosifiers in EOR processes should exhibit increased thickening efficiency in the presence of surfactants and also act cooperatively with surfactants to reduce interfacial tension and to solubilize oil [166].

1.4.2 Polyampholytes as rheology enhancer and fluid-loss control agents for salt tolerant water-based drilling fluids (WBDFs)

Drilling fluids are typically thixotropic shear-thinning fluids, which have low viscosity at high shear rates, but have high viscosity at low shear rates. There are mainly three types of drilling fluids, including synthetic drilling fluids (SDFs), oil-based drilling fluids (OBDFs), and water-based drilling fluids (WBDFs). Water based drilling fluids are widely used, because they are cheaper than the other types of fluids and easy to prepare. Water-based drilling fluids are often a mixture of water, bentonite, rheology thickener, filtration control agent, and weighting materials. Drilling fluids, such as WBDFs play an important role in the oil well drilling operations, including cleaning of the wellbore, carrying and suspending cuttings, cooling and lubricating drilling tools, and maintaining stability of the wellbore and formation [167]. As studies show, the viscosity increases slowly when the content of polyanionic cellulose is less than 1.5%, and viscosity increases rapidly when the content of polyanionic cellulose is more than 1.5% [168]. Salt hydrated lime, gypsum (hydrated calcium sulfate) and synthetic polymers are often used to stimulate flocculation and to remove colloiddally sized drilled solids. Guar gum and some acrylic polymers are also very effective common flocculants when used at low concentrations in clear water drilling fluids. Lime and gypsum are also used to increase the permeability of water-based sediments by flocculating bentonite and drilled solids [169].

Because of the fact that the filtrate volume of the drilling fluids decreases linearly with the increase in the amount of polyanionic cellulose (PAC) and carboxymethyl cellulose (CMC), these substances were successfully used in the oil industry for the preparation of drilling fluids due to its thickening, flocculation and rheological properties [170]. In drilling fluids calcium salts are present in large amounts because of the calcium chloride is used as an additive, which leads to excessive fluid loss, increased fluid viscosity and reduced circulation. It can also lead to the accidents as a result of the expansion of the wellbore and its instability. Currently, water-based drilling fluids are prepared using saturated or unsaturated mineralized water to reduce the dissolution of salts and anhydrite formations [170,171]. In this regard, the application of polyanionic cellulose for water based drilling fluids is limited due to the low resistance to harsh environmental conditions [172].

Bentonite, which is an absorbent clay consisting mostly of montmorillonite, has been used to modify performance properties of conventional WBM systems. Due to its inherent, good rheological properties and ability to contribute to the formation of a thin and low-permeability filter cake, bentonite is used widely for drilling oil and gas wells Nevertheless, bentonite in WBM formulations by itself exhibits insufficient rheological properties, not enough to transmit shear and suspend cuttings satisfactorily during drilling operations [172]. However, the unfeasible application of bentonite becomes realistic in high-temperature environments. Montmorillonite clay chemically breaks down when the vicinity temperature begins to exceed 120 °C (250 °F) [173]. The degradation causes a reduction in shear-thinning behavior and capacity

to carry drilled cuttings and increases the filtration-loss behavior of the drilling mud, consequently rendering the drilling mud ineffective at elevated temperatures [174].

Rheology and fluid-loss properties are very important aspects of drilling muds. Rheology refers to the deformation and flow behavior of all forms of matter. It is an important drilling mud property for removal of the drill cuttings and influences drilling progress in many other ways. Unsatisfactory mud rheology can lead to serious problems such as bridging the hole, filling the bottom of the hole with drill cuttings, reduced penetration rate, borehole enlargement, stuck pipe, loss of circulation, and even a blowout [175]. Meanwhile, fluid loss refers to the volume of the filtrate lost to the permeable material due to the process of filtration. Fluid-loss prevention is a crucial performance attribute of drilling muds. Excessive fluid loss leads to several challenges from formation damage due to the invasion of the mud filtrate to formation and instability of the borehole due to an irreversible change in the drilling fluid properties, for example, density and rheology [176,177].

Several studies have been conducted to improve the rheology [176-179] and filtration-loss properties [180-185] of drilling fluids. Drilling mud additives (nonpolymeric and polymeric additives) have been successfully applied in combination with bentonite to enhance mud performance under harsh drilling conditions. These additives have the potential to better the performance of drilling muds to meet the functional requirements such as appropriate mud rheology, density, mud activity, and fluid loss [175,181]. Naturally occurring polymers (for example, cellulose, starch, xanthan gum, and guar gum) and modified natural polymers (for example, polyanionic cellulose (PAC), carboxymethyl cellulose (CMC), nanocellulose, and nanostarch) have been used extensively with bentonite to achieve desirable drilling mud properties. The extensive use of these additives is attractive due to their environmental friendliness, availability, and low cost [180,181]. However, natural polymers and their modified forms are susceptible to microbial degradation and low stability at temperatures above 115 °C [181].

At elevated temperatures, these additives degrade, reducing the active components, and consequently, the drilling muds are likely to exhibit undesirable properties. The loss of rheological properties and fluid loss control of the drilling mud may cause serious operational problems such as barite sag and fluid invasion, thereby increasing drilling costs significantly [184].

To overcome the aforementioned technical challenges, the application of synthetic additives, in particular, synthetic polymers, has attracted attention. Academics and drilling practitioners have been attentively focusing on synthetic polymers as a promising rheology enhancer and fluid-loss reducer of drilling muds [168,169,175]. Synthetic polymers are more thermally stable than natural polymers and their modified forms; they are suitable to use in formulating smart drilling fluids at elevated temperatures [181].

Jain et al. studied the effect of synthesized graft copolymers on inhibitive water-based drilling fluid systems [182]. In their study, they compared the performance of the graft copolymer with that of CMC, which is the modified cellulose. It was found that the synthesized graft copolymer had the favorable rheological and filtration properties required for optimal performance in the oil-gas

well drilling industry. The synthesized polymer exhibited better thermostability than CMC. They predicted that the synthesized graft polymer can be used for the drilling of water-sensitive shale formations. Quan et al. synthesized a ternary copolymer and studied it as a fluid-loss additive for drilling fluids with high salt and calcium contents [183]. The synthetic polymer demonstrated high thermal resistance and salt tolerance, and it was effective in controlling fluid loss at high temperatures. Moreover, Chu and Lin studied a series of synthetic polymers as drilling fluid additives for controlling rheological and filtration properties [184]. In their study, they investigated the effect of molecular flexibility on the rheological and filtration properties of synthetic polymers in WBMs. The studied polymers demonstrated better thermal stabilities, and the rigidity of the polymer molecule was found to increase the thermostability [185].

1.4.3 Application of polymers as tracer agents for monitoring of oil reservoirs

Many inter-well tracers have been widely used to monitor the displacement into reservoirs and to obtain information on the interaction between producer and injector. These include chemical tracers [186], nuclear tracers [187] and isotope tracers [188]. However, some chemical tracers are easily absorbed onto the surface of rocks in the stratum, and the instruments required to detect radioactive isotopes are extremely expensive.

The fluorescent method was simple and convenient with high precision and accuracy. The detection ranges for fluorescein and calcein were 0-0.35 and 0-0.89 mg/L, respectively, with a measurement error within 2.5 %. Yan et al. (2012) synthesized a fluorescent tracer copolymer (AM-AMCO) by emulsion polymerization of acrylamide and coumarin in the presence of $(\text{NH}_4)_2\text{S}_2\text{O}_8\text{-NaHSO}_3$ as a redox initiator. Characterization of the copolymer (AM-AMCO) indicated that fluorescent polyacrylamide can be used as an oilfield tracer and has good heat and salt resistance [188].

Coumarin, a benzopyrone, which has a large Stokes shift, high fluorescence quantum yield, and excellent light stability, is an attractive choice as a fluorescent candidate. Its derivatives have been widely used as fluorescent probes, fluorescent indicator, and as fluorescent dye [189]. Field test results in Shengli, Dagang and Jidong Oilfields in China showed that polymer microsphere was a promising conformance control agent in the development of heterogeneous reservoirs, especially the fractured reservoirs [190]. [191] Hua and Lin et al. investigated the shape, size, rheological properties, plugging properties, profile control mechanism and oil displacement mechanism of the nanoscale

It was found that polymer microspheres could reduce water permeability because the microspheres adsorbed, accumulated and bridged in the pore throat, and the adsorbed layers would be collapsed under the pressure, entering deep into the reservoir due to the good deformation properties of the microspheres. [190] Yao and Wang et al. researched the effects of ionic strength on the transport and retention of polyacrylamide microspheres in porous media. Yang and Kang et al. researched the mechanism and influencing factors on the initial particle size and swelling capability

of polymer microspheres from the synthesis and reservoir condition. [191] Yang and Xie et al. optimized the injection parameters of polymer microspheres and polymer composite flooding system, and they found that the composite system could better improve polymer flooding at the displacement rate of 3.5 m.d⁻¹ and the injection volume of 530 mg.L⁻¹ PV [192].

During the application of polymer microspheres, polymer solution was injected into the reservoir along with polymer microspheres. [192] Due to the same amide functional groups in polymer microspheres and polymer solutions, the conventional concentration method of polymer microspheres such as starch–cadmium iodide method, chemiluminescent nitrogen method, ammonia electrode method and organic carbon content method were not accurate. Therefore, it is difficult to research the plugging behavior and conformance control mechanism from a quantitative perspective.

For these reasons, fluorescent polymer microspheres could overcome the limits of conventional methods and achieve the real-time detection of polymer microspheres concentration and the distribution of polymer microspheres in the reservoir during the flooding process. Fluorescent polymer microspheres have a dual function, one is the conformance agent and the other is the oil field tracer. The oil field tracer will be a new application of fluorescent polymer microspheres in the development of oilfields [193].

Under most circumstances, fluorescent polymer microspheres are physically dyed through absorption or embedment, which results to the problem of dye leakage and limits the field applications of these fluorescent polymer microspheres. To avoid dye leakage, dyes could be covalently incorporated into polymer microsphere by the inverse suspension polymerization. Rhodamine B (RhB), which has been widely used in medicine, environmental protection, textiles, colored glass, and cosmetics etc., is a commonly used commercial fluorescent dye. Herein, we report one kind of fluorescent polymer microspheres P (AM-BA-RhB) acted as a novel conformance control agent [194].

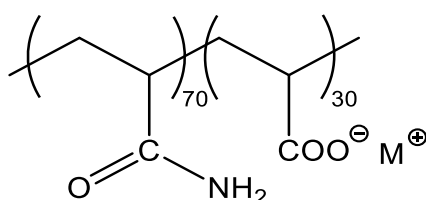
CHAPTER 2. EXPERIMENTAL PART

2.1 Materials

2.1.1 Chemicals

The monomers including: acrylamide (AAm, 97% purity), 2-acrylamido-2-methylpropanesulfonic acid sodium salt (AMPS, 50 wt.%), (3-acrylamidopropyl) trimethylammonium chloride (APTAC, 75 wt.% in water), acrylamide nile blue (ANB, dark blue crystals, purity 99%) and ammonium persulfate (APS, 98% purity) $(\text{NH}_4)_2\text{S}_2\text{O}_8$, N, N, N', N'- tetramethylethylenediamine were purchased from Sigma-Aldrich (USA).

Commercially available HPAM (Flopaam 3630S, 98% purity, SNF) with a hydrolysis degree of 30% and an average molecular weight of $17.2 \cdot 10^6$ Dalton was used for the core flooding. The hydrolysis degree of HPAM 30% means that the sample contains 70 mol.% of AAm and 30 mol.% of sodium acrylate (SA) in the macromolecular chain (Figure 2.1).



where M^+ is Na^+ or K^+

Figure 2.1 - Repeating monomeric units and composition (mol.%) of HPAM

Polyanionic cellulose (PAC-LV, 95% purity) was obtained from “Shandong Look Chemical co., Ltd” (Shandong province, China). The structure formula of PAC is showed in Figure 2.2.

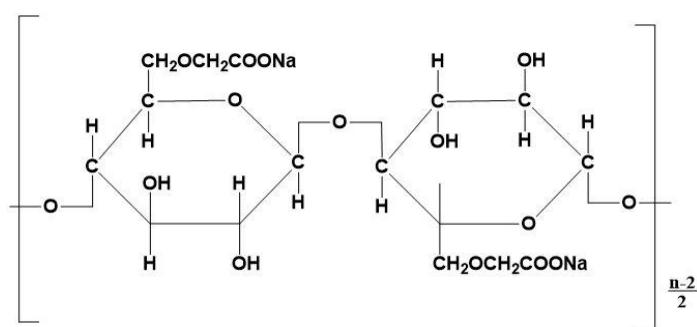
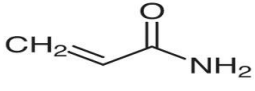
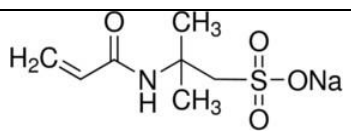
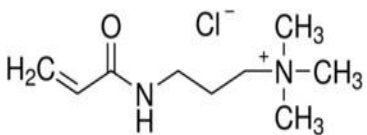
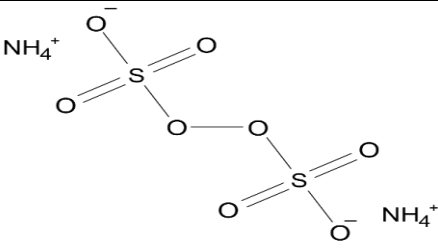
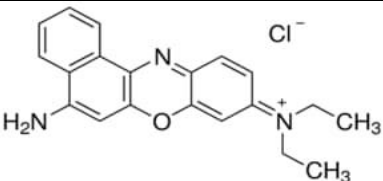
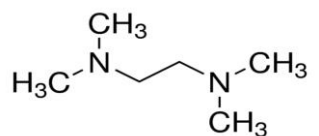


Figure 2.2 - Repeating monomeric units of polyanionic cellulose.

Salts – magnesium chloride (MgCl_2), sodium chloride (NaCl), calcium chloride (CaCl_2) with purity 99%” were purchased from “Titan Biotech LTd”. Organic solvents – ethanol and acetone were obtained from “Format” company and used without further purification. Nitrogen (purity 99.995 wt. %) was obtained from

“Ikhsan TechnoGas” Ltd. (Almaty, Kazakhstan). Table 2.1 lists some other chemicals used in this study.

Table 2.1- Chemical structure of the chemicals used in this research

Name, Abbreviation	Chemical structure
Acrylamide (Aam, 97% purity) Mr = 71.08 g/mol, “Sigma-Aldrich”, was used without further purification.	
2-Acrylamido-2-methyl propane sulfonic acid sodium salt (AMPS, 50 wt. % in water), Mr = 229.23 g/mol from “Sigma- Aldrich”, was used without further purification.	
3-acrylamidopropyl) trimethyl-ammonium chloride (APTAC, 75 wt.% in water), Mr = 206.71 g/mol, “Sigma-Aldrich”, was used without further purification.	
Ammonium persulfate (APS), Mr = 228.2 g/mol, made by Changzhou Qi Di Chemical Co. (China), was used without further purification.	
Acrylamide Nile Blue, Mr = 407.89 g/mol, “Reachim”, was used without further purification.	
N, N, N', N' Tetramethylethylenediamine TMEDA. Mr = 116.20 g/mol, “Sigma-Aldrich, Purity ≥99.5%” was used without further purification	

2.1.2 Sand pack models and core samples

Sand packs were made by packing 250-500 μm sand grains into 8.6 cm-length and 4.3-cm-diameter steel cylinder and PET plastic pipe with sized 5 cm-length and 3 cm-diameter, respectively (Fig.2.3 a and b). Regular quartz river sand was used in this study.

The core flooding experiments were carried out with 2.9-cm-diameter and 4.4-cm-length artificial high porosity core (Fig. c). 0.25 or 0.5% polymer solutions were injected into the sand/core at the rate of 0.15-1 cm³·min⁻¹.

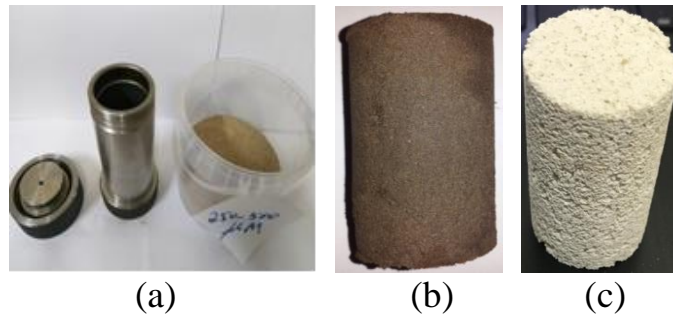


Figure 2.3 - Sand pack (a, b) and artificial high porous core samples (c)

Table 2.2 - presents the petro-physical properties of the porosity and permeability calculations of used sand packs and core samples

Sand packs /Core samples	Size, (cm)	Permeability, K (Darcy)	Pore Volume, (cm ³)	Porosity, ϕ (%)	Salinity, g·L ⁻¹	Injection, T (°C)
1. Sand pack	4.3x8.6	16	50	55	101	20-25
2. Carbonate core	2.9x4.4	5	24.12	83	163	60
3. Sand pack	3x5	1.8	10.95	31	200	30
4. Sand pack	3x5	0.62	10.6	30	200	30
5. Sand pack	3x5	1.77	11.9	33.7	200	30

2.1.3 Brine

The model was saturated with 101 g·L⁻¹ or 163 g·L⁻¹ East Moldabek (well#2092 M-II) brines and East Moldabek oil (well# 2027 M-III-U-I), respectively. the salinity and chemical composition of the different brines that were used in the present work are listed in table 2.3.

Table 2.3 - Chemical composition of synthetic brines

Salinity (g·L ⁻¹)	Concentration of salts (g·L ⁻¹)		
	NaCl	CaCl ₂	MgCl ₂
200	180	10	10
232	208.8	11.6	11.6
250	225	12.5	12.5
300	270	15	15

The water-based drilling fluids (WBDF) were prepared by using the following concentrations of NaCl in brine 1, 7, 15, 25 and 35 wt. %.

2.1.4 Crude oil

Different types of crude oils were used in this study, with the lower temperatures representing the conditions of the oil wells themselves:

East Moldabek (oil well #2027) with density and viscosity at 25 °C equal to 0.89 g/cm³ and 138.8 cp, respectively.

Karazhanbas (oil well #1913) with density and viscosity at 30 °C equal to 0.93 g/cm³ and 420 cp or at 60 °C equal to 0.907 g/cm³ and 64 cp, respectively.

2.1.5 Bentonite clay

BENTO LUX LLC, Tatarstan, Russia, supplied bentonite clay in accordance with the API standard. It is widely used for drilling wells in the oilfields of Kazakhstan. Bentonite was used without further purification to study the rheology and fluid loss properties of water-based drilling fluids.

The average particle size of pure bentonite was found to be 5.34 μm, as determined by zeta-potential measurements.

The chemical composition of the bentonite sample was determined by using X-ray fluorescence spectrometer (XRF) with the RFA analyzer Epsilon (Netherlands), 2015 (see Fig. 2.4). The composition of the bentonite clay, given in weight percent (wt.%) is listed in table 2.4.

Table 2.4 - Chemical compositions of pure bentonite clay (BT)

Metal oxides	SiO ₂	Fe ₂ O ₃	Al ₂ O ₃	K ₂ O	CaO	MgO	TiO ₂	P ₃ O ₄	FeO	MnO ₂
wt. %	25.5	7.92	6.8	3.28	1.57	0.92	0.71	0.46	0.19	0.052
Metal oxides	ZrO ₂	SrO	Rb ₂ O	Cr ₂ O ₃	ZnO	V ₂ O ₅	Ni ₂ O ₃	CuO	Y ₂ O ₃	Ga ₂ O ₃
wt.%	0.032	0.025	0.022	0.016	0.015	0.018	0.007	0.005	0.005	0.004

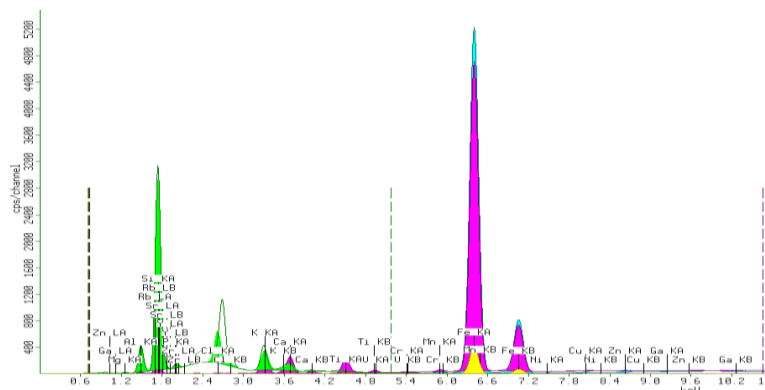


Figure 2.4 - X-ray fluorescence (XRF) spectroscopy of the bentonite clay

2.2 Research methods

2.2.1 FTIR spectroscopy

A sample of the AAm-co-AMPS-co-APTAC copolymers was ground into a powdered state using an agate mortar. Then, a 2 mg sample of the powder was measured out and transferred to a Cary 660 FTIR IR spectrophotometer (Agilent Technologies, USA) using a single-bounce diamond attenuated total reflectance (ATR) accessory equipped with a liquid nitrogen-cooled mercury-cadmium-telluride detector, and the spectrum of the sample was recorded. As the samples of linear

polymers already had a powder-like texture, they were studied without preliminary sample preparation on the FTIR IR spectrophotometer, and the spectra of the samples were recorded.

2.2.2 ^1H and ^{13}C -NMR spectroscopy

^1H and ^{13}C -NMR spectra of the copolymers dissolved in D_2O (10 mg/mL) were recorded at room temperature on a Bruker 400 MHz Fourier NMR spectrometer using tetramethylsilane as an internal standard. The peaks between $\delta = 1.8\text{-}2.0$ ppm are assigned to methyl groups of amide, while the peaks between 3.4 and 3.6 ppm characterize the methyl groups of the AMPS. The ionic segment content of the copolymers was determined from the area ratio of meta-protons to methyl proton peaks in ^1H and ^{13}C -NMR spectra of AMPS-*co*-APTAC linear polymers in D_2O .

2.2.3 UV-Vis and fluorescence spectroscopy

Absorption and fluorescence spectra of amphoteric terpolymer AMPS-*co*-APTAC-*co*-ANB in aqueous solution were registered on UV-Vis spectrophotometer (Specord 210 plus BU, Germany), F97 Pro spectrophotometer (China).

2.2.4 Dynamic light scattering (DLS) and zeta-potential measurements

The dynamic light scattering (DLS) and zeta-potential measurements were completed using a Zetasizer NanoZS 90 (Malvern, UK), equipped with a 633nm laser source.

2.2.5 Gel-permeable chromatography (GPC)

The average molecular weights (M_w and M_n) of aqueous solutions of AAm-*co*-AMPS-*co*-APTAC were measured by gel permeation chromatography (GPC) using a Viscotek (Malvern) chromatograph equipped with 270 dual detectors (Malvern) and VE 3580 RI detector (Malvern). Two 6000M columns (Malvern) were used, and the flow rate of DMF in mobile phase was 0.7 mL/min. Polystyrene standard samples (PolyCALTM, Malvern) were used to plot the calibration curve. The injection volume of the sample was equal to 100 μL .

2.2.6 Differential scanning calorimetry (DSC) and thermogravimetric analysis (TGA)

10 mg of AAm-*co*-AMPS-*co*-APTAC copolymer powder was placed in a cuvette for thermogravimetric analyses (TGA) tested using LabSys Evo equipment (Setaram, France), at a temperature range of 30 to 500 $^\circ\text{C}$ and heating rate of 10 $^\circ\text{C}/\text{min}$.

2.2.7 Scanning electron microscopy (SEM) and transmission electron microscopy (TEM)

The SEM images were obtained on a Crossbeam 540 (Germany) by placing dry polymer powder coated with gold nanoparticles on carbon tape. The TEM images were made on a JEOL JEM 1400 Plus (USA) by placing one drop of 0.01 wt.% polymer solution in D₂O on a copper cell (d=2mm) and drying the sample overnight in a refrigerator.

2.2.8 Chemical analysis

The elemental composition of bentonite clay sample was determined by X-ray fluorescence spectroscopy (XRF) by using RFA analyzer Epsilon (Netherlands), 2015.

2.2.9 Elemental analysis

The elemental analysis of ATP and HPAM samples were performed using Vario EL-III elemental analyzer (Elementary Analyze System GmbH, Hanau, Germany).

2.2.10 Rheological study

The viscosities of polymer solutions were measured using glass capillary Abbehole viscometer with diameter 1.47-mm (BIIЖ 4d) or AMETEK Brookfield viscometer (Spindle-0) at a stable shear rate of 7.32 s⁻¹. The oil density and viscosity were determined by Stabinger viscometer. The temperature in the rheological tests varied from room temperature to 60 °C. However, an Anton Paar Rheolab QC viscometer was used to measure the viscosity of the effluent samples for the HPAM experiment on the 8.6-cm-length sand pack.

The apparent viscosity and shear stability of 4 wt.% bentonite with 2 wt.% polymer BT/TPA and BT/PAC-LV dispersions in 1-35 wt.% NaCl brine at 25±1 °C were determined using an Anton Paar Rheolab QC rotational rheometer (Austria). The measurements were conducted with a temperature control device (C-LTD80/QC) and a cylindrical measuring system (CC39/QC-LTD). Shear stress (τ) and viscosity (η) were determined over a wide range of shear rates ($\dot{\gamma}$ = 1-1000 s⁻¹) at 25 °C. The rheological properties of the bentonite and bentonite/polymer formulations were analyzed using the Herschel-Bulkley model [198, 199].

$$\tau = \tau_0 + K (\dot{\gamma})^n \quad (2.1)$$

Where K (Pa·sⁿ), n and τ_0 (Pa) are consistency coefficient, flow behavior index and yield stress, respectively [200].

Gel strength (GS) was measured by using API standard procedure at a low shear rate of 5.1 s⁻¹ [198]. Prior to the measuring of the 10 s GS, the samples were

pre sheared for 1 min at 510 s^{-1} and left undisturbed for 10 s. Then the sample was again left undisturbed for 10 min before measuring 10 min GS.

2.2.11 Permeability and porosity measurements of sand pack and core samples

The permeability of sand pack and core samples before flooding was calculated using Darcy's law for single phase expressed in equation (2.2):

$$u = -\frac{k\Delta P}{\mu} \quad (2.2)$$

Where:

v - Flux of fluid (mL/s.cm^2);

k - Permeability (Darcy);

ΔP - Pressure gradient across the core (atm/cm);

μ - Fluid viscosity (mPa.s);

The porosity of the models was determined by using the following formula (see equation (2.3)) :

$$\varphi = \frac{V_{in} - V_d}{V_t} \cdot 100\% \quad (2.3)$$

Where:

φ -porosity, %.

V_{in} -injected volume, cm^3 .

V_d -dead volume, cm^3 .

V_t -total volume of the sand pack, cm^3 .

2.2.12 Core/sand pack flooding experiments

The sand pack and core flooding experiments were carried out with the help of a special core flooding setup called "UIC-C (2)" from Russia (as seen in Fig 2.5).



(a)

(b)

Figure 2.5 - Special sand pack (a) and core (b) flooding system

Sand pack flooding was conducted with the help of a special core flooding set up “UIC-C (2)” in the following sequence (see Fig.2.6):

- 1) Vacuuming of the sand pack;
- 2) Saturation with brine;
- 3) Porosity and permeability measurements;
- 4) Brine displacement with oil till irreducible water saturation was reached;
- 5) Water flooding simulation using 1 pore volume of brine injection;
- 6) Polymer flooding simulation using 1-3 pore volumes of 0.25-0.5 wt. % polymer solution injection.

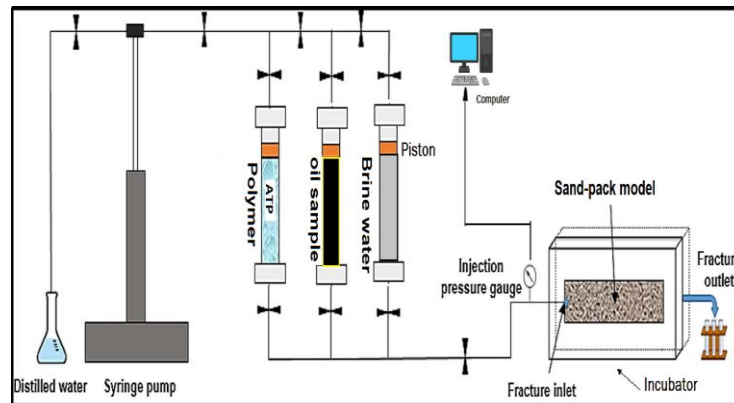


Figure 2.6. Experimental setup “UIC-C (2)” used in the sand-pack flooding

The confining pressure was set at 2 MPa, ambient temperature was equal to 30 °C, and the fluids were injected at $0.15 \text{ cm}^3 \cdot \text{min}^{-1}$. The outlet section of the model was open to atmosphere. The fluids were injected using high-pressure piston pumps, the temperature was supported by wrapping a heating tape around the model, and PC connected pressure transducers were used to register the inlet pressure values during the tests.

2.2.13 Preparation of bentonite/water and bentonite/polymer dispersion

As a first step, 2 wt.% polymer solutions were prepared in 1-35 wt. % NaCl brines using a magnetic stirrer. The solutions were stirred for 24 hours at 1000 rpm and then aged under static conditions for an additional 24 hours to allow for complete hydration of the polymers. The second step, bentonite/polymer dispersions were prepared by slowly adding 4 wt.% of bentonite powder to the polymer solutions were being stirred. Each bentonite/polymer dispersion was poured in a covered container and left for 24 h for the complete swelling of the bentonite clay at room temperature. As a result, several bentonite/ternary polyampholyte (BT/TPA-I) and bentonite/low viscosity polyanionic cellulose (BT/PAC-LV) dispersions were prepared using brines with a wide range of NaCl concentrations. Moreover, bentonite dispersions (without polymer) were prepared in deionized water and 35 wt.% NaCl brine in order to compare their rheological and fluid-loss properties with those of bentonite/polymer dispersions. In order to keep bentonite particles uniformly suspended in the drilling fluid before starting rheological experiments the samples were agitated for 1 h.

The measured pH of the bentonite/polymer dispersions was found to be 5.6 ± 0.04 . that is unfavorable especially for stabilization of the bentonite/PAC-LV system. This is attributed to the negative charges of both bentonite particles (-16 mV, as per zeta-potential measurement) and PAC-LV, which is categorized as an anionic polyelectrolyte. However, in case of bentonite/TPA system due to the presence of 10 mol.% of positively charged monomer APTAC the bentonite-TPA mixture might have bigger stability. This positively charged APTAC component can contribute to the stabilization of the bentonite particles. In our case the pH value was measured only for the TPA/Bentonite + 35wt.% drilling fluid. Before conducting rheological measurements, the sample was stirred in the viscometer for 1 minute at a shear rate of 5.1 s^{-1} followed by a resting period of two minutes.

2.2.14 Fluid loss tests

Fluid loss tests were performed according to the API standard procedure for the evaluation of water-based drilling fluids. The fluid loss volume of the BT/polymer dispersions was measured using a VM-6-type medium-pressure filtration apparatus through a filter paper (Fann, U.S.A.) with a pore size of 25-30 μm . In a single test, 120 mL of drilling fluid was forced to pass through the filter paper by applying a pressure of 0.7Mpa for 30 minutes .The filtrate volume was recorded after each 5 min. After the filtration, the filter paper was carefully detached from the filter press cup in order to measure the thickness of the available cake on the paper.

2.2.15 Permeability of filter cake, and SEM analysis

For the measurement of permeability of filter cakes and SEM analysis was carried out for the study of filter cake morphology after drying overnight at 100 °C using JEOLJSM-6490 LA (JEOL Ltd, Japan). The permeability of the filter cake was calculated from Darcy's law [198]:

$$dV_f/dt = k \cdot A \cdot \Delta P / \mu h_c \quad (2.4)$$

Where:

- filtrate volume (V_f) in cubic centimeters;
- filtration time (t) in seconds;
- pressure drop across the filter cake (ΔP) in kPa;
- area of the filter cake medium (A) in cm^2 ;
- viscosity of the filtrate (μ) in Pa·s;
- thickness of the filter cake (h_c) in cm;

Moreover, permeability of the filter cake (k) typically expressed in microdarcsies (μD). When measuring the permeability of the filter cake, it is assumed that three parameters remain constant: the pressure drop across the filter cake (690 kPa), the area of the filter medium (22.3 cm^2), and the viscosity of the filtrate ($8.90 \times 10^{-4} \text{ Pa}\cdot\text{s}$).

CHAPTER 3. RESULTS AND DISCUSSION

3.1 Synthesis of acrylamide-based ternary polyampholytes (AAm-*co*-AMPS-*co*-APTAC) derived from acrylamide (AAm), 2-acrylamido-2-methyl propane sulfonic acid sodium salt (AMPS) and 3-acrylamidopropyl trimethylammonium chloride (APTAC)

Linear polymers were prepared using solution polymerization of AAm, AMPS and APTAC in the presence of APS as an initiator at 60°C. Initial monomer concentration were fixed at different compositions of [AAm]:[AMPS]:[APTAC] = 50:25:25; 60:20:20; 70:15:15; 80:10:10 and 90:5:5 mol.% were synthesized by free-radical polymerization, with respect to the solution mass (Table 3.1, Figure 3.1).

Table 3.1 - Synthetic protocol of various molar ratios of AAm-*co*-AMPS-*co*-APTAC terpolymers (total 10 g)

Initial feed composition, mol. %			AAm, g	AMPS, g	APTAC, g	APS, mg	H ₂ O, mL
AAm	AMPS	APTAC					
50	25	25	1.94	5.5	3.31	11	3.04
60	20	20	1.66	2.2	2.64	11	2.98
70	15	15	1.94	3.3	1.99	11	2.934
80	10	10	2.75	2.22	1.33	11	3.2
90	5	5	3.07	1.11	0.653	11	3.45

To prepare polyampholyte terpolymers with different composition of AAm (g), AMPS (g), APTAC (g) and were mixed at 0-20 °C and stirred for 30 minutes to form a homogeneous solution. After adding APS (11 mg) and stirring for 1-2 minutes, nitrogen was bubbled for 30 minutes to eliminate oxygen from the reaction mixture. The solution was then transferred into cylindrical vessels with a volume of approximately 10 mL and placed in a thermostatically controlled environment at 60 °C. The reaction mixtures were kept at this temperature for 4 hours. The synthesized polymer samples were used without further purification.

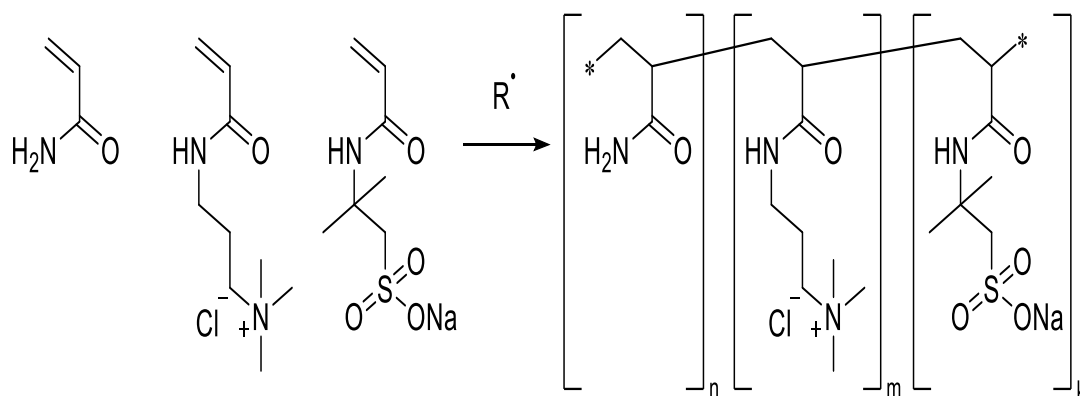


Figure 3.1 - Synthesis of AAm-*co*-AMPS-*co*-APTAC

The results of ^1H NMR spectra of AAm-*co*-AMPS-*co*-APTAC registered in D_2O along with initial and final molar compositions of monomers are shown in Fig 3.2. The molar composition of AAm-*co*-AMPS-*co*-APTAC terpolymers was estimated from the integral peaks of methyl groups that belong to AMPS and APTAC monomer units. It is seen that experimentally found molar compositions of terpolymers deviate from the theoretically prescribed by 1-2 mol.% that are within the experimental error.

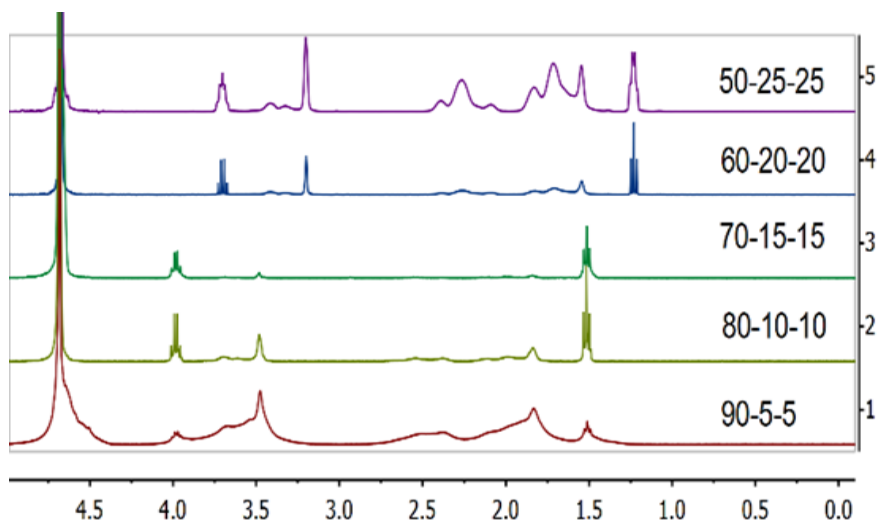


Figure 3.2 - ^1H NMR spectra of [AAM]:[AMPS]:[APTAC] = 90:5:5(1), 80:10:10(2), 70:15:15(3), 60:20:20(4) and 50:25:25 (5), in D_2O

The molar composition of AAm-*co*-AMPS-*co*-APTAC copolymers was estimated from the integral peaks of methyl groups that belong to each monomer as shown in Table 3.2.

Table 3.2 - Theoretical and experimentally found molar composition of AAm-*co*-AMPS-*co*-APTAC terpolymers

#. samples	Molar composition of AAm- <i>co</i> -AMPS- <i>co</i> -APTAC , mol.%	
	Theoretical prescribed	Experimentally found from ^1H NMR spectra
1	90:5:5	92:3:5
2	80:10:10	81:9:10
3	70:15:15	70:14:16
4	60:20:20	60:20:20
5	50:25:25	50:24:26

3.1.1 Synthesis and characterization of AAm-*co*-AMPS-*co*-APTAC (80:10:10 mol. %)

The ternary polyampholyte (TPA) AAm-*co*-AMPS-*co*-APTAC (80:10:10 mol. %) was synthesized via-conventional free radical (co)polymerization of monomers according to synthetic protocol given in Table 3.3.

Initially, the dry acrylamide (AAm) monomer was dissolved in deionized water while being stirred in a beaker at relevant temperature. Then, the liquid monomers, AMPS and APTAC, were added in equimolar concentrations to the aqueous solution of AAm, total concentration of the monomers in water was kept constant (50 wt.%), however the amount of water was changed between 50 and 30 wt.%. The monomer mixture was purged with nitrogen over 1 h continually to remove the dissolved oxygen. Afterward, the mixture of 0.005-0.01 mol.% APS as initiator and 0.008-0.03 mol.% tetramethylethylene diamine (TMEDA) as catalyst was added to speed up the radical polymerization. The polymerization process, accompanied by increasing of solution viscosity, occurred over 2 hrs.

Table 3.3 - Synthetic protocol ternary polyampholyte AAm-co-AMPS-co-APTAC (80:10:10 mol. %) in deionized water

Initial feed composition, mol. %	#.Samples Monomers	I	II	III	IV	V	VI	VII
		80	AAm (g)					
10	AMPS (g)							4.84
10	APTAC (g)							2.91
[Initiator]:[Catalyst] ([APS]/[TMEDA]), mol/mol		6:1	8:1	6:1	4:3	12:1	18:1	12:1
H ₂ O, (wt.%)		50	40	30	50	50	50	50
Yield mass (g)		15.8	20.9	14.7	14.3	-	18.2	18.3
Temperature (°C)		0±1	0±1	0±1	24±1	24±1	0±1	24±1
Apparent viscosity (mPa·s)		27.3	11.4	5.2	9.7	-	14.5	7.1

In order to select appropriate samples with optimal viscosity, apparent viscosity measurements were conducted using an AMETEK Brookfield viscometer at a shear rate of 7.32 s⁻¹ and room temperature. As a result, the 0.5 wt.% TPA-I in 23.2 wt.% NaCl brine was selected to make water-based drilling fluids due to its highest apparent viscosity among all the samples presented in Table 3.3.

An FTIR spectrum of the amphoteric terpolymer is shown in Fig.3.3. The wide absorption band in the region of 3200-3500 cm⁻¹ corresponds to the NH₂ groups of AAm, and the absorption bands in the region of 2800-3000 cm⁻¹ correspond to the asymmetric and symmetric vibrations of the CH groups. The absorption bands at 1660 and 1546 cm⁻¹ belong to the vibrations of the N-substituted groups, Amide I and Amide II, respectively. The absorption band at 1450 cm⁻¹ is characteristic of the deformation vibrations of the CH groups. Finally, the absorption band in the region of 1190 cm⁻¹ is related to the symmetrical S=O stretching vibration of AMPS.

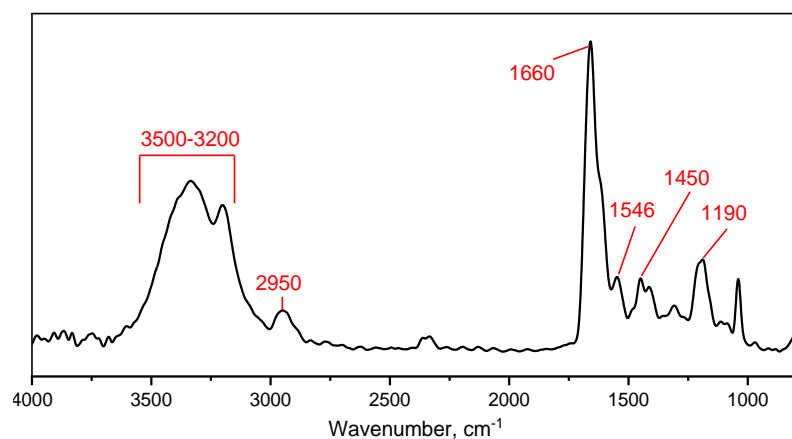


Figure 3.3 - FTIR spectrum of AAm-*co*-AMPS-*co*-APTAC= 80:10:10 mol. %

The structure of AAm-*co*-AMPS-*co*-APTAC terpolymer was established using ^1H NMR spectroscopy (Figure 3.4). The broad resonance peaks at 1.6-1.8 and 2.3 ppm were attributed to the protons of the methylene and methine groups of the main polymer chain, respectively. However, these peaks overlap with those of the methyl and methylene protons of AMPS and APTAC. The peaks at 3.1-3.3 ppm were assigned to the suspended protons of the methyl and methylene groups of AMPS and APTAC. Two methylene groups of AMPS are responsible for the appearance of the peak at 1.4 ppm.

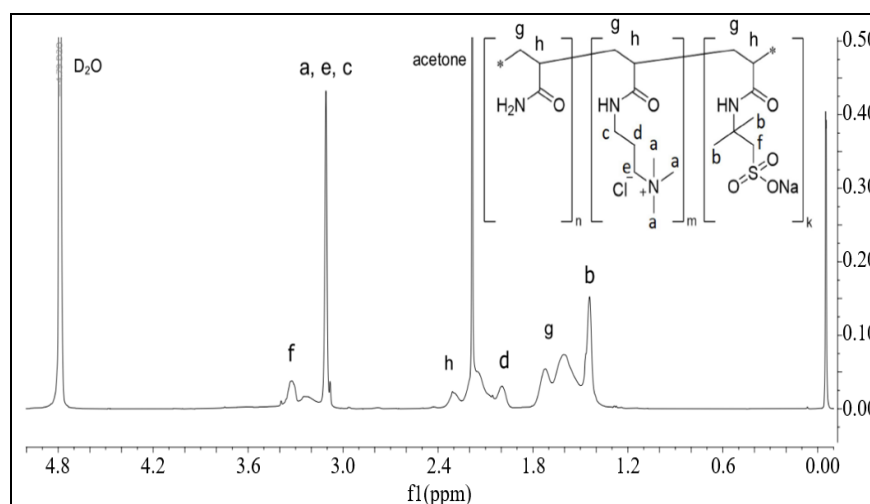


Figure 3.4 - ^1H NMR spectrum of AAm-*co*-AMPS-*co*-APTAC = 80:10:10 mol. %

As seen from ^{13}C -NMR spectra (Figure 3.5.), the peak at 16.78 ppm is related to $-\text{CH}_2$ carbons (a), and the peak at around of 3.72 ppm belongs to $-\text{CH}_3$ and $-\text{CH}-$ carbons (b and c) of APTAC or Na-AMPS backbone, the peak at 52.99 ppm was for $-\text{CH}_2-\text{SO}_3^-$ (d) in Na-AMPS segment, the peaks at 57.43 and 64.74 ppm belong to the $-\text{CN}$ (e) in APTAC segment. The peak at 179.48 ppm is characteristic for $\text{C}=\text{O}$ (g) groups in acrylamide units. Meanwhile, there was no peak at the region of 100–150 ppm, indicating that there was no monomer [195-197]. Thus, the ^1H and

^{13}C -NMR spectra confirm that the ternary polyampholyte AAm-co-AMPS-co-APTAC) was successfully obtained.

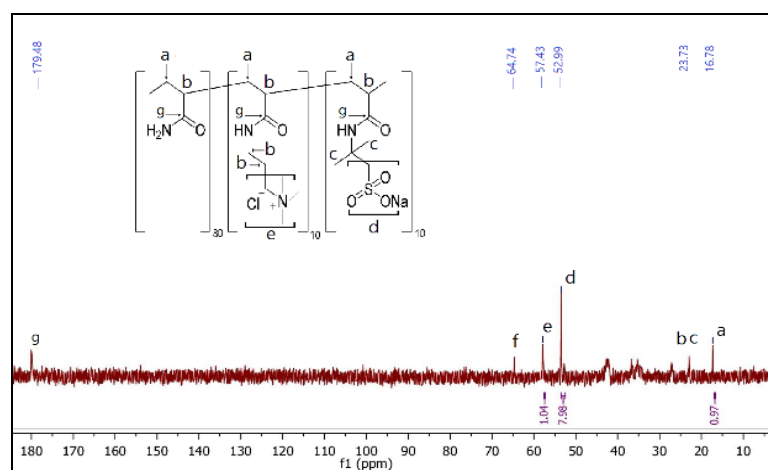


Figure 3.5 - ^{13}C -NMR spectrum of AAm-co-AMPS-co-APTAC = 80:10:10 mol. %

Elemental analysis (C, H, N and S) was conducted to determine the composition of TPA at high temperature, in the presence of oxygen and catalyst. The S and N elements were oxidized to SO_2 and N_2 , respectively. The gases were separated in chromatographic column by the carrier gas. Finally, the different elements were detected in the thermal conductivity cell and analyzed. Based on the principles of mass conservation and the element conservation, the ratios of different monomers in the copolymer were calculated as shown in Figure 3.6. The elemental analysis of the copolymer synthesized at molar ratio of monomers AAm-co-AMPS-co-APTAC= 80:10:10 mol.% indicates that the measured value of the element content in the copolymer was consistent with the theoretical value. This suggests that the resulting product was the intended target product.

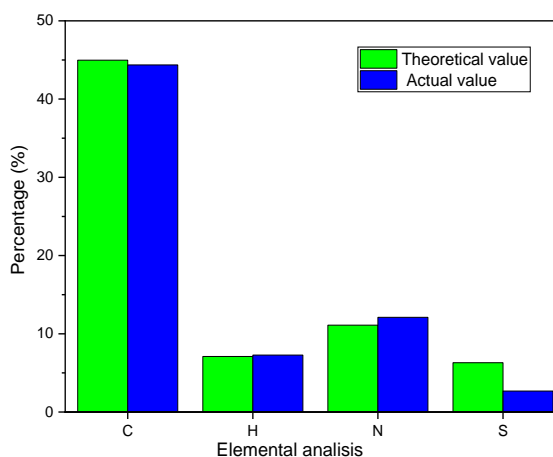


Figure 3.6 - Elemental analysis of the copolymer synthesized at molar ratio of monomers AAm-co-AMPS-co-APTAC= 80:10:10 mol.%

3.1.2 Determination of molecular weights of the AAm-co-AMPS-co-APTAC (80:10:10 mol.%)

Table 3.4 and Figure 3.7 represent the GPC data and molecular weights of AAm-co-AMPS-co-APTAC terpolymer measured in an aqueous solution. The weight-average molecular weight (M_w) and the average-number molecular weight (M_n) of the terpolymer were equal to 2.9×10^6 and 2.1×10^6 Daltons, respectively. The polydispersity index (PDI) of the terpolymer is quite low for conventional free radical polymerization. The relatively high monomer concentration in the reaction mixture is considered to be responsible for the low PDI. The high molecular weight and low PDI of the terpolymers are expected to be suitable for oil recovery.

Table 3.4 - M_w , M_n and PDI of AAm-co-AMPS-co-APTAC terpolymer

Composition, mol. %			$M_w \cdot 10^6$, Dalton	$M_n \cdot 10^6$, Dalton	PDI = M_w/M_n
AAm	AMPS	APTAC			
80	10	10	2.9	2.1	1.36

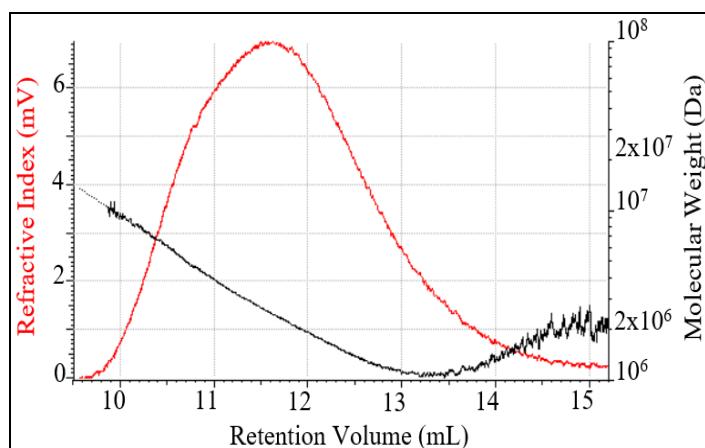


Figure 3.7 - Gel Permeable Chromatogram of AAm-co-AMPS-co-APTAC = 80:10:10 mol.% terpolymer in aqueous solution

3.1.3 TGA and DTA analysis of AAm-co-AMPS-co-APTAC (80:10:10 mol. %)

The Figure 3.8 shows the TGA curve of AAm-co-AMPS-co-APTAC terpolymer (black line), and differential thermogravimetric curve DTG (red line) registered in N_2 atmosphere. The mass loss of the copolymer can be divided into several stages that are shown by dotted lines. The fluctuated stages between 117 and 239 °C, where the mass loss is 12 %, can probably be attributed to evaporation of moisture containing in sample. The second significant mass loss ranging from 239 to 343 °C and the peak occurred at 318 °C with mass loss about 21 %, probably corresponds to the decomposition of the amide group of the copolymer. The third stage between 343 and 487 °C, resulting in weight loss of 31 %, with the peak at 402 °C, may be related to decomposition of sulfonic groups and C-C backbones of polymer chain. The latest stage between 402 and 500 °C can be the result of fully carbonization of polymer chain. It is concluded that the thermal stability of TPA is rather high and suitable for use as temperature resistant polymeric additive in EOR and WBDFs.

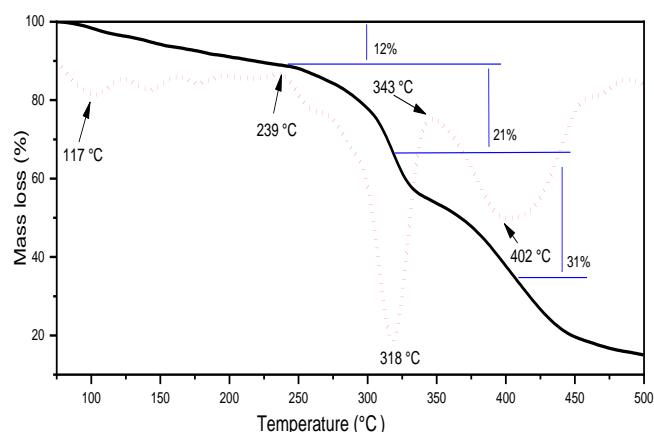


Figure 3.8 - TGA thermogram of AAm-*co*-AMPS-*co*-APTAC=80:10:10 mol.% terpolymer (black line), and its differential curve DTA (red line). Dotted lines indicate the values of T_g and decomposition temperature

3.1.4 DLS measurement of AAm-*co*-AMPS-*co*-APTAC (80:10:10 mol.%) terpolymer in pure water and brine solution

The average hydrodynamic size of AAm-*co*-AMPS-*co*-APTAC terpolymer is shown in Figure 3.10. In pure water, the terpolymer has a broad size distribution with a maximum at 50-60 nm and a small shoulder at 350-400 nm. In brine solutions, a bimodal size distribution is observed, and two well-separated maxima appear at 25-30 nm and 300-340 nm. It is supposed that in pure water the macromolecular chains are mostly in aggregated state. At high salt solutions (200-250 g/L) these aggregates destruct and are fractionated to lower (25-30 nm) and higher (300-340 nm) molecular weight fractions. Increasing of the intensity of both low molecular weight and high molecular weight fractions is probably due to unfolding and increasing of hydrodynamic volume of macromolecules. These data are in good agreement with increasing of the dynamic viscosities of AAm-*co*-AMPS-*co*-APTAC terpolymer measured at 200-250 g.L⁻¹ brine (see Fig.3.9).

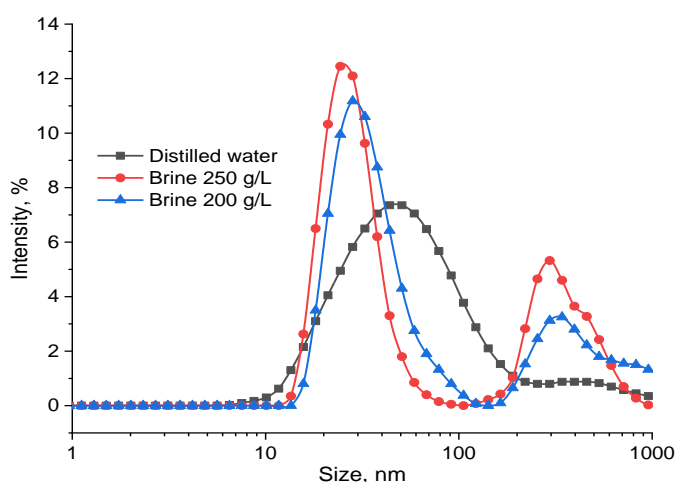


Figure 3.9 - The effect of brine solution on the average hydrodynamic size of AAm-*co*-AMPS-*co*-APTAC (80:10:10 mol. %)

The zeta potential of the terpolymer solutions, dissolved in pure water in a concentration range of 0.25-0.016 %, was negligible negative at -3.4 to -6.8 mV. This negative charge is due to a small excess of AMPSNa in the main polymer chain and is indicative of the different reactivity of the monomers.

3.1.5 SEM and TEM results of AAm-co-AMPS-co-APTAC (80:10:10 mol.%)

Figure 3.10 shows the SEM and TEM images of AAm-co-AMPS-co-APTAC terpolymer in the form of powder and thin film, respectively. The micron-sized SEM image of the terpolymer is specific to the most amorphous polymers, and not very informative. In contrast, the TEM image of the terpolymer exhibits two kinds of spherical nanoparticles, small and large, with average sizes of 25-30 nm and 200-250 nm, respectively. Moreover, the number of small nanoparticles is vastly larger than the quantity of large ones. This result coincides well with the average hydrodynamic size of the terpolymer determined by DLS (see Fig.3.9). As follows from the DLS data, the number of small nanoparticles with an average size of 50-60 nm is far in excess of the quantity of large nanoparticles with an average size of 350-400 nm. A discrepancy is observed between the particle sizes determined by DLS and TEM. The particle sizes registered by TEM represent the compact polymer particles without hydrated shells. Whereas, DLS results show greater sizes of polymer particles due to the swollen state of the macromolecules in aqueous solution and formation of hydrated shells around the polymer chains.

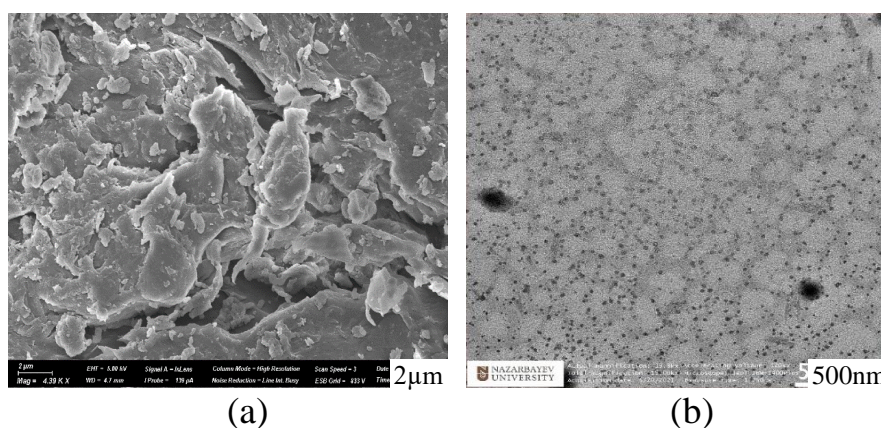


Figure 3.10 - SEM (a) and TEM (b) images of AAm-co-AMPS-co-APTAC (80:10:10 mol.%)

3.1.6 Zeta potential measurements of AAm-co-AMPS-co-APTAC (80:10:10 mol.%) and bentonite clay

Zeta potential study was conducted using 0.1% bentonite and AAm-co-AMPS-co-APTAC terpolymer in deionized water. Figure 3.11 (a) and Figure 3.11 (b) illustrate the zeta potential values of the pure bentonite dispersion and the aqueous solution of TPA, respectively. In the aqueous solution, the average hydrodynamic size and zeta potential of bentonite were determined to be 5.34 μm and $\xi = -16$ mV, respectively. On the other hand, the average hydrodynamic size and zeta potential of

the TPA in the aqueous solution were found to be 5.8 nm and $\xi = -2.57$ mV, respectively. The small negative charge of TPA can be attributed to a small excess of AMPSNa monomer in the polymer chain, indicating different reactivity among the monomers. The slightly negative surface charge ($\xi = -2.57$ mV) of the AAM-co-AMPS-co-APTAC terpolymer is expected to facilitate the adsorption and intercalation of positively charged monomers on the edges of bentonite pellets, making it resistant to salt cations.

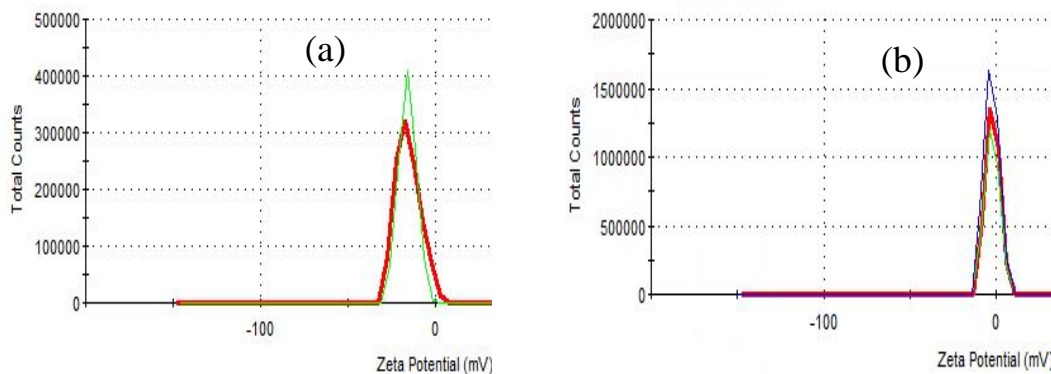


Figure 3.11 - Zeta potential values of pure bentonite dispersion (a) and TPA (b) in aqueous solution

3.2 Rheological study

3.2.1 Viscosity of ternary polyampholytes in aqueous solution

0.5 wt.% of terpolymer solutions were prepared by addition of [AAM]:[AMPS]:[APTAC] - (1) 90:5:5, (2) 80:10:10, (3) 70:15:15, (4) 60:20:20 and (5) 50:25:25 various molar ratios of polyampholyte terpolymers dissolved in a 163.3 g·L⁻¹ and oil field brine for 24 h stirring at 400 rpm in room temperature. The water samples were taken from the oil well # 2092. Polymer solutions for oil displacement experiments were prepared in brine water from the East Moldabek oil field (mineralization 163.3 g·L⁻¹). The viscosity measurements carried out by using Abbeholle viscometer BИЖ 4d – (d=1,47mm) as it can be seen in Figure 3.12.

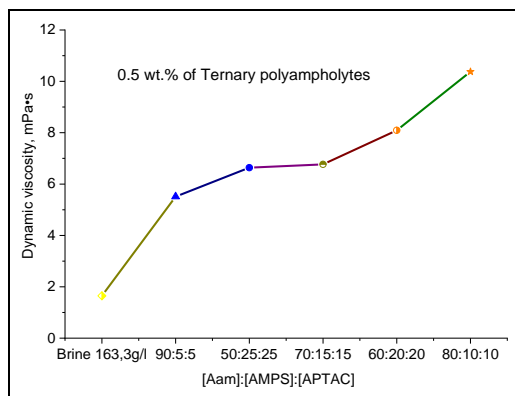


Figure 3.12 - Dynamic viscosity vs polymer type at room temperature

The viscosity measurements identified that their viscosifying ability with respect to reservoir water (salinity is $163 \text{ g}\cdot\text{L}^{-1}$) at 24°C has the highest viscosity than others. It was found that due to polyampholytic nature, the AAm-*co*-AMPS-*co*-APTAC terpolymers exhibited improved viscosifying behavior at high salinity water are shown in Table 3.5 and Figure 3.13.

Table 3.5 - Dependence of the dynamic viscosity of AAm-*co*-AMPS-*co*-APTAC on composition of terpolymers

Molar composition of TPA, (mol.%)	90:5:5	80:10:10	70:15:15	60:20:20	50:25:25
Dynamic viscosity, mPa·s	5.5	10.4	6.7	8.0	6.6

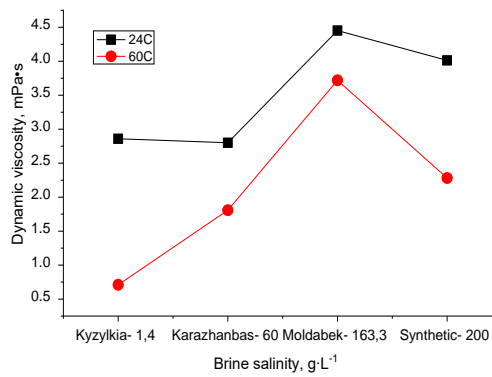


Figure 3.13 - Dynamic viscosity of 0.2 % AAm]:[AMPS]:[APTAC] =80:10:10 mol.% in various oilfield brine at 24 and 60 °C

Based on the viscosity results, the optimal salt-tolerant sample AAm-*co*-AMPS-*co*-APTAC with a molar composition of 80:10:10 mol. % was chosen for all polymer flooding experiments.

3.2.2 Salt- and temperature-dependent viscosity of AAm-*co*-AMPS-*co*-APTAC

The effect of polymer concentration on the dynamic and reduced viscosities of AAm-*co*-AMPS-*co*-APTAC terpolymer in $250 \text{ g}\cdot\text{L}^{-1}$ synthetic brine is shown in Figure 3.14.

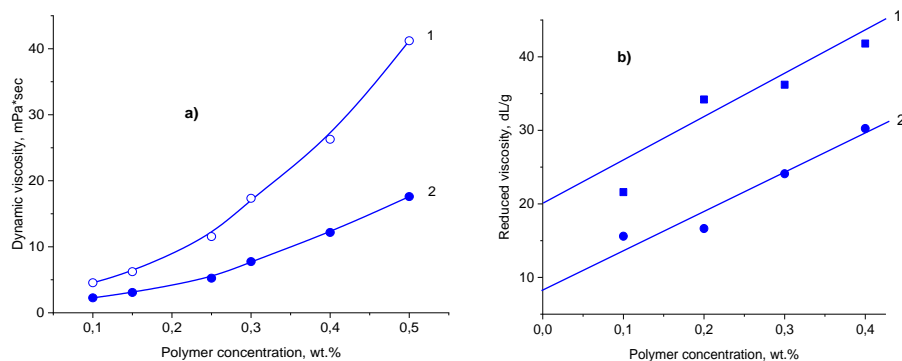


Figure 3.14 - Dependence of the dynamic (a) and reduced (b) viscosities of TPA on polymer concentration at 24 (1), 60 °C (2) in $250 \text{ g}\cdot\text{L}^{-1}$ synthetic brine

The intrinsic viscosity $[\eta]$ of the terpolymer is found by extrapolation of η_{sp}/C to $C \rightarrow 0$ to be equal to 20 and 8.3 dL·g⁻¹ at 24 and 60 °C, respectively. The high values of the intrinsic viscosities of the terpolymer in 250 g·L⁻¹ salt solution confirm the preparation of high molecular weight quenched polyampholyte by radical polymerization. The dynamic viscosity of the 0.25 wt.% terpolymer solution was found to increase with a rise in brine salinity from 200 to 300 g·L⁻¹ at 24 and 60 °C (Figure 3.15).

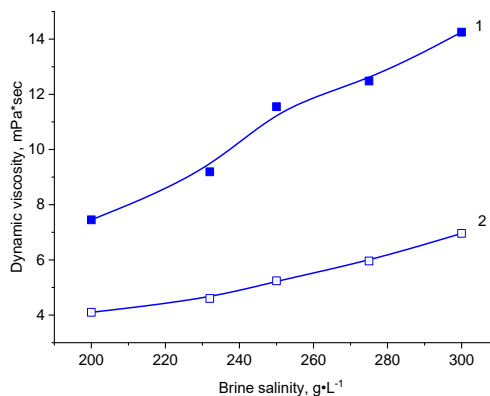


Figure 3.15 - Salt-dependent dynamic viscosity of the TPA at 24 (1), 60 °C (2)

In the case of charge-balanced AAm-*co*-AMPS-*co*-APTAC terpolymer, the polyelectrolyte effect is fully suppressed due to mutual compensation of oppositely the charged monomers, AMPS and APTAC. The low values of the dynamic and reduced viscosities at a high temperature of 60 °C are probably accounted for by destruction of intra- and inter-macromolecular hydrogen bonds between acrylamide monomers, and by enhancement of hydrophobic interactions between the backbones of the main polymer chain.

3.2.3 Salt- and concentration dependent dynamic viscosities of ATP and HPAM in synthetic brine

Figure 3.16 demonstrates the dynamic viscosities of amphoteric terpolymer AAm-*co*-AMPS-*co*-APTAC and HPAM versus the polymer concentrations at 24 and 60 °C in 250 g·L⁻¹ synthetic brine.

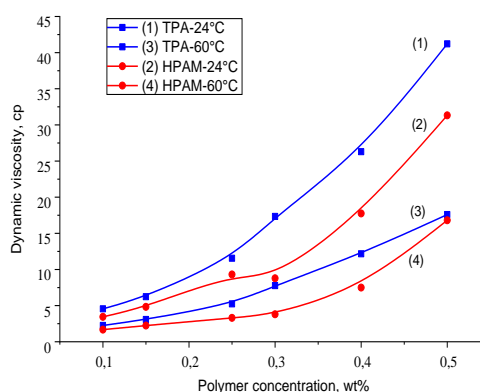


Figure 3.16 - Dependence of the dynamic viscosity of TPA and HPAM on polymer concentration in 250 g·L⁻¹ synthetic brine at 24 and 60 °C

The gradually decreasing of dynamic viscosities of amphoteric terpolymer and HPAM upon dilution testify the absence of polyelectrolyte effect leading to unfolding of macromolecular coils.

Figure 3.17 represents the dynamic viscosities of AAm-*co*-AMPS-*co*-APTAC terpolymer and HPAM in high salinity brine. The dynamic viscosity 0.25 wt.% amphoteric terpolymer solutions increases steadily from 7.45 mPa·s to 14.25 mPa·s with increase of the salinity from 200 to 300 g·L⁻¹. Whereas the dynamic viscosity of HPAM solution increased from 6.78 to 9.31 mPa·s when the salinity increases from 200 to 250 g·L⁻¹, however the further increasing of the salinity up to 300 g·L⁻¹ causes sharp decreasing of the viscosity of HPAM. This is probably accounted for precipitation of HPAM as a result of “salting out” effect.

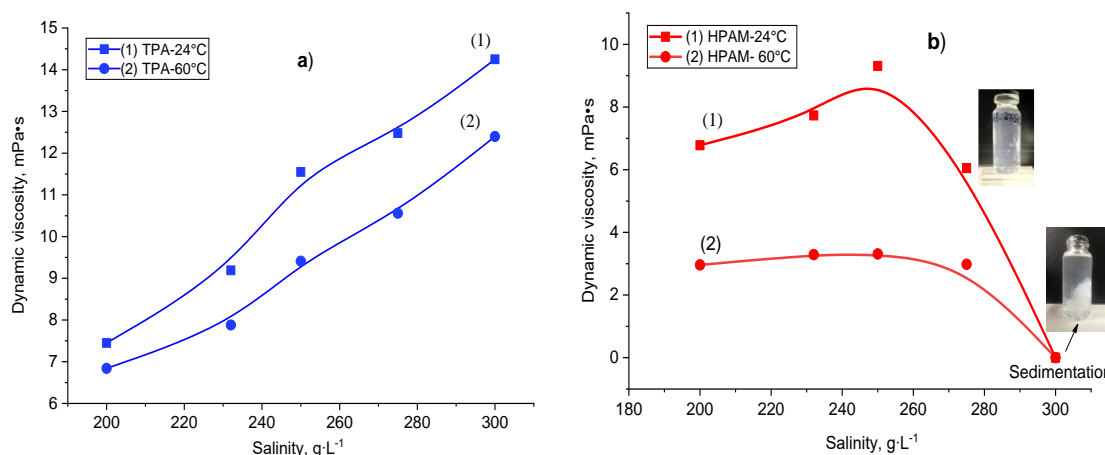


Figure 3.17 - Salt-dependent dynamic viscosities of 0.25 wt.% TPA (a) and HPAM (b) at 24 (1) and 60 °C (2) in a salinity range of 200 - 300 g·L⁻¹ brine

The dynamic viscosities of AAm-*co*-AMPS-*co*-APTAC terpolymer solutions are higher than that of HPAM. This phenomenon is attributed to the expanding of TPA molecule under high-temperature and high-salinity conditions in brine.

3.2.4 Comparative viscosity measurements of TPA and HPAM in high salinity brine

The dynamic viscosity of a 0.25 wt. % solution of an amphoteric terpolymer and polyacrylamide, depending on the salinity of water, is shown in Figure 3.18. As can be seen from the figure, terpolymer solutions retain their relatively high viscosity in the salinity range from 200 to 300 g·L⁻¹. However, the viscosity of polyacrylamide solutions decreases sharply in the same salinity range. The structures of HPAM, a polyelectrolyte, and TPA, a polyampholyte, dictate their behaviors in saline solutions. The HPAM chains tend to shrink with an increase in salinity, because the added salts, illustrating the polyelectrolyte effect, screen the electrostatic repulsion between negatively charged carboxylic groups.

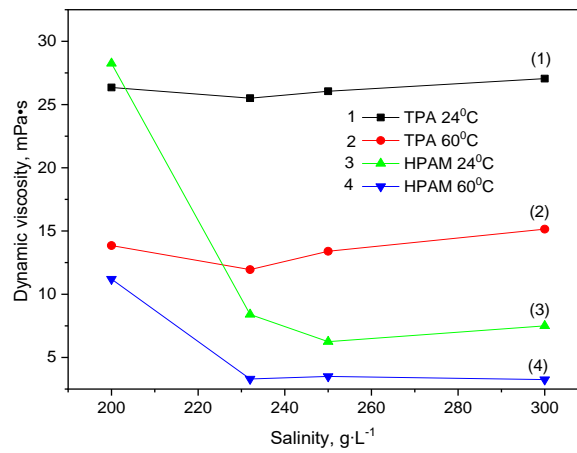


Figure 3.18 - Dynamic viscosities of 0.25 wt.% TPA (curves 1,2) and HPAM (curves 3,4) in high salinity brine at 24 and 60 °C, with a shear rate of 7.32 s⁻¹

Moreover, bivalent cations (Ca²⁺ and Mg²⁺) present in saline solution can bridge the carboxylic ions in the HPAM, effectively shrinking the macromolecules. On the other hand, the TPA macromolecule chains tend to unfold in saline solutions, due to the screening of the electrostatic attraction between negatively charged AMPS and positively charged APTAC moieties, demonstrating the antipolyelectrolyte effect.

The rheological results show that the viscosity of 0.25 wt.% HPAM solution in 200 g·L⁻¹ decreases over 15 days of aging by 27.5 %, whereas the viscosity of 0.25 wt.% TPA solution in 200 g·L⁻¹ decreases over the same time period by only 18.2 % (Figure 3.19, Table 3.6).

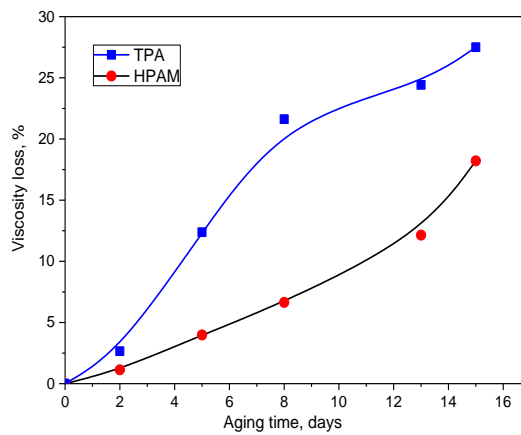


Figure 3.19 - Viscosity loss for 0.25 wt.% TPA and HPAM solutions in 200 g·L⁻¹ synthetic brine while aging at 24 °C

Table 3.6 - Viscosity of 0.25 wt.% TPA and HPAM solutions in 200 g·L⁻¹ synthetic brine while aging at 24 °C

Date	Aging time, days	Dynamic viscosity, (± 0.5 cp)	
		TPA	HPAM
06.10.2021	0	26	28
08.10.2021	2	26	27
11.10.2021	5	25	25

Continuation of the table 3.6

14.10.2021	8	25	22
19.10.2021	13	23	21
21.10.2021	15	22	20

The increase of dynamic viscosity with an increase in brine salinity is explained by the screening of the electrostatic attraction between positively and negatively charged monomers by anions and cations of salts, which leads to expansion of the polymer chain. This phenomenon is called the antipolyelectrolyte effect, which is illustrated in Figure 3.16. Increasing the dynamic viscosity of the high molecular weight terpolymer in brine is favorable for viscosification of hot reservoir water containing up to 200-300 g·L⁻¹ salts.

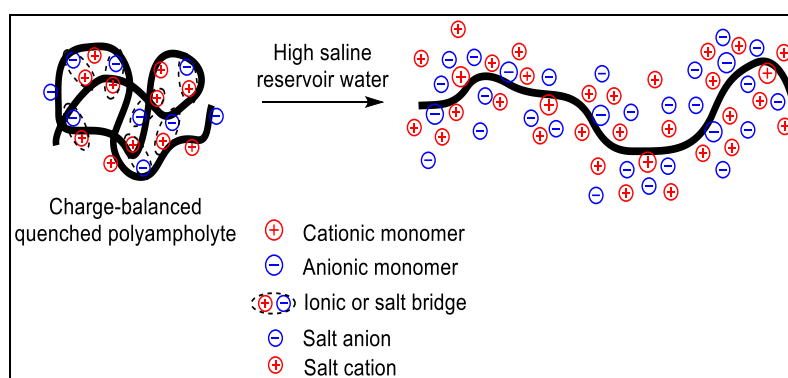


Figure 3.16 - Schematic illustration of the behavior of AAm-co-AMPS-co-APTAC=80:10:10 mol. % terpolymer in high saline water. Black thick line represents polymer backbone

CHAPTER 4. Results of core/sand pack flooding experiments

4.1 Oil displacement ability of amphoteric terpolymers in reservoir water

Table 4.1- Core/sand pack flooding conditions and results

Core/ sand pack flooding experiments	Polymer concentration, (wt.%)	Viscosity, (mPa*s)	Flow rate, (cm ³ /min)	ORF by water flooding, (%)	ORF by polymer flooding, (%)	Total ORF, (%)
1. Sand pack (16 D)	0.5- 5 TPA	(LW)	0.1	25.7	0.51	26.21
2. Carbonate core (5 D)	0.5 - TPA (Mw=5-6·10 ⁵ Da),	10.4	1	19.7	4.8-5	24.5
3. Sand pack (1.8 D)	0.25 - TPA (Mw = 2.9·10 ⁶ Da),	14.25	0.15	30	23	53
4. Sand pack (0.62D)	0.25 - TPA (Mw = 2.9·10 ⁶ Da)	14.25	0.15	36	28	64
5. Sand pack (1.77 D)	0.25 - HPAM (Mw =17.2·10 ⁶ Da)	9.6	0.15	34.7	18	52.7

Figure 4.1 demonstrates mass of produced oil versus injected water volume and photos of effluents. The volume of each effluent sample is 10 cm³, whereas the pore volume (PV) of the model is 55 cm³. As seen from Fig. 4.1 water breakthrough occurred before the injection of the first 10 cm³ water (≈ 0.18 PV) and oil production started to decline after 0.18PV of injected water into the model. Water flooding oil recovery factor (ORF) demonstrates that the water flooding resulted in displacement of approximately 25.7% of oil initially in place (OIIP) (Figure 4.1).

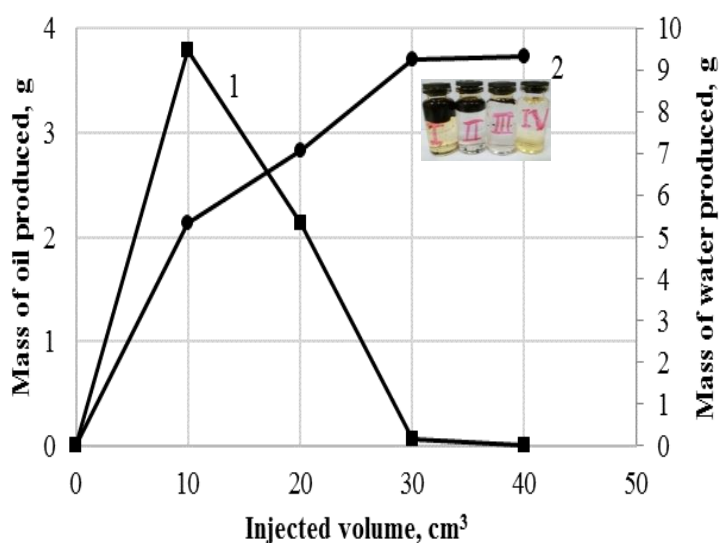


Figure 4.1 - Dependence of mass of produced oil (curve 1) and water (curve 2) vs injected water volume. Insert is photos of each effluent containing 10 cm³ of fluid

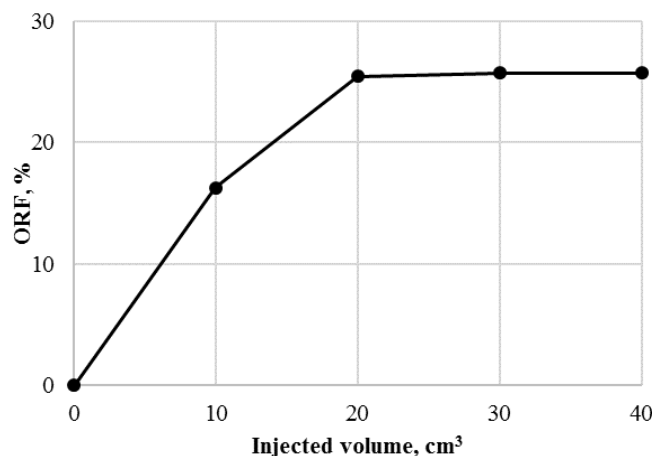


Figure 4.2 - Dependence of ORF vs injected volume of water

Injection of 0.5% brine solution of AAm-*co*-AMPS-*co*-APTAC terpolymers into high permeable sand pack model stepwise increases oil production (Figure 4.3). For instance, injection of AAm-*co*-AMPS-*co*-APTAC (50:25:25 and 60:20:20 mol.%) increases the oil recovery up to 0.35 %, while ORF is 0.51 % when terpolymers 70:15:15, 80:10:10 and 90:5:5 mol.% are injected. Thus, polymer flooding experiments on high permeable sand pack model demonstrated that only 0.51 % oil is recovered by amphoteric terpolymers in comparison with water flooding.

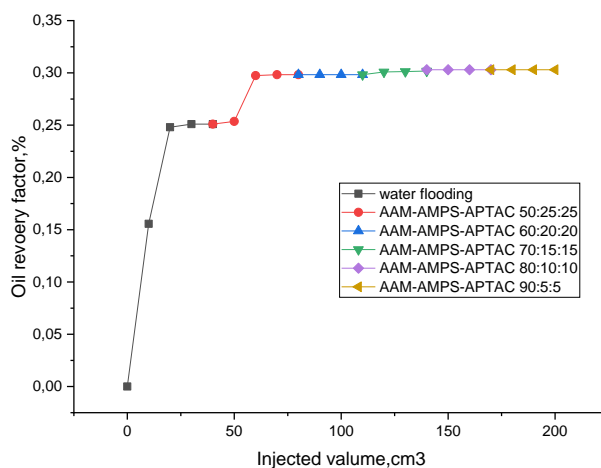


Figure 4.3 - Oil recovery vs polymers injected volume. Polymer concentration 0.5 wt.% in 101 g·L⁻¹ brine. Flow rate 0.1 cm³/min. Room temperature

4.2 Core flooding experiment using TPA

In the next series of experiments 0.5 wt.% solution of AAm-*co*-AMPS-*co*-APTAC (80:10:10 mol.%) in 163 g·L⁻¹ brine was injected into preliminarily water-flooded core sample. The reason is that among the tested AAm-*co*-AMPS-*co*-APTAC terpolymers have highest viscosity in brine exhibited amphoteric terpolymer with composition of 80:10:10 mol.%. (see Table 3.5).

The injection of 0.5 wt.% solution of TPA (80:10:10 mol.%) in brine into the prewater flooded core sample resulted in a notable oil recovery increase. Figure 4.4 clearly shows the increasing of the mass of produced oil in the course of polymer flooding.

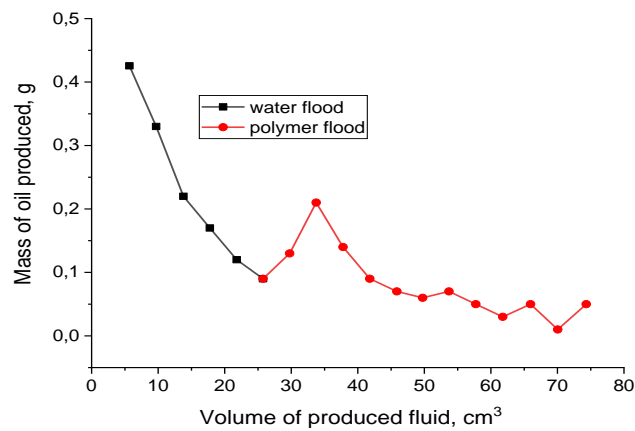


Figure 4.4 - Mass of produced oil vs the produced volume of fluid in the course of water flood (■) and polymer flood (●). Karazhanbas oil 64 cp at 60 °C. The injection rate is 1 cm³·min⁻¹

The increase of the pressure drop at the beginning of polymer flooding also indicates that the *in-situ* polymer solution viscosity is higher than that of water, and the higher viscosity results in more favorable oil mobility ratio between the displacing and the displaced fluids (Figure 4.5).

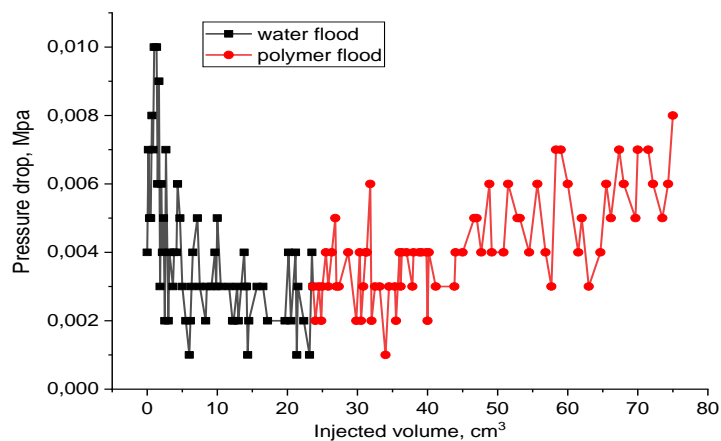


Figure 4.5 - Change of pressure drop vs injected volume in the course of water flood (■) and polymer flood (●)

As seen from Figure 4.6 the ORF increased by 4.8-5% due to injection of 0.5% polymer solution. This is explained by increasing of the viscosity of brine solution (or viscosifying) due to disruption of intra- and interionic contacts between oppositely charged AMPS and APTAC moieties demonstrating *antipolyelectrolyte* effect. In pure water, the electrostatic attraction between oppositely charge macroions leads to formation of compact structure and low viscosity. In saline water the anions and

cations of salts screen the electrostatic attraction between positively and negatively charged microions and the macromolecular chain expands. This phenomenon leads to increasing of the solution viscosity and consequently to viscosifying effect. In its turn the viscosification of brine solution leads to decreasing of the mobility ratio (M_r) which is defined as ratio of displacing phase mobility (water) to displaced phase mobility (oil). It is commonly accepted that in polymer flooding, favorable M_r is achieved by increasing the viscosity of water.

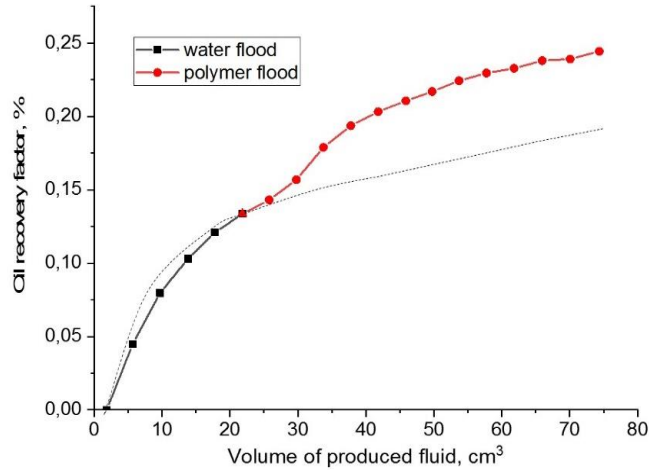


Figure 4.6 - Dependence of ORF vs produced volume in the course of water flood (■) and polymer flood (●). Water flooding trend is shown by the dotted line (•••)

It is interesting to evaluate the state of core samples after polymer flooding experiment. For this purpose, the sand pack model was cut into two pieces and the interior walls along with injection and outlet faces were analyzed (Figure 4.7). Interior walls of core sample contain some amount of adsorbed polymer solution while the injection face of the core is less oil saturated than the outlet face. This fact confirms the oil displacement by amphoteric terpolymer in the course of injection of polymer solution.

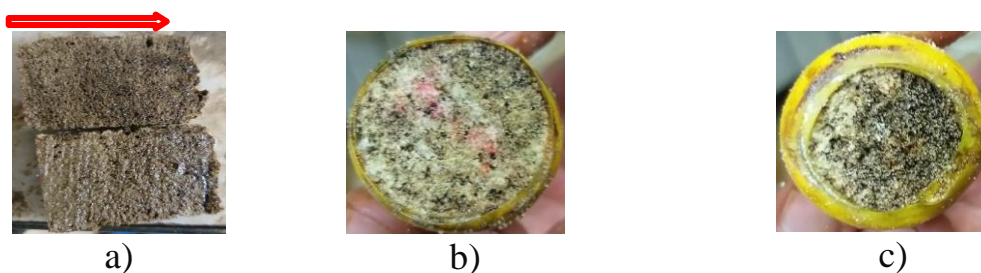


Figure 4.7 - The view of core sample after the testing. Core cut along the axis (a), injection (b) and outlet (c) face of the core sample

4.3 Sand pack flooding experiments using TPA

4.3.1 Oil saturation

Figure 4.8 shows changing of injection pressure versus time in the course of the oil saturation process for the 0.62 D and 1.8 D sand pack models.

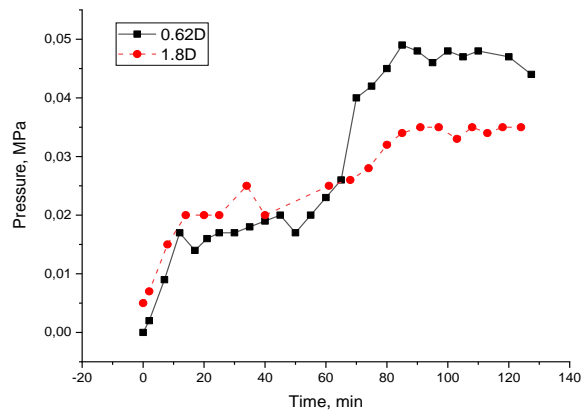


Figure 4.8 - Injection pressure versus time in the oil saturation process

At a high oil injection pressure of 0.044-0.047 MPa, stabilization occurs in the lower permeability model, as seen in Figure 3.23. For the higher permeability model (1.8 D), the oil injection pressure leveled off at 0.035 MPa. The mass of oil in each model was calculated based on material balance, and was found to be equal to 8.78 g and 9.47 g for the 0.62 D and 1.8 D models, respectively.

4.3.2 Water and polymer flooding

The Figure 4.9 shows that immediately following the start of polymer injection, oil production increases up to 0.35 g, then reaches a limit as indicated by a decline in the oil flow rate. The injection pressure is slightly increased in the case of the low permeability sand pack (1.8 D).

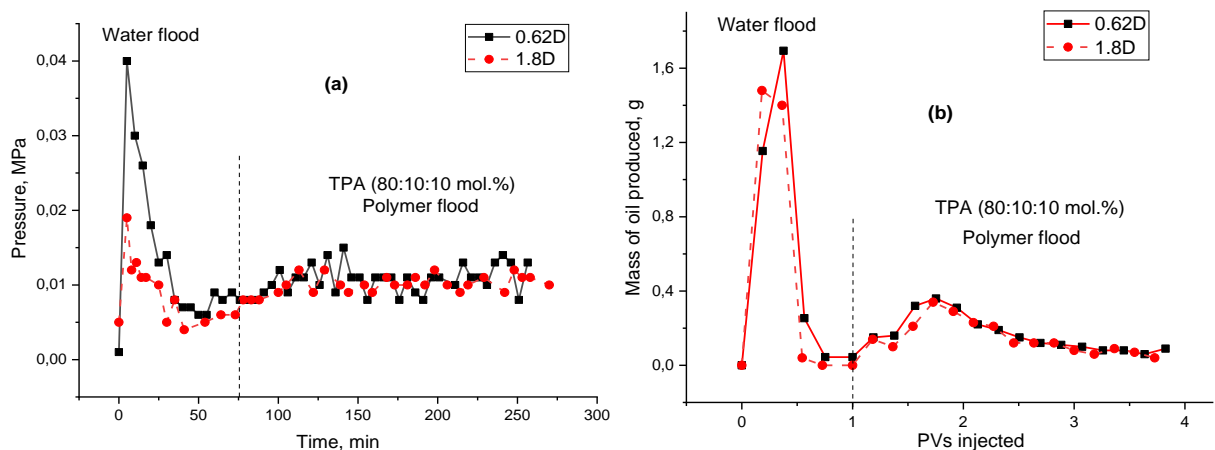


Figure 4.9 - Injection pressure versus time (a), and mass of oil produced versus injected PVs (b) during the water and polymer flooding process

Figure 4.9 (b) shows the mass of produced oil versus pore volumes injected into the sand packs during the water flooding. In spite of large permeability differences, the oil production curves are not substantially different. However, the

injection pressure is notably higher in the case of the lower permeability sand pack (Figure 4.9 (a)).

4.3.3 Oil recovery factor (ORF)

The oil recovery factor (ORF) during water and polymer flooding is demonstrated in Figure 4.11. In the case of water flooding, the ORF curves leveled off at around 36 % and 30 % for the 0.62 D and 1.8 D models, respectively. The injection of 0.25 wt. % polyampholyte dissolved in $250 \text{ g}\cdot\text{L}^{-1}$ brine resulted in a rise of incremental oil recovery by 28 and 23 % for the 0.62 D and 1.8D sand pack models, respectively.

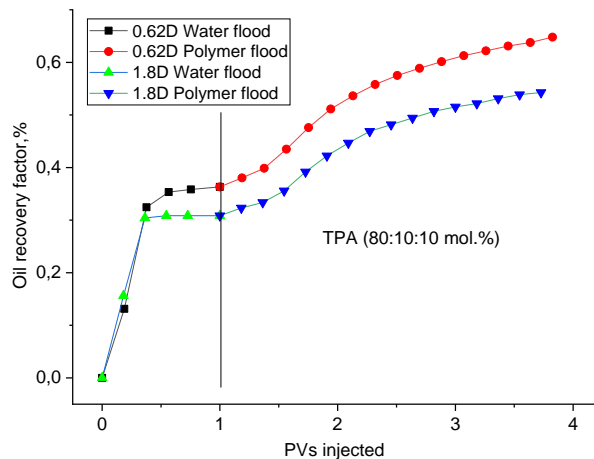


Figure 4.11 - Oil recovery factor versus injected PVs of water and TPA solution

4.4 Comparison of oil recovery efficiency with TPA and HPAM

4.4.1 Sand pack flooding tests with TPA and HPAM

As shown in Figure 4.12, the flooding of the 8.6 cm long high permeability (15.8 Darcy) sand pack saturated with East Moldabek oil and $100 \text{ g}\cdot\text{L}^{-1}$ reservoir brine at room temperature.

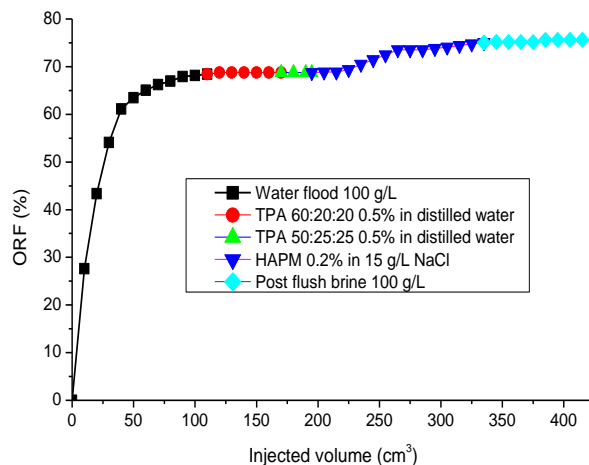


Figure 4.12 - Oil recovery factor versus injected volume. 1 PV is 64 cm^3 . Flow rate set at $0.1 \text{ cm}^3/\text{min}$

The results of the experiment demonstrated that 0.2 wt.% HPAM solution in low salinity brine ($15 \text{ g}\cdot\text{L}^{-1} \text{ NaCl}$), with initial viscosity equal to 31cp at 14.7 sec^{-1} , provides a notable increase in oil recovery (5-6 %), even after the injection of 3 PVs ($1\text{PV}= 64 \text{ cm}^3$) of pre-flush with 1.7 PV of $100 \text{ g}\cdot\text{L}^{-1}$ brine and 1.3 PV of various TPA solutions, which themselves were not effective in oil displacement (Figure 4.12).

This is a remarkable result, because the injection of 3 PVs of fluid into the homogeneous sand pack drives the model almost to its irreducible oil saturation value, at which point the incremental oil recovery increase of 5-6% shows that HPAM is an effective polymer for enhanced oil recovery when dissolved in low salinity brine. Moreover, the analysis of the effluent samples shows that after the injection of 1 and 2 PVs of the HPAM solution, the viscosity of the effluents rose to 28.5 cp and 29.8 cp, respectively (Figure 4.13), which corresponds to 8% and 3.8% viscosity reductions, respectively, in comparison with the initial value (31 cp), demonstrating the good propagation ability of HPAM in a high permeability sand pack.

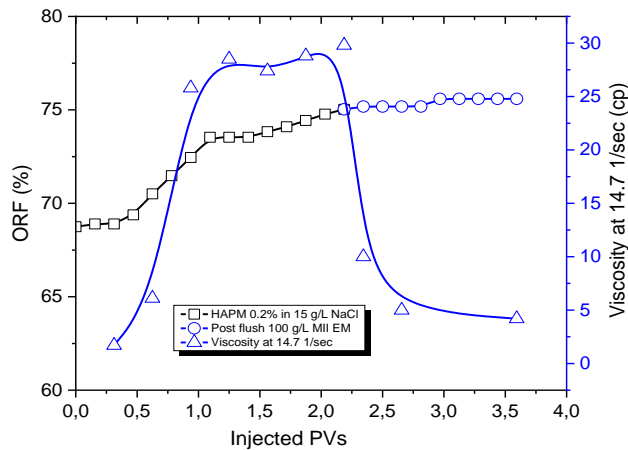


Figure 4.13 - Viscosity of effluents and ORF versus injected PVs of HPAM solution. HPAM 0.2 wt. % with initial viscosity 31 cp at 14.7 s^{-1}

4.4.2 Core/sand pack flooding tests with TPA and HPAM

The next two experiments were conducted using high porosity (83-85 %) 4.4-4.5 cm long and 2.9 cm diameter aerated concrete cores with permeability of 5.06 Darcy (2nd experiment) and 4.72 Darcy (3rd experiment). 0.5 wt.% TPA (2nd experiment) and HPAM (3rd experiment) solutions in $163 \text{ g}\cdot\text{L}^{-1}$ reservoir brine were prepared and injected at $60 \text{ }^{\circ}\text{C}$ and $1\text{cm}^3/\text{min}$ into cores previously saturated with Karazhanbas oil and the same brine. As a preliminary, the cores were subjected to the injection of 1 PV of water. Figure 4.14 shows the produced oil mass versus the total mass of all other fluid for both the TPA and HPAM experiments. As can be seen, the water flooding results are very similar for both experiments. However, HPAM, at its maximum, allowed displacement of 3 times more oil than did TPA. The photos of the core inlet (face) and outlet (backside) show that the core used in the HPAM experiment contains less oil than that used in the TPA test, especially at the outlet

side. Moreover, Figure 4.15 (b) shows that the HPAM pressure drop was around 3 times higher than that of TPA. This demonstrates that the apparent viscosity of HPAM is higher, and explains its better performance in terms of greater oil production.

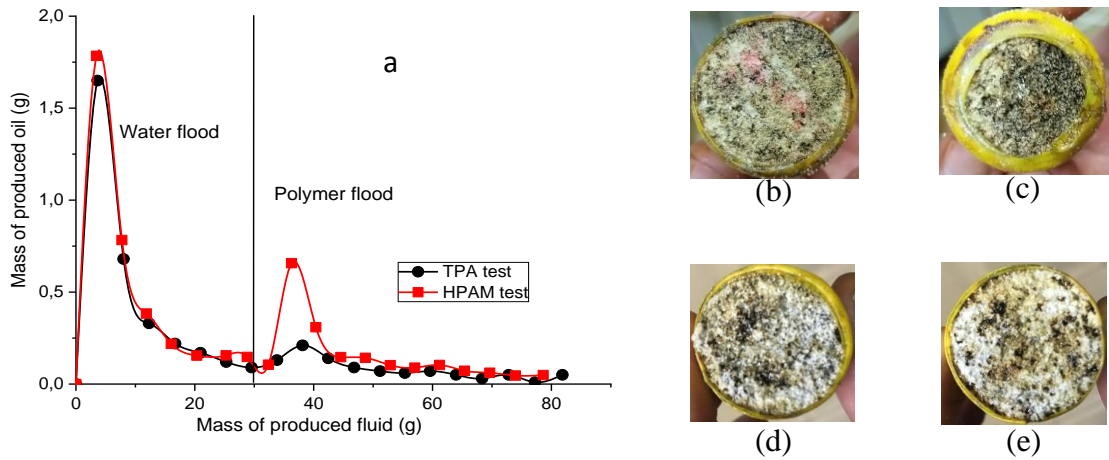


Figure 4.14 - (a) Mass of oil produced during water and polymer injections in the aerated concrete cores, (b) core inlet and (c) outlet after testing with ATP, (d) core inlet and (e) outlet after testing with HPAM

Figure 4.15 (a) shows that water injection for the two tests is characterized by similar pressure values. However, when injecting polymers, higher pressures were recorded in the HPAM test, as seen in Figure 4.15 (b). This indicates a higher viscosity of this polymer and helps explain the results presented in Figure 4.15.

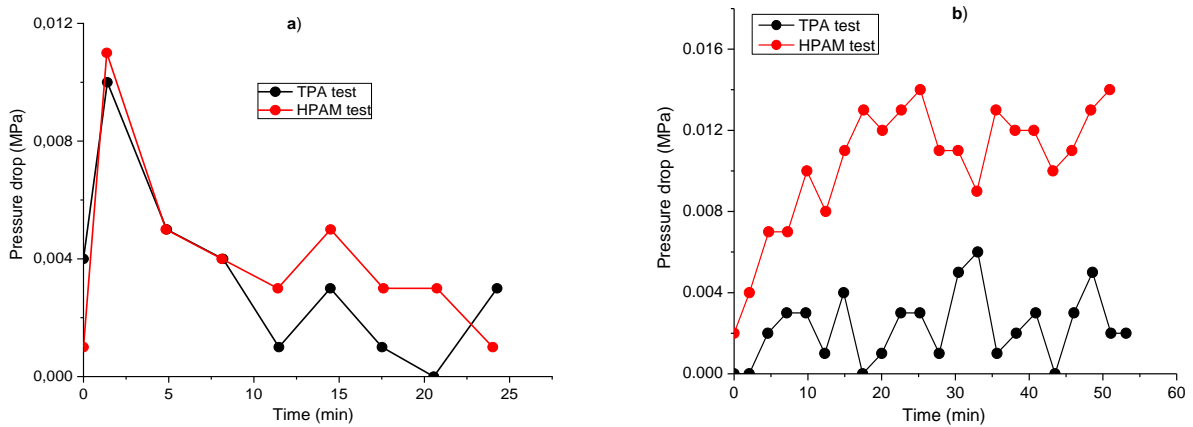


Figure 4.15 - Pressure drops registered during flooding tests in cores with TPA and HPAM for water (a) and polymer (b) floods

The following tests were conducted using 0.25 wt.% polymer solutions prepared in $200 \text{ g}\cdot\text{L}^{-1}$ brine injected into sand packs of 5 cm in length 3 cm diameter saturated with Karazhanbas oil and brine salinity $200 \text{ g}\cdot\text{L}^{-1}$ at $30 \text{ }^\circ\text{C}$ and $0.15 \text{ cm}^3/\text{min}$. Before injection of polymer solutions, the models were pre-washed with 1 PV of water to simulate the flooding process. As can be seen from Figure 4.16, water injection in the model showed similar results. Injecting 0.25 wt.% TPA solutions into

the model showed positive results in two experiments with good reproducibility. However, injection of 0.25 wt.% HPAM solutions showed different results, one of which (HPAM 1st test) can be considered negative compared to the rest. This can be explained by the fact that 200 g·L⁻¹ seems to be the critical point for HPAM, as can be seen from the viscosity graph (Figure 3.18), in which the use of this polymer is not recommended.

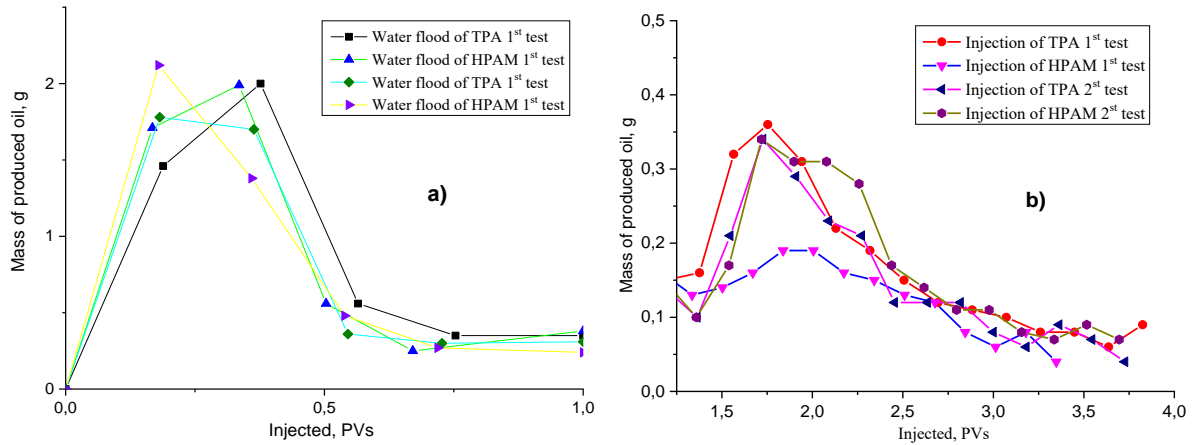


Figure 4.16 - The mass of the displaced oil depends on the injected volume of water (a) and polymer solutions (b)

A graph of pressure versus time for experiments by the 5 cm long sand pack models is shown in Figure 4.17. As can be seen from the graph, the pressure during TPA injection in all tests was greater than the pressure during HPAM injection. This once again confirms that TPA has a higher viscosity when filtered through a porous medium and provides more reliable results than HPAM.

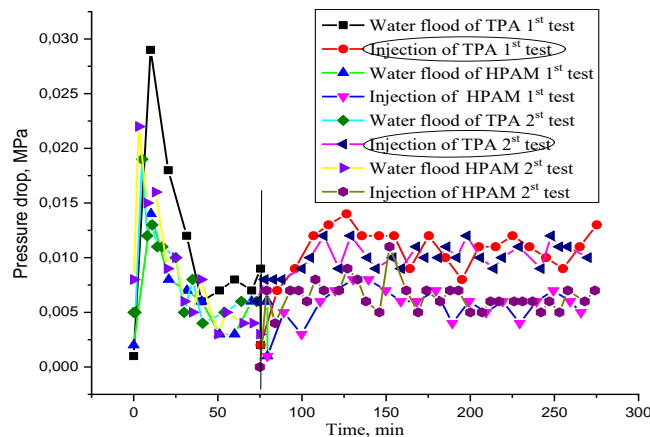


Figure 4.17 - Dependence of pressure drop on the time of fluid injection into sand pack models 5 cm long

Figure 4.18 shows the oil displacement coefficients obtained by injecting TPA (1st test) and HPAM (1st test) polymers into the model. As seen in the figure, the oil displacement coefficients resulting from the injection of 0.25 wt. % TPA and HPAM solutions through the sand pack models were 28 % and 18 %, respectively.

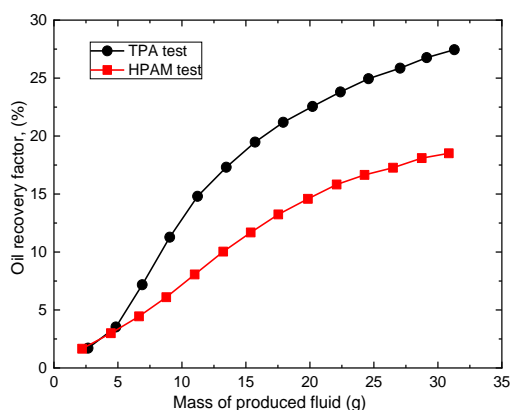


Figure 4.18 - Oil recovery factor versus the mass of produced fluid registered during the water and polymer flooding experiments using 5 cm long sand packs

4.4.3 Comparative oil displacement experiments of TPA and HPAM

At the next stage, sand pack flooding experiments were carried out on large sand pack models made of sand from the Karazhanbas deposit (diameter 4.3 cm, length 8.6 cm) using brine with a salinity of $250 \text{ g}\cdot\text{L}^{-1}$ (contain of $225 \text{ g}\cdot\text{L}^{-1}$ NaCl, $12.5 \text{ g}\cdot\text{L}^{-1}$ CaCl₂, and $12.5 \text{ g}\cdot\text{L}^{-1}$ MgCl₂ salts) and oil from the Karazhanbas field with a viscosity of 420 cp, as seen in Figure 3.18. The pore volume of the models is 58-64 cm³. Tests were carried out at a temperature of 30 °C and a flow rate of 0.3 cm³/min. After saturation with oil, 1 pore volume of water and 3 pore volumes of polymer were pumped through the models. As can be seen in Figure 4.19 (c,d), injecting HPAM with a salinity of $250 \text{ g}\cdot\text{L}^{-1}$ into the model allowed for an additional displacement of oil ranging from 16 % to 28.6 % after water flooding Figure (a,b). Injecting an TPA solution into a 5 cm long model resulted in an additional 23% displacement of oil. Thus, the oil displacing capability of TPA is comparable to that of modern brands of HPAM produced by SNF Company.

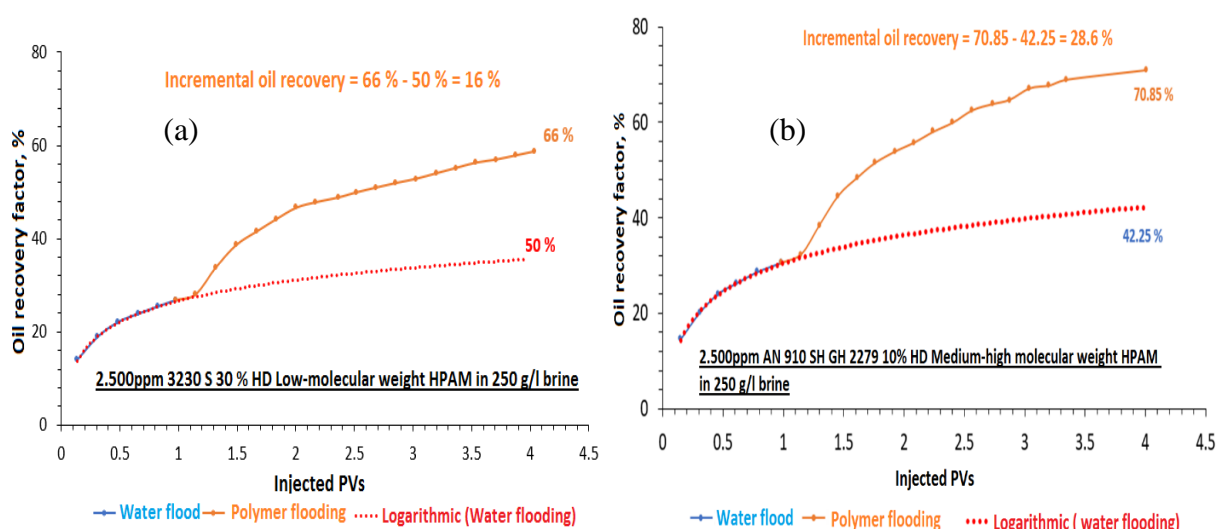
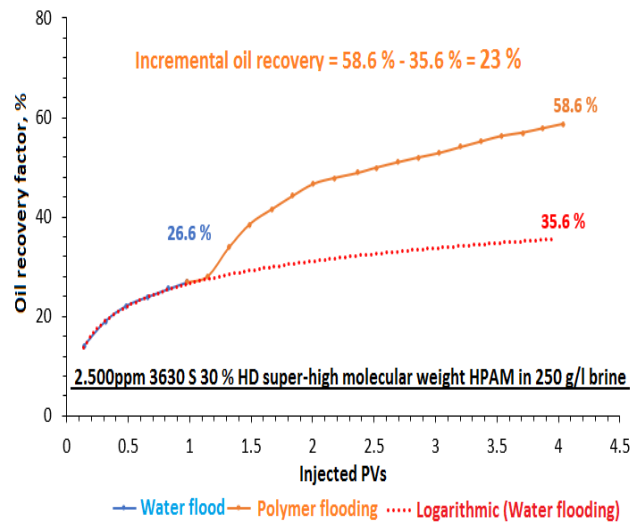
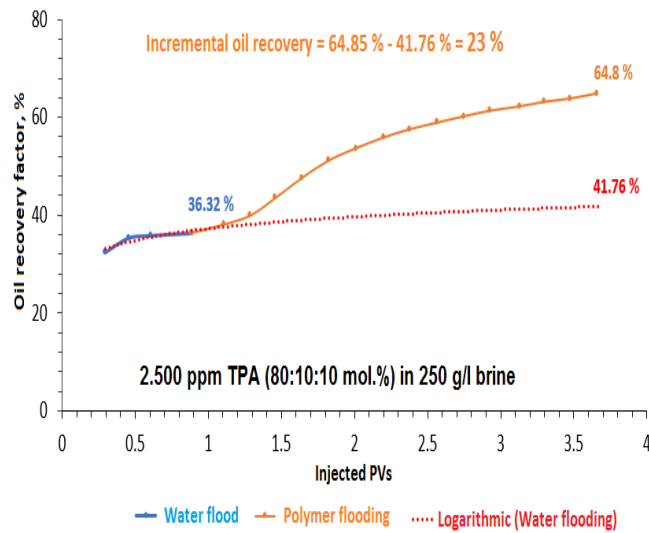


Figure 4.19 - Dependence of the oil recovery factor on the injected volume for experiments with 10 % HD low-molecular weight (a) and 30 % HD medium-high molecular weight (b) of 0.25 wt.% HPAM in $250 \text{ g}\cdot\text{L}^{-1}$



c) HPAM with 30% degree of hydrolysis and super-high molecular weight



d) TPA (80:10:10 mol.%) in 250 g·L⁻¹ brine

Figure 4.19 - Dependence of the oil recovery factor on the injected volume for experiments with HPAM TPA (80:10:10 mol.%) (d)

4.4.4 Issuing recommendations for the use of heat- and salt-resistant amphoteric terpolymers as reagents to enhance the thickening and leveling of injectivity profiles

The oil displacement experiments were conducted enabled to perform theoretical calculations for relative permeability to oil and water by the Brooks-Corey formulas (4.1):

$$k_{rw} = k_{rwo} [(S_w - S_{wi}) / (1 - S_{or} - S_{wi})]^{nw}, \quad (4.1)$$

$$k_{ro} = [(1 - S_w - S_{or}) / (1 - S_{or} - S_{wi})]^{no},$$

Where k_{rw} is the relative permeability to water
 k_{rwo} – final relative permeability to water
 S_w – current water saturation
 S_{wi} – initial water saturation
 S_{or} – residual oil saturation
 k_{ro} – relative permeability to oil

In this process, the parameters S_{wi} (initial water saturation) and S_{or} (residual oil saturation) were determined experimentally. The parameters n_w and n_o were then carefully selected to maximize convergence between the experimental and calculated water cut data (see Figure 4.20). The water cut, in turn, was calculated using the following formula (4.2):

$$f_w = \frac{1}{1 + \frac{k_{ro} \mu_w}{\mu_o k_{rw}}} \quad (4.2)$$

Where k_{ro} is the relative permeability to oil
 k_{rw} – relative water permeability
 μ_w – viscosity of water (or polymer solution)
 μ_o – oil viscosity

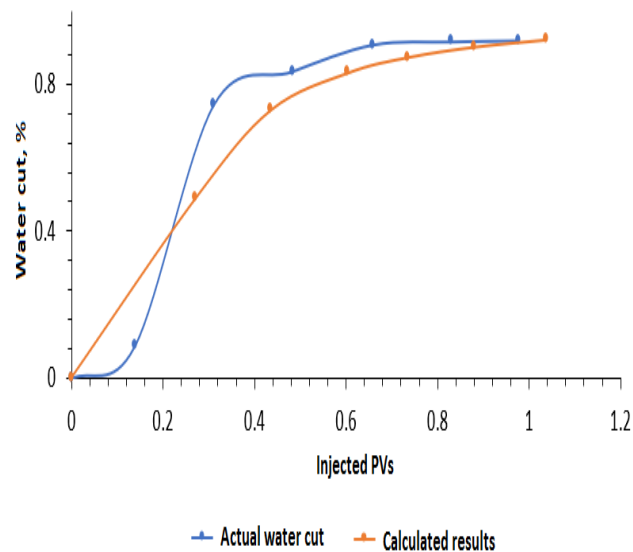


Figure 4.20 - Dependence of water cut on injected volume

Next, calculations were performed for various water (or polymer solution) viscosities (see Figure 4.21). The resulting dependencies can aid in selecting the optimal polymer concentration for displacing oil with a viscosity of approximately 400-450 cP. The resulting relationships between oil production, viscosity, and the injected volume of polymer allow for the selection of the polymer type and concentration, while considering the budget for the polymer flooding project.

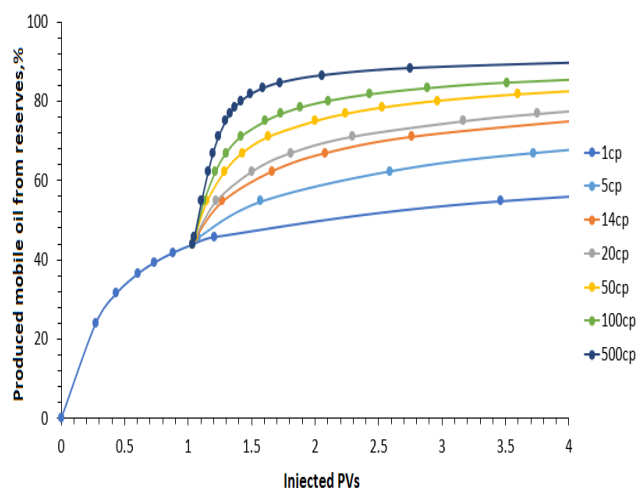


Figure 4.21 - Relationship between oil production, injected volume, and polymer solution viscosity

Based on the above results, the following recommendations can be made:

Under conditions of low water salinity and temperature, HPAM is an effective oil-displacing agent. At a mineralization of $160 \text{ g}\cdot\text{L}^{-1}$ and a temperature of $60 \text{ }^\circ\text{C}$, HPAM provides greater oil displacement than TPA. However, unlike HPAM, the viscosity of the terpolymer does not decrease with increasing water salinity above $200 \text{ g}\cdot\text{L}^{-1}$.

1. The optimal terpolymer composition should be consist of 80 mol.% acrylamide (AAm), 10 mol.% sodium salt of 2-acrylamido-2-methyl-1-propanesulfonic acid (AMPS), and 10 mol.% (3-acrylamidopropyl) trimethylammonium chloride (APTAC), $[\text{AAm}]:[\text{AMPS}]:[\text{APTAC}] = 80:10:10$ mol.%;

2. The optimal concentration of amphoteric terpolymer for injection into oil reservoir should be 0.2-0.3% within the salinity range of brine ($5\text{-}300 \text{ g}\cdot\text{L}^{-1}$).

3. To inject a 0.2-0.3% solution of an amphoteric terpolymer into the oil reservoirs, its temperature should not exceed $100 \text{ }^\circ\text{C}$.

4. A 0.2-0.3 % solution of an amphoteric terpolymer with the composition $[\text{AAm}]:[\text{AMPS}]:[\text{APTAH}] = 80:10:10$ mol.% is recommended for use at the South-West Kamyshtovoye field, where the mineralization of brine exceeds $200 \text{ g}\cdot\text{L}^{-1}$.

CHAPTER 5. Development of water-based drilling fluids based on the ternary polyampholyte AAm-co-AMPS-co-APTAC (80:10:10 mol. %) and bentonite clay

This chapter is divided into three sections. The first section presents the rheological properties of TPA-I and PAC-LV aqueous solutions without bentonite. The second section describes the rheological properties of bentonite/polymer dispersions. The third section discusses the results of fluid loss tests, including measuring the permeability of filter cakes, as well as SEM analysis of formulated filter cakes derived from bentonite/polymer dispersions following the filtration tests.

5.1 Rheological properties of TPA and PAC-LV solutions without bentonite

5.1.1 The intrinsic viscosities $[\eta]$ of polymer solutions

The intrinsic viscosities $[\eta]$ of TPA-I and PAC-LV measured in 35 wt.% NaCl brine is shown in Figure 5.1. The method of determination of the intrinsic viscosity of TPA-I can be found in [173]. The reduced viscosity η_{sp}/C of TPA-I and PAC-LV decreased from 270.5 to 75 dL·g⁻¹ and from 69 to 12.4 dL·g⁻¹, respectively, in the concentration range of polymers from 2 to 0.25%. Extrapolation of η_{sp}/C to $C \rightarrow 0$ allows to determine the intrinsic viscosities of TPA-I and PAC-LV that are equal to 41 and 7.5 dL/g, respectively. The high value of the intrinsic viscosity of TPA-I in 35 wt.% NaCl salt solution confirms the high molecular weight of prepared polyampholyte.

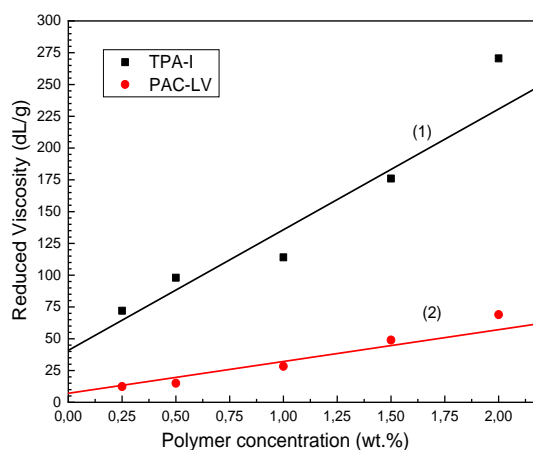


Figure 5.1 - Reduced viscosities of TPA-I (1) and PAC-LV (2) in a saline solution containing 35 wt. % NaCl at 24 °C

5.1.2 The apparent viscosities of polymer solutions

Figure 5.2. shows a significant difference in the apparent viscosity and shear stress versus shear rate of the polymer solutions (without bentonite) in salinity of brine at 25 °C.

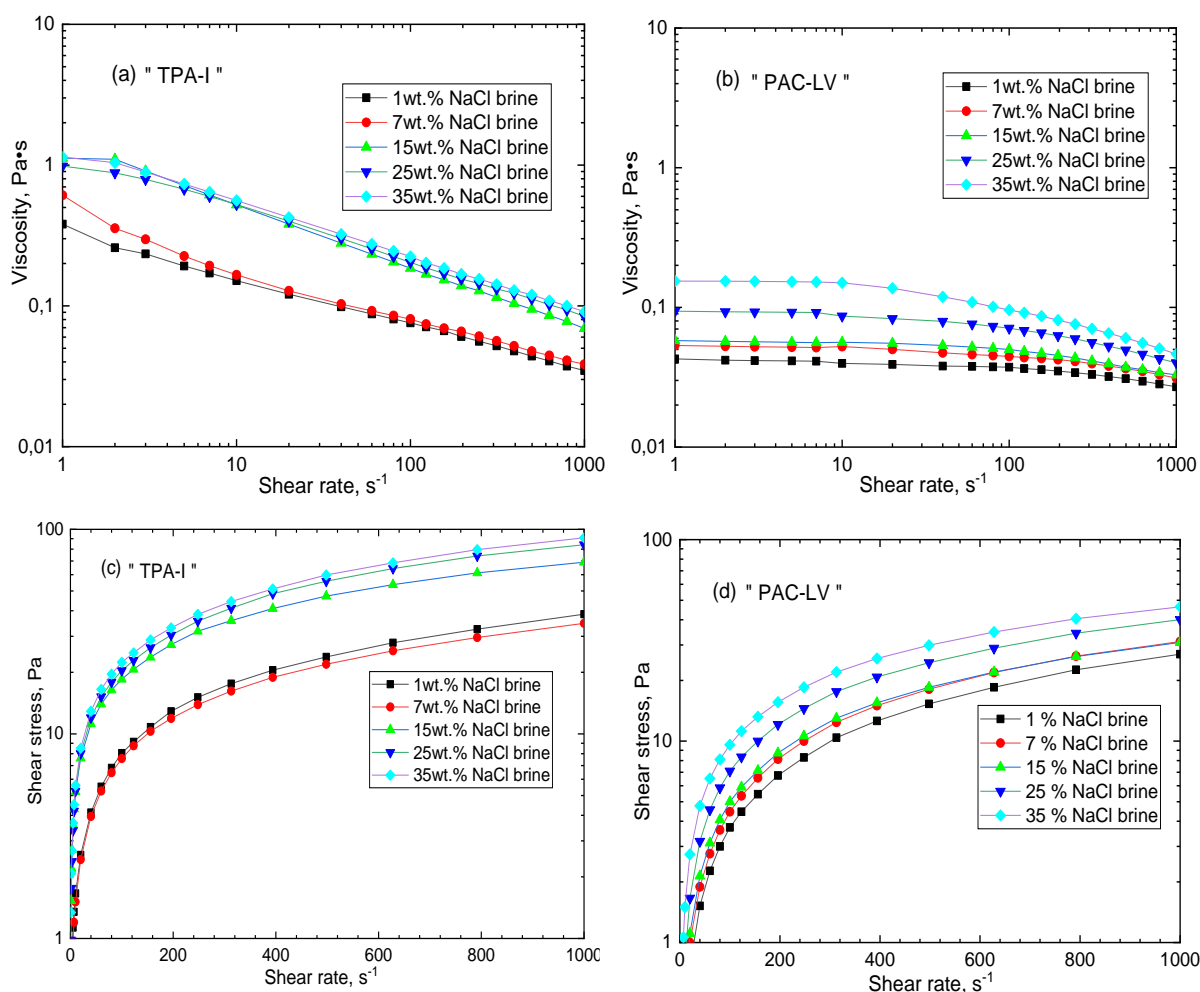


Figure 5.2 - Steady shear viscosity (a, b) and shear stress (c, d) versus shear rate for 2 wt.% TPA-I and PAC-LV polymer solutions in concentration 1, 7, 15, 25 and 35 wt.% of NaCl brine at 25 °C

As shown in Figure 5.2 (a), at 1% and 7% NaCl salinity and a wide range of shear rates, the apparent viscosity of TPA-I polymer decreased from 0.38 to 0.04 Pa·s and 0.6 to 0.04 Pa·s, respectively. It is noteworthy that with the increase of the shear rate from 1 to 1000 s⁻¹, the viscosity values of TPA-I prepared in 1, 7, 15, 25 and 35 wt.% NaCl brines decrease from 0.38 to 0.035 Pa·s and from 1.14 to 0.09 Pa·s, respectively.

As can be seen from Figure 5.2 (b), the increase of NaCl concentration from 1 to 35 wt.% results in the increase of apparent viscosity of PAC-LV from 0.04 to 0.15 Pa·s (3.7 times increase) at a shear rate of 1 s⁻¹. However, at a high shear rate of 1000 s⁻¹, there is only 1.7-fold increase in viscosity (from 0.027 to 0.046 Pa·s) with the increase in salinity.

In 35 wt.% NaCl brine at a shear rate of 1 s⁻¹, there is a substantial difference in viscosity values between the polymer solutions, ranging from 1.14 to 0.15 Pa·s for TPA-I and PAC-LV, respectively. These results demonstrate that in high salinity conditions (35 wt.% NaCl) the viscosity values of TPA-I solutions are notably higher than those of PAC-LV at low and high shear rates.

The flow curves (shear stress versus shear rate) of TPA-I and PAC-LV polymer solutions are depicted in Figure 6.2 (c) and (d). At a constant shear rate of 5.1 s^{-1} (API standard procedure), the PAC-LV polymer solution exhibits lower shear stress compared to the TPA-I polymer solution. In fact, the yield stress (G') values of TPA-I and PAC-LV polymer solutions in a 35 wt.% NaCl brine are equal to 2.99 Pa and 0.24 Pa, respectively. Across the entire range of shear rates ($1\text{-}1000 \text{ s}^{-1}$), the shear stress values observed for TPA-I and PAC-LV polymer solutions, prepared by using 1-15 wt.% NaCl brines, are lower than those observed for the same polymer solutions prepared by using 25-35 wt.% NaCl brines. Of note, TPA-I polymer solution prepared by using 35 wt.% NaCl brine exhibits the highest shear stress value among tested solutions.

As shown in Figure 5.2 (c) and (d), the shear stress values observed for TPA-I and PAC-LV polymer solutions in 35 wt.% NaCl saline water are ranging from 1.34 to 90.9 Pa and from 0.063 to 46.4 Pa, respectively. This indicates that the shear stress of TPA-I is sufficiently higher compared to PAC-LV. Therefore, it can be observed that polyampholyte terpolymers exhibit higher gel strength under similar temperature and shear rate conditions. For both polymer solutions the shear stress increases with salinity.

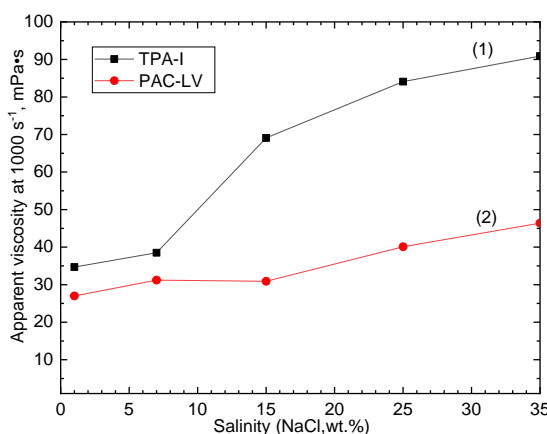


Figure 5.3 - Apparent viscosity of 2 wt.% TPA-I (1) and PAC-LV (2) polymer solutions versus NaCl concentration at 1000 s^{-1} and $25 \text{ }^\circ\text{C}$

Figure 5.3 demonstrates the change of apparent viscosity of TPA-I and PAC-LV polymer solutions across a wide range of NaCl concentrations (1-35 wt.%). The TPA-I (1) curve shows that the lowest viscosity values (34.7 and 38.5 mPa·s) were observed when the concentration of NaCl was equal to 1 and 7 wt.% NaCl. The increase of salinity to 15 and 35 wt.% resulted in the viscosity increase up to 69.1 and 90.9 mPa·s, respectively. This behavior is a characteristic feature observed for TPA terpolymers that contain charge balanced anions and cations [111,173].

Of note is that the viscosity increase of PAC-LV with salinity was less significant. In fact, the increase of salinity from 1 to 35 wt.% NaCl resulted in the increase of viscosity from 27 to 46.4 mPa·s. This observation suggests that in high salinity and under high shear rate the polyanionic cellulose solution is less effective than TPA-I terpolymer.

Based on the obtained results TPA-I was chosen for the further tests with bentonite in order to make a brine water based drilling fluids. At the same time the properties of those drilling fluids were compared with those of PAC-LV/bentonite/brine.

5.2 Rheological properties of bentonite/polyampholyte dispersions

The rheological properties of bentonite/TPA-I or bentonite/PAC-LV dispersions were investigated at 25 °C across a wide range of shear rates and NaCl concentrations. Figure 5.4 (a) shows the steady shear viscosity of BT/TPA-I dispersion versus shear rate. The comparison of Figure 5.2 (a) and Figure 5.4 (a) shows that the addition of bentonite to TPA-I solution increases the viscosity of the formulations in 35 wt.% NaCl brine at a shear rate of 1 s⁻¹ from 1.14 to 3.83 Pa·s.

The interactions between bentonite and amphoteric terpolymer molecules in brine can be explained by two distinct mechanisms. The first mechanism is adsorption of terpolymer onto bentonite. The second mechanism is ionic interactions between the negatively charged functional groups of polymer molecules and the positively charged edges of bentonite platelets [198].

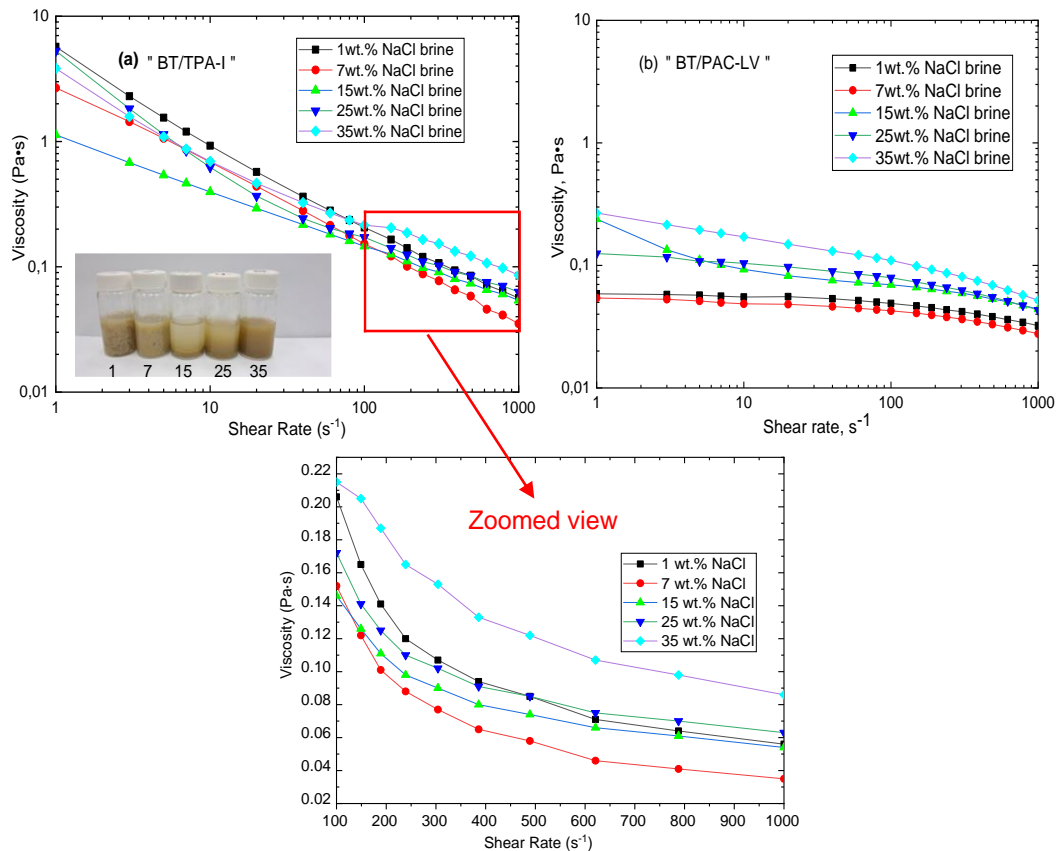


Figure 5.4 - Steady shear viscosity of 2% BT/TPA-I (a) and BT/PAC-LV (b) polymer dispersions over a wide range of shear rates and NaCl concentrations at 25 °C

As observed in Figure 5.4 (b), the viscosity of BT/PAC-LV formulations in 35 wt.% NaCl brine exhibited significantly lower values across a wide range of shear

rates, ranging from 0.26 to 0.05 Pa·s, compared to BT/TPA-I formulations, which ranged from 3.83 to 0.08 Pa·s. Additionally, upon comparing Figure 5.2 (b) and Figure 5.4 (b), it can be noted that the presence of bentonite did not have a substantial impact on the viscosity of PAC-LV, which measured 0.15 and 0.26 Pa·s, respectively, at a shear rate of 1 s⁻¹ in 35 wt.% NaCl brine.

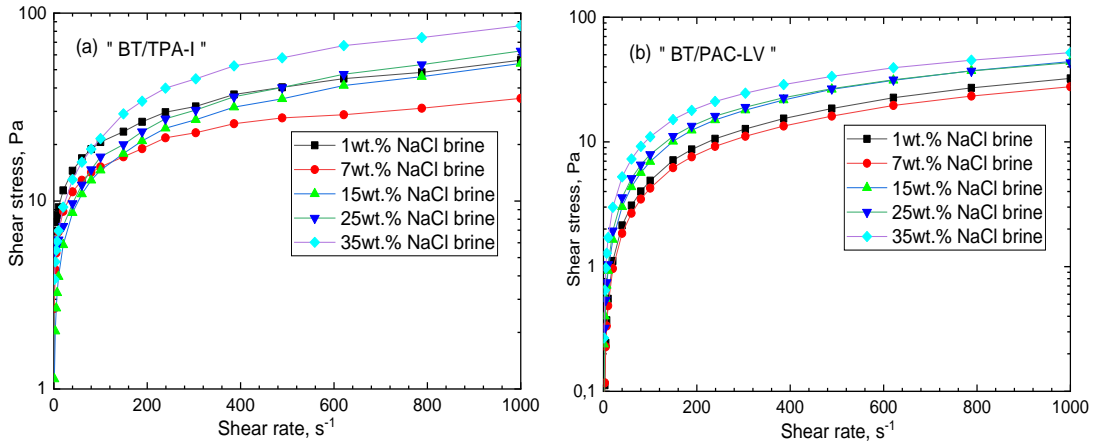


Figure 5.5 -Flow curves of the BT/TPA-I (a) and BT/PAC-LV (b) polymer dispersions across a wide range of shear rate and NaCl concentrations at 25 °C.

The flow curves of bentonite/ternary polyampholyte (BT/TPA-I) and bentonite/polyanionic cellulose (BT/PAC-LV) dispersions are shown in Figure 5.5 (a) and (b), respectively, at 25 °C. All the curves exhibit non-Newtonian shear thinning behavior. As can be seen, BT/TPA-I terpolymer dispersions demonstrate higher shear stress values compared to BT/PAC-LV dispersions. Of note is that the shear stress increases with salinity.

The rheological parameters obtained for bentonite/polymer dispersions using the Herschel-Bulkley model are presented in Table 5.1. Consistency coefficient ‘K’ shows the relation between the shear stress and shear rate, interactions between the components of the drilling fluid and its cleaning efficiency. The yield stress values at zero shear rate for the BT/TPA-I dispersions were found to be maximum at 5.29 Pa and 2.99 Pa in 25 and 35 wt.% NaCl brines, respectively (refer to Table 6.1). In contrast, the BT/PAC-LV dispersions exhibited significantly lower yield stress values (Table 5.1).

A high yield stress value is an important factor for the application of drilling fluid in drilling well operations as it facilitates the easy transport of shale cuttings to the surface of the hole and improves the efficiency of cleaning the drilling well.

With regards to the consistency coefficient (K), in the case with BT/TPA-I the increase of salinity from 1 to 15 wt.% NaCl resulted in the decrease of K from 1.54 Pa·sⁿ to 0.54 Pa·sⁿ. However, the further increase of salinity up to 35 wt.% NaCl resulted in the increase of K to the value of 1.1 Pa·sⁿ. Of note, in the case with BT/PAC-LV the value of K did not exceed 0.19 Pa·sⁿ over a wide range of NaCl concentrations.

Table 5.1- Parameters of Herschel-Bulkley model for bentonite/terpolymer drilling fluids prepared in different brines at 25 °C

Concentration of brine, wt.%		1	7	15	25	35
BT with TPA-I	YS (pa)	4.08	1.68	1.13	5.29	2.99
	K (pa*s ⁿ)	1.54	1.06	0.54	1.14	1.1
	n	0.31	0.54	0.11	0.23	0.22
	GS 10s (Pa)	18.8	1.14	3.54	10.7	20.5
	GS 10min (Pa)	25.8	1.1	3.68	11.1	21
BT with PAC-LV	YS (pa)	-0.12	-0.07	0.15	0.08	0.24
	K (pa*s ⁿ)	0.05	0.05	0.11	0.11	0.19
	n	0.01	0.01	0.02	0.02	0.04
	GS 10s (Pa)	0.41	0.18	0.54	0.054	0.81
	GS 10min (Pa)	0.36	0.21	0.39	0.47	0.75

* YS - yield stress, K - consistency coefficient, n - flow behavior index, GS - gel strength.

The value of the flow behavior index 'n' is determined by evaluating the slope of a logarithmic plot depicting the relationship between shear stress and shear rate. A value of n greater than 1 indicates that the fluid exhibits shear-thickening characteristics, whereas a value of n less than 1 signifies shear-thinning behavior. It is worth emphasizing that the effective viscosity of a non-Newtonian fluid is influenced not only by rheological parameters but also by the local shear rate, which is significantly impacted by the movement of particles in a two phase flow. When n is less than 1, the fluid is categorized as pseudo-plastic, which is commonly observed in solutions of polymers or suspensions containing fine solid particles [198,199].

Indeed, the value of the flow behavior index 'n' indicates that all BT/TPA-I formulations exhibit shear-thinning (pseudo-plastic) behavior within the salinity range of 1-35 wt.% NaCl. This confirms that the bentonite/terpolymer composites display shear-thinning behavior at high concentrations of NaCl. These rheological properties make the amphoteric terpolymer suitable for use in combination with bentonite as a rheology modifier in salt-resistant brine water-based drilling fluids (WBDF). The gel strength of BT/TPA-I and BT/PAC-LV formulations prepared in different brines are shown in Figure 5.6.

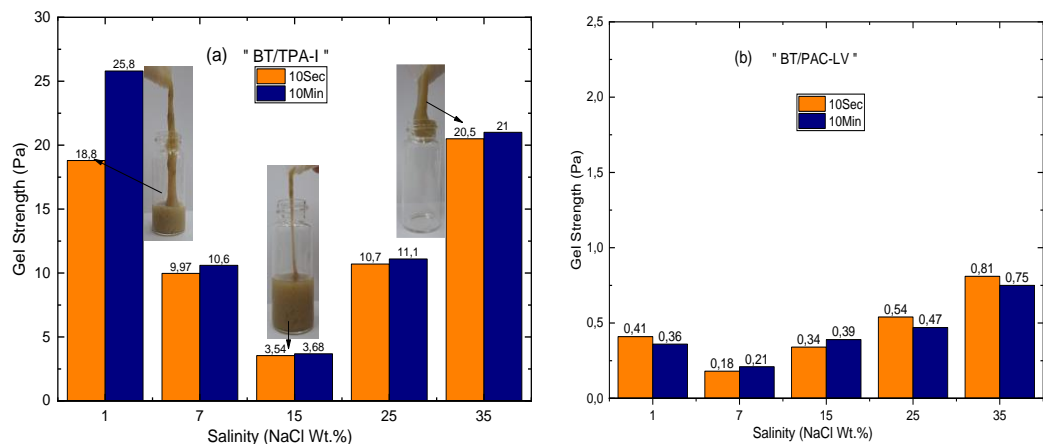


Figure 5.6 - Gel strength of bentonite/TPA-I (a) and bentonite/PAC-LV (b) dispersions within a wide range of NaCl concentration at 25 °C

As figure 5.6 (a) shows, both 10-seconds and 10-minutes gel strength values decrease with the increase of salinity from 1 to 15 wt.% NaCl. However, the further increase of salinity to 35 wt.% NaCl results in the increase of the gel strength values. Of note is that BT/TPA-I formulation failed to provide a gel strength value required by the API standard only in 15 wt.% NaCl brine. Whereas for other concentrations of NaCl the gel strength values were notably higher than the numbers required by the standard. At the same time, BT/PAC-LV could not provide the required gel strength values in the same conditions. This proves the effectiveness of BT/TPA-I over BT/PAC-LV.

The ability to control the rheological behavior of drilling fluids is crucial for efficient drilling operations, and the incorporation of amphoteric terpolymer can contribute to achieving the desired flow characteristics under high salinity conditions.

To summarize, the use of amphoteric terpolymers, specifically TPA-I terpolymer, significantly enhances the rheological properties of bentonite/polymer dispersions. The use of TPA-I increased viscosity, yield stress, and gel strength of drilling formulations. The BT/TPA-I dispersion demonstrates particularly superior rheological properties at high salinity levels of 25 and 35 wt.% NaCl and 25 °C. As a result, it is considered a suitable choice for drilling fluid applications.

5.3 Comparative rheological behavior of different drilling fluids at a high salinity (35 wt. %) of brine

Figure 5.7 (a) demonstrates the viscosity versus shear rate for bentonite suspensions prepared in distilled water and 35 wt.% NaCl brine. As can be seen, bentonite suspension in distilled water possesses sufficiently higher viscosity values within the range of shear rates from 1 to 1000 s⁻¹. This can be explained by the swelling of bentonite in distilled water. However, in high salinity brines the effect of swelling the clay particles is less pronounced due to the presence of ions.

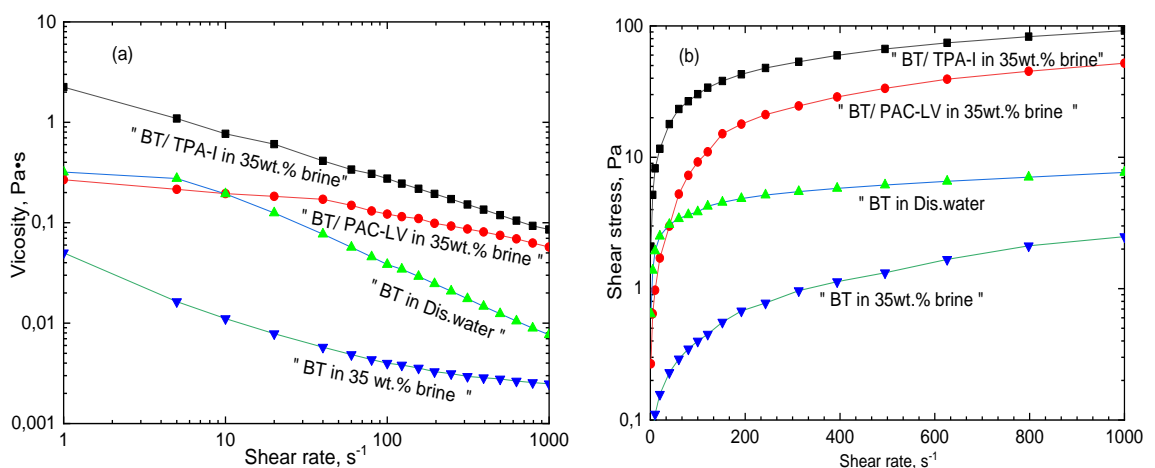


Figure 5.7 - Viscosity (a) and flow curves (b) of different drilling fluid formulations prepared in 35 wt.% NaCl brine at 25 °C

The introduction of PAC-LV resulted in the increase of viscosity at 5 s^{-1} from 0.0164 to 0.215 Pa·s. However, the introduction of TPA-I resulted in the increase of viscosity to 1.09 Pa·s in the same conditions. Of note is that at 1000 s^{-1} the viscosity of BT/TPA-I was 1.5 times higher than that of BT/PAC-LV.

BT in distilled water (base fluid) and BT/TPA-I in 35 wt.% NaCl dispersions exhibited the highest yield stress values of 0.64 and 2.99 Pa, respectively (Fig.6.7(b)). However, when 4% bentonite was added to a high salinity solution (35 wt.% NaCl) and stirred at 1000 rpm for 30 minutes, it formed a suspension. Subsequently, the suspension was left undisturbed for 24 hours to allow the bentonite particles to swell. Afterward, a portion of the bentonite particles separated from the suspension, with some settling and others remaining in suspension.

The comparative filter cakes in deionized water and 35 wt.% brine after their API filtration tests are shown in Fig.5.8.

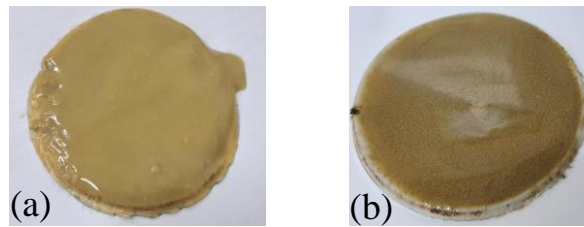


Figure 5.8 - The bentonite-based filter cakes formed by BT in deionized water (a) and 35 wt. % NaCl brine (b)

Table 5.2 - Rheological parameters of Herschel-Bulkley model for different formulations of bentonite and bentonite/polymers

Drilling fluid formulations	YS(pa)	K(Pa·s ⁿ)	n
BT + 35wt.% brine	0.05	0.01	0.02
BT + Dis. water	0.64	0.27	0.05
BT/PAC-LV + 35 wt.% brine	0.24	0.12	0.04
BT/TPA-I + 35 wt.% brine	2.99	1.1	0.22

* YS - yield stress, K - consistency coefficient, n- flow behavior index

As Table 5.2 shows, the lowest yield stress (0.05 Pa) and consistency coefficient (0.01 Pa·sⁿ) were observed for bentonite suspension prepared by using 35 wt.% NaCl brine. Whereas the highest yield stress (2.99 Pa) and consistency coefficient (1,1 Pa·sⁿ) were observed for bentonite/TPA-I formulation in 35 wt.% NaCl brine.

5.4 Fluid loss tests

In all filtration tests the resulting filtrate appeared colorless, indicating that it mainly consisted of water. However, the initial attempt to perform the fluid-loss filtration test using BT/35 wt.% NaCl brine was unsuccessful. The filter cake formation was inadequate, leading to the complete loss of water from the bentonite/brine dispersion. This failure could be attributed to the presence of a channel at the center of the filter cake.

Figure 5.9 shows the fluid loss versus time for different formulations. The findings reveal a notably higher initial filtration rate in the first 5 minutes, which can be attributed to the absence of a filter cake structure at the beginning of the filtration process. Following this, the filtration rate progressively decreases in 5 minute intervals, indicating the gradual formation of the filter cake. Among the different formulations, the bentonite/distilled water dispersion demonstrates the highest fluid loss. This discovery suggests that the addition of polymers to the bentonite dispersion enhances filtration performance and mitigates the extent of fluid loss.

In the fluid-loss tests with bentonite/distilled water, the filter cake exhibited small pores and channels, which allowed for increased water flow and resulted in a high volume of filtrate. However, upon the addition of polymers to the bentonite dispersions, the filtration rate and total fluid loss noticeably decreased. This reduction in fluid loss can be attributed to the adsorption of polymer molecules onto the bentonite platelets. The presence of long linear chain molecules in the terpolymer prevents water penetration through the filter cake and forms a stable, thin layer that blocks the filter cake pores. This is depicted in Figure 5.9 The filtration performance of the bentonite and bentonite/polymer dispersions exhibited a distinct trend in terms of fluid-loss values. Specifically, for a filtration duration of 30 minutes, the observed trend was the following: BT/TPA-I < BT/PAC-LV < BT + Distilled water (base fluid).

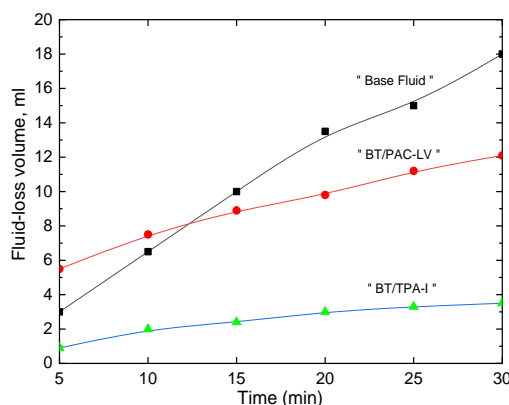


Figure 5.9 - Fluid loss volume vs time for bentonite/dis. water (base fluid), bentonite/ATP terpolymer and bentonite/PAC-LV polymer dispersions in 35 wt.% NaCl at 25 °C

5.4.1 Permeability of filter cakes and SEM analysis

The BT/TPA-I formulation with high salinity exhibited a significantly lower fluid-loss volume, measuring only 3.5 ml, which is well below the API standard limit of 12 ml. Furthermore, the filter cake thickness was measured at 0.09 cm, and the permeability of the filter cake was determined to be 1.17 mD. The thinness and low permeability of the filter cake contributed to the minimal volume of fluid loss.

The results suggest that the TPA-I terpolymer shows promising potential in reducing fluid loss in water-based drilling fluids (WBDF) when operating under high salinity conditions and at room temperature.

Table 5.3 - Fluid loss, thickness and permeability of filter cakes after fluid-loss filtration tests

Drilling fluid formulations	Filtrate volume V_f, cm^3	Filter cake thickness h_c, cm	Permeability of filter cakes K, mD	Ratio of permeability to thickness $k/h_c, \text{mD/cm}$
BF	18	0.35	15.3	43.71
BT + 35% brine	loss	0.41	26.7	65.12
BT/PAC-LV + 35% brine	12.1	0.18	7.9	43.89
BT/TPA-I + 35% brine	3.5	0.09	1.17	13

Table 5.3 presents the permeability of the filter cakes after fluid-loss filtration. Among the tested formulations, the BT/35 wt.% brine dispersion exhibited the highest permeability value (26.7 mD), along with a filter cake thickness of 0.41 cm. In comparison, the addition of PAC-LV and TPA-I polymers to the BT dispersion resulted in a significant reduction in permeability to 7.9 and 1.17 mD, respectively, accompanied by a decrease in filter cake thickness to 0.18 and 0.09 cm, respectively.

Specifically, PAC-LV dispersion shows a 3.3 times reduction in permeability, while the BT/TPA-I dispersion exhibits a substantial 22.8 times reduction in permeability. In addition to its lower permeability, the BT/TPA-I dispersion exhibits the minimum filter cake thickness compared to all other BT and BT/polymer dispersions.

Four SEM images of the filter cakes were taken to examine the impact of bentonite and terpolymers on their surface morphology. Among all the filter cake SEM analyses, the filter cake produced by the BT/TPA-I dispersion exhibited the most compact structure compared to the filter cakes of other BT and BT/polymer dispersions (see Fig.5.10).

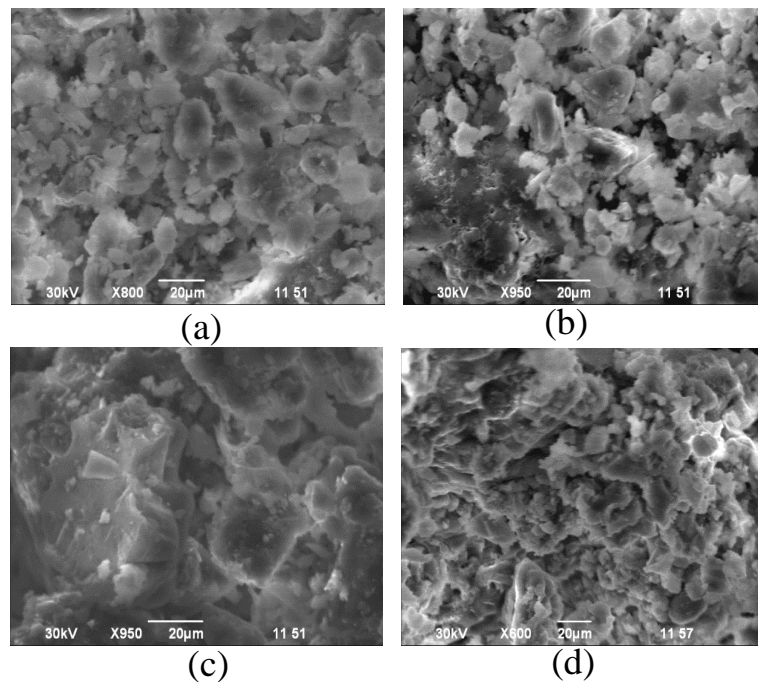


Figure 5.10 - SEM images of bentonite/polymer based mud cakes after fluid-loss filtration test at 25 °C;

(a) sample 4% BT in deionized water (without polymer); (b) sample 4% BT + 35 % NaCl brine (without polymer); (c) sample 4 % BT + 2 % TPA-I + 35 % NaCl brine; (e) sample 4 % BT+2 % PAC-LV+ 35 % NaCl brine

The images represented in Figures 5.10 (a) and 5.10 (b) display the filter cake formed by BT dispersions, exhibiting an open structure characterized by numerous micro cracks, scattered arrangements, and nanopores. The presence of these nanopores contributes to the highest levels of permeability and thickness observed in the filter cake of BT dispersions. However, when TPA-I terpolymer is incorporated into the BT dispersions containing high salinity, notable improvements in the texture of the filter cakes are observed.

The reduced permeability of the BT/polymer dispersion filter cakes can be attributed to the bridging mechanism between BT micro-particles and nanoscale polymer chains. The bridging between BT platelets and polymer chains leads to the formation of a multilayer thin structure in the filter cake, resulting in a more compact and compressed structure. Upon evaluating all the filter cakes, it becomes apparent that the filter cake derived from the BT/TPA-I dispersion, as shown in Figure 5.10 (c), exhibits a highly compact structure with the lowest permeability and thickness compared to the filter cakes of other formulations (Table 5.3).

It is important to note that the filter cake obtained from the BT/TPA-I dispersion outperforms the BT/PAC-LV filter cake. The BT/TPA-I filter cake is characterized by a homogeneous nanostructure, suggesting a more uniform and compact arrangement.

5.5 On the mechanism of stabilization drilling fluids by ternary polyampholyte

Earlier [110, 111] we have shown that the charged-balanced polyampholyte based on AAm-*co*-AMPS-*co*-APTAC (80:10:10 mol.%) exhibits excellent salt tolerance in high saline synthetic brine (containing NaCl, KCl, MgCl₂, and CaCl₂ salts) in the range of salt concentrations from 250 to 300 g.L⁻¹. Such behavior of TPA was explained by so called antipolyelectrolyte effect as a result of screening the positively and negatively charged monomers by added salts leading to expansion (or unfolding) the macromolecular chains. Therefore, for ternary polyampholyte AAm-*co*-AMPS-*co*-APTAC (80:10:10 mol.%) an increase in solution viscosity and a significant enhancement in rheological properties in high salinity brine is observed. Authors [85,195-198] also developed highly salt-resistant drilling fluids based on various polyampholytes with bentonite and cationic copolyelectrolytes additives on drilling fluids for shales [199, 200]. In our case, application of the ternary polyampholyte (TPA-I) noticeably enhanced the rheological properties of bentonite/polymer dispersions, such as apparent viscosity, yield stress, and gel strength, even in high salinity (35 wt. %) NaCl brine at 25 °C. As a result, it was considered a suitable choice for drilling fluid applications. The excellent rheological properties of the BT/TPA-I dispersion can be attributed to the strong chemical interactions between the functional groups of the terpolymer and the positively

charged edges of the bentonite platelets. The interaction between bentonite and ternary polyampholyte in brine can be explained by two distinct mechanisms. The first mechanism is adsorption of terpolymer onto bentonite. The second mechanism is ionic interaction between the negatively charged functional groups of macromolecules and the positively charged edges of bentonite platelets [175] (see Fig. 5.11).

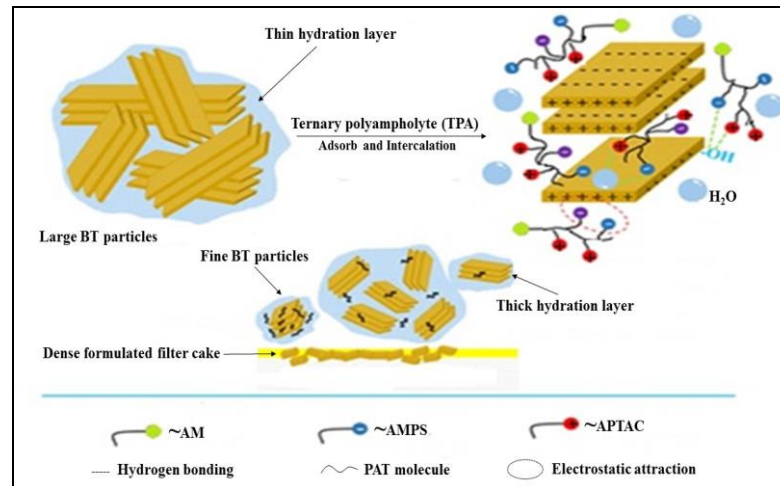


Figure 5.11 - Schematic representation of interaction between bentonite platelets and TPA chains

CHAPTER 6. Application of AMPS-*co*-APTAC-*co*-ANB (50:49:1 mol.%) terpolymer as tracer agent

6.1 Synthesis and identification of AMPS-*co*-APTAC-*co*-ANB terpolymer

Ternary polyampholyte AMPS-*co*-APTAC-*co*-ANB containing acrylamide Nile Blue (ANB) was synthesized *via* conventional free radical (co)polymerization at the molar ratio of initial monomers [AMPS]:[APTAC]:[ANB] = 50:49:1 mol.% in the presence of APS at 60 °C during 4 h (Figure 6.1).

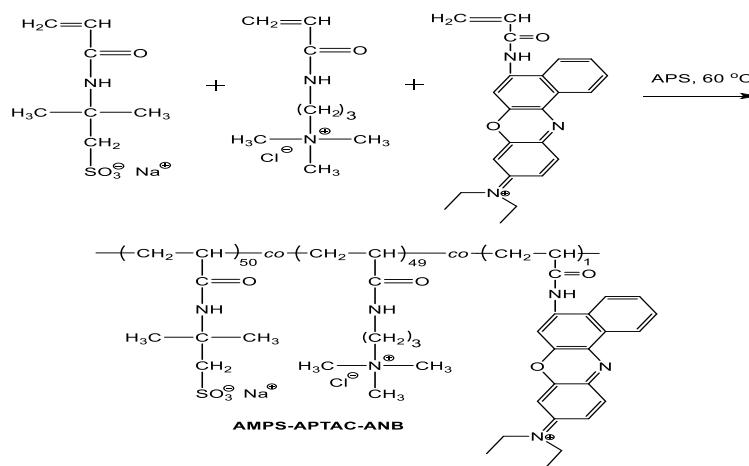


Figure 6.1- Synthetic protocol of AMPS-*co*-APTAC-*co*-ANB terpolymer

6.2 Identification of AMPS-*co*-APTAC-*co*-ANB terpolymer from FTIR spectrum

FTIR spectra of AMPS-APTAC (50:50 mol.%) and AMPS-*co*-APTAC-*co*-ANB (50:49:1 mol.%) are identical, meaning that 1 mol.% of ANB in terpolymer composition does not influence on the characteristic bands of polyampholytes [202].

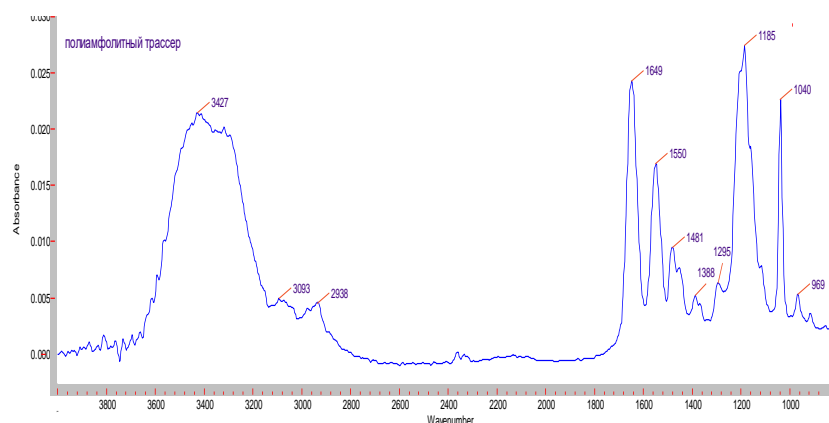


Figure 6.2 - FTIR spectrum AMPS-*co*-APTAC-*co*-ANB

Identified functional groups of the AMPS-*co*-APTAC-*co*-ANB terpolymer from FTIR spectrum (as seen in Figure 6.2) are shown in Table 6.1.

Table 6.1- Identification of FTIR spectrum of AMPS-*co*-APTAC-*co*-ANB

Functional groups	ν (NH)	ν (CH)	ν (CONH) Amide I	ν (CONH) Amide II	(CH)	ν (S=O)
Band assignments, cm^{-1}	3427	2938	1649	1550	1185	1040, 969

6.3 The average hydrodynamic size and zeta potential of AMPS-*co*-APTAC-*co*-ANB terpolymer

The average hydrodynamic size and zeta potential of AMPS-*co*-APTAC-*co*-ANB in aqueous solution are equal to 4.3 nm and $\xi = -1.6$ mV that indicate on globular conformation of amphoteric macromolecules with slightly negative surface charge (see Fig. 6.3).

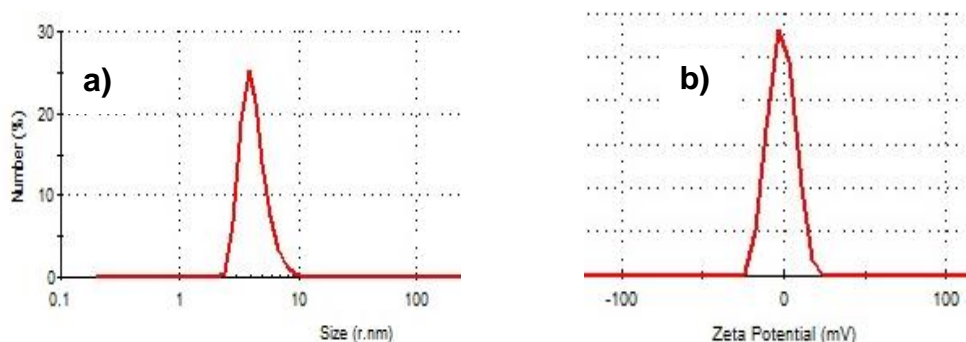


Figure 6.3 -The average hydrodynamic diameter (a) and the value of zeta-potential (b) of AMPS-*co*-APTAC-*co*-ANB in aqueous solution

6.4 UV-Vis spectra of AMPS-*co*-APTAC-*co*-ANB in aqueous solution

The UV-Vis spectra of AMPS-*co*-APTAC-*co*-ANB in aqueous solution exhibit well defined absorption maximum at $\lambda_{\text{max}} = 586$ nm that is attributed to ANB group of terpolymer (Fig.6.4).

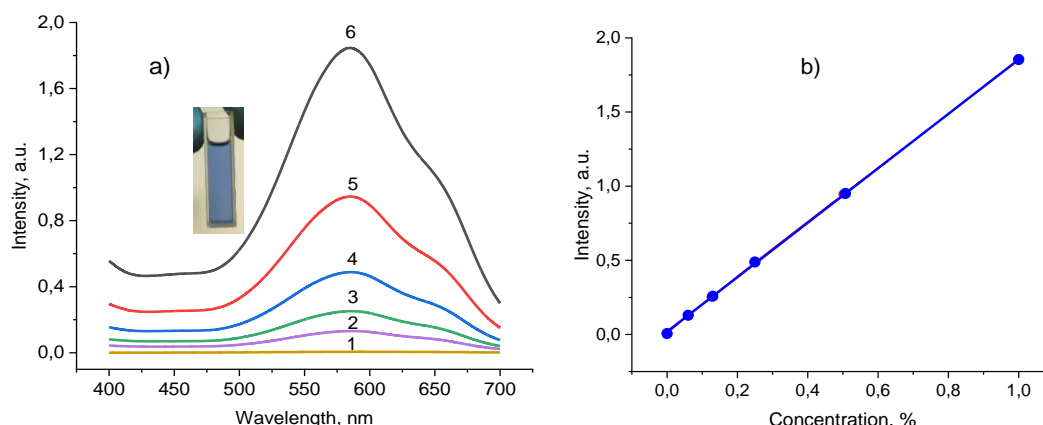


Figure 6.4 - UV-Vis spectra of AMPS-*co*-APTAC-*co*-ANB in aqueous solution (a) and calibration graph (b) plotted in coordinates “intensity-concentration” at concentration of [AMPS-APTAC-ANB] = 0 (1), 0.0625 (2), 0.125 (3), 0.25 (4), 0.5 (5) and 1.0 wt.% (6)

In pure water the AMPS-*co*-APTAC-*co*-ANB macromolecules are in globular state due to electrostatic attraction between oppositely charged monomer units. It is likely that the ANB molecules due to more hydrophobic character are replaced inside of globules as shown in Fig.6.5. It is expected that due to slightly negative surface charge of the AMPS-*co*-APTAC-*co*-ANB ($\xi = -1.6$ mV) its adsorption to negatively charged surface of core materials is minimal or even excluded.

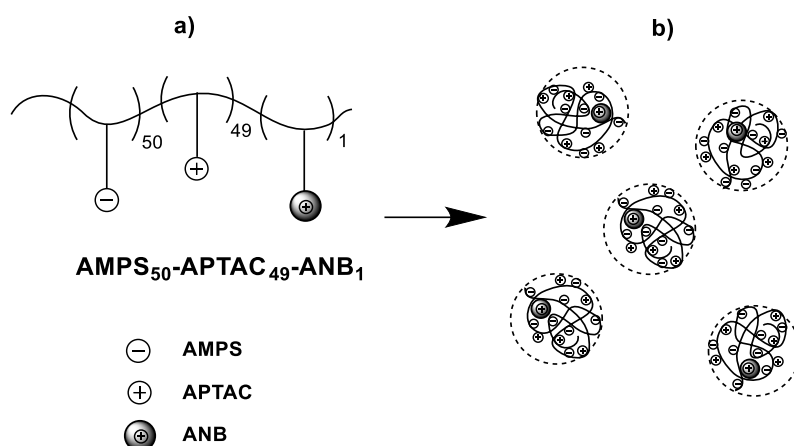


Figure 6.5 - Schematic representation of structural unit of amphoteric terpolymer AMPS-*co*-APTAC-*co*-ANB (a) and formation of globular structure (b) in dilute aqueous solution

6.5 Core flooding experiment with AMPS-*co*-APTAC-*co*-ANB solution

The fluorescence-detection technology attracts considerable interest in oilfield operations [203] due to many advantages over radioactive isotopes, ionic and organic tracers [204]. For evaluation of inter-well permeability and porosity, the authors [205] used fluorescent polyacrylamide microspheres, which fluoresce under ultraviolet irradiation. A water-soluble fluorescent polymer was prepared as a combination of a flooding agent and tracer by introducing a polymerizable rigid fluorescent coumarin monomer into polyacrylamide chains [206]. Fluorescent polymer microspheres were also obtained via the inverse suspension polymerization method with Rhodamine B as a fluorescence functional monomer [207]. As distinct from the abovementioned researches, in our case we have introduced a trace amount of fluorescent monomer ANB into the composition of AMPS-APTAC quenched polyampholyte to obtain globular and fully electroneutral macromolecular chains to minimize or exclude their adsorption to the rock. The advantages of our approach are that the QPA of equimolar composition is water-soluble, salt tolerant and adopts globular and quasi-electroneutral conformation in aqueous solution due to mutually compensation of positive and negative charges. The core flooding experiments were conducted in the following sequence. At first, 40 mL of distilled water was injected into the core sample at 1 mL·min⁻¹. In the course of water injection, the pressure sharply increased during 5 min and leveled off at P=0.08-0.10 MPa during 10-90 min. The effluents were slightly turbid due to washing out of fine dispersed microparticles containing in core sample. On the next stage 50 mL, 0.1 wt.% (or

$1.3 \cdot 10^{-3} \text{ mol} \cdot \text{L}^{-1}$) aqueous solution of AMPS-*co*-APTAC-*co*-ANB were injected into the core sample preliminary washed out by distilled water (Fig.6.6). The injection rate of AMPS-*co*-APTAC-*co*-ANB was equal to $0.1 \text{ mL} \cdot \text{min}^{-1}$. In the course of the test the injection pressure was increasing gradually and blue color appeared in the collected effluents.

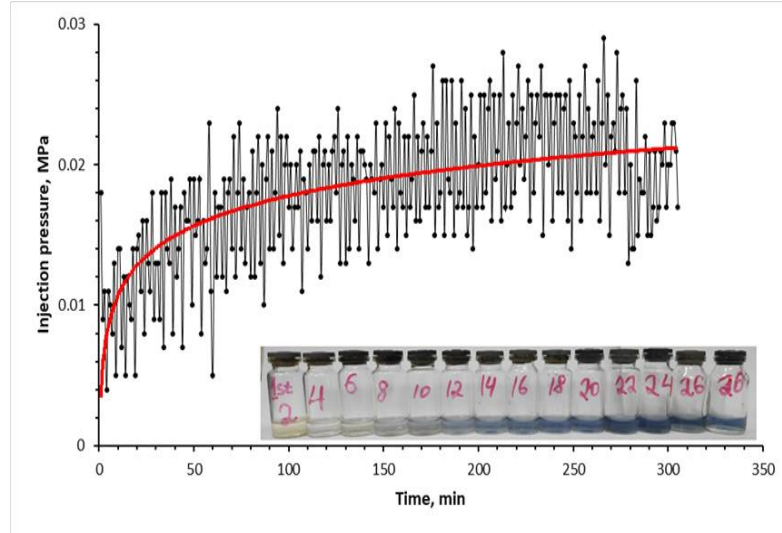


Figure 6.6 -Time-dependent change of pressure upon injection of AMPS-*co*-APTAC-*co*-ANB solution into core sample and vials of collected effluents at $T = 25 \text{ }^{\circ}\text{C}$

Chase saline water flooding with salinity $100 \text{ g} \cdot \text{L}^{-1}$ shows the linear increasing of the pressure and replacement of residual amount of AMPS-*co*-APTAC-*co*-ANB entrapped within the core (see Fig.6.7).

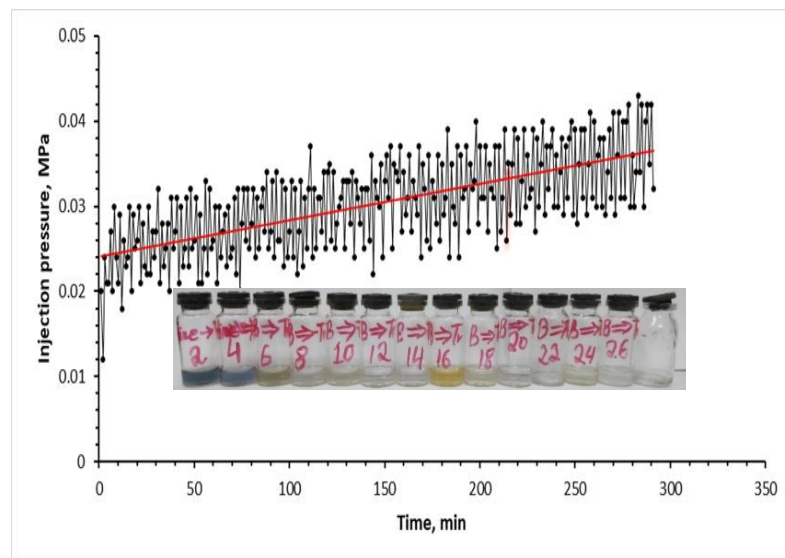


Figure 6.7 -Time-dependent change of pressure upon injection of saline water from “Vostochnyi Moldabek” with salinity $100 \text{ g} \cdot \text{L}^{-1}$ into the core sample after the injection of AMPS-*co*-APTAC-*co*-ANB and vials of collected effluents at $T = 25 \text{ }^{\circ}\text{C}$. The injection rate is $0.1 \text{ mL} \cdot \text{min}^{-1}$

6.6 The absorption tests of amphoteric terpolymer AMPS-*co*-APTAC-*co*-ANB aqueous solution on the rock

Colorization of initial 3 fractions of passed saline water confirm the replacement of AMPS-*co*-APTAC-*co*-ANB in core sample by saline water. The effluents were analyzed by UV-Vis at $\lambda_{\max} = 586$ nm and fluorescence spectrophotometer at emission wavelength $\lambda_{\max} = 660$ -680 nm (λ_{\max} of pure ANB in water is 674 nm) to determine the concentration of AMPS-*co*-APTAC-*co*-ANB passed through the core and displaced by saline water (see Fig.6.8).

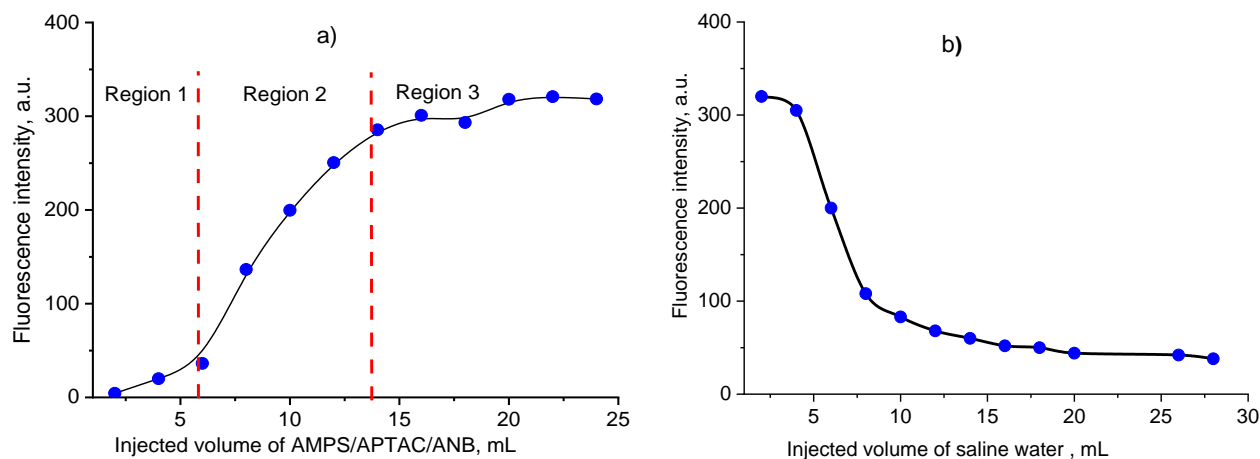


Figure 6.8 - Dependence of the fluorescent intensity of 0.1 wt.% aqueous solution of AMPS-*co*-APTAC-*co*-ANB on injected volume of polymer (a) and saline water (b)

The fluorescence intensity of AMPS-*co*-APTAC-*co*-ANB gradually increases after injection of the first 6 mL of polyampholyte solution (Region 1). This is probably due to dilution of polyampholyte by residual distilled water left in core sample. Sharp increase of the fluorescence intensity takes place after injection of 7 mL of polyampholyte solution through the core. It means that the main portion of AMPS-*co*-APTAC-*co*-ANB passes through the core in Region 2. The fluorescence intensity of AMPS-*co*-APTAC-*co*-ANB levels off in Region 3 after injection of 12-25 mL of polyampholyte solution meaning that the core sample is fully saturated by fluorescence-labeled polyampholyte. Pumping of saline water with mineralization $100 \text{ g}\cdot\text{L}^{-1}$ to the core saturated by 0.1 wt.% AMPS-*co*-APTAC-*co*-ANB leads to gradually decreasing of the fluorescence intensity of polyampholyte solution. It is connected with replacement of AMPS-*co*-APTAC-*co*-ANB by saline water. After injection of 28 mL saline water the fluorescence, intensity of AMPS-*co*-APTAC-*co*-ANB decreases up to 38.5 a.u. It is 10 times lower than the initial concentration of AMPS-*co*-APTAC-*co*-ANB solution injected to the core (389 a.u.). Thus, approximately 90% of AMPS-*co*-APTAC-*co*-ANB is replaced from the core sample by saline water without precipitation, destruction and adsorption on the rock. Thus, the novel QPA based on AMPS-*co*-APTAC-*co*-ANB may be promising tool for evaluation of interwell and interlayer connections, as well as heterogeneities of oil reservoirs.

CONCLUSION

A novel high molecular weight ternary polyampholyte (TPA) was successfully synthesized and characterized, comprising 50-90 mol.% acrylamide (AAM) as a nonionic monomer, 5-25 mol. % 2-acrylamido-2-methyl-1-propanesulfonic acid sodium salt (AMPS) as an anionic monomer, and 5-25 mol. % (3-acrylamidopropyl) trimethylammonium chloride (APTAC) as a cationic monomer. The sample AAm-co-AMPS-co-APTAC=80:10:10 mol. % was chosen for the further sand pack and core flooding tests due to its highest viscosifying ability in high salinity brine.

The amphoteric terpolymer with an 80:10:10 mol. % composition showed improved viscosifying behavior in high salinity media (163 g·L⁻¹ brine), attributed to its polyampholytic nature, making it promising for enhanced oil recovery (EOR) applications.

Sand pack flooding experiments with different AAm-co-AMPS-co-APTAC recipes resulted in only a 0.5 % increase in oil recovery factor (ORF). However, core flooding tests using AAm-co-AMPS-co-APTAC (80:10:10 mol.%) solution showed a significant 4.8-5 % ORF increase.

The increase in brine salinity from 200 to 300 g·L⁻¹ at 24 °C results in a noticeable increase in the dynamic viscosity of the 0.25 % TPA solution compared to the HPAM solution. However, the viscosity of HPAM suddenly falls at 300 g·L⁻¹ due to severe polymer precipitation. This phenomenon is explained by the poor solubility of HPAM at 270-300 g·L⁻¹. The obtained viscosity measurement results clearly demonstrate that the amphoteric terpolymer is more stable at high brine salinity than HPAM.

The injection of 0.25 % ternary polyampholyte (TPA) and HPAM solutions, prepared in 200 g·L⁻¹ brine, into the 0.62 and 1.77 Darcy sand packs, resulted in an increase of the ORF by 28 % and 18 %, respectively. These results demonstrate that the amphoteric terpolymer has a higher oil displacement capacity than HPAM. Moreover, the TPA solution showed greater resilience to viscosity reduction after aging at room temperature compared to HPAM. After 15 days of aging, the viscosity reduction was 18.2 % in TPA, but 28 % in HPAM.

The application of ternary polyampholytes significantly enhances the rheological properties of bentonite/polymer drilling fluids, with all BT/TPA formulations exhibiting shear-thinning behavior within the 1-35 wt. % NaCl salinity range. TPA addition notably reduces the filter cake thickness to 0.09 cm, outperforming bentonite/PAC-LV (0.18 cm) and bentonite alone (0.41 cm). Moreover, the bentonite/TPA drilling fluid shows the lowest permeability-to-thickness ratio at 13 mD/cm, indicating its potential as a rheology enhancer and fluid loss additive for salt-resistant Water-Based Drilling Fluids. It is considered a suitable choice for drilling fluid applications due to these favorable properties. The excellent rheological properties of the BT/TPA dispersion can be attributed to the strong chemical interactions between the functional groups of the terpolymer and the positively charged edges of the bentonite platelets.

A novel ternary polyampholyte consisting of 50 mol. % of the anionic monomer – AMPS, 49 mol. % of the cationic monomer – APTAC, and 1 mol. % of

the cationic fluorescent dye – ANB, was synthesized and characterized as an oilfield tracer. The globular, electroneutral, and nanometric-sized macromolecules of AMPS-*co*-APTAC-*co*-ANB = 50:49:1 mol.% in aqueous and aqueous-salt solutions have proven to be efficient in minimizing adsorption on the rock, leading to a 90 % recovery factor upon injection of a 0.1 wt.% (or $1.3 \times 10^{-3} \text{ mol}\cdot\text{L}^{-1}$) aqueous solution of AMPS-*co*-APTAC-*co*-ANB into the core. It is expected that the novel AMPS-*co*-APTAC-*co*-ANB formulation might be useful as an appropriate polymer tracer for monitoring oil wells.

ACKNOWLEDGMENTS

This research was funded by the Science Committee of the Ministry of Education and Science of the Republic of Kazakhstan (Grant No. AP08855552, Grant No. AP09260574, Grant No. AP14972771). I thank Prof. Nurxat Nuraje and PhD. Munziya Abutalip at Nazarbayev University for provision of assistance in providing of H^1 and ^{13}C -NMR, TEM and elemental analysis.

REFERENCES

1. Kudaibergenov, S. E. (n.d.). Recent Advances in the Study of Synthetic Polyampholytes Solutions. *Advances in Polymer Science*, 115–197. doi:10.1007/3-54068384-4_3
2. Kudaibergenov S.E. (2002). *Polyampholytes: Synthesis, Characterization and Application*. Kluwer Academic/Plenum Publishers, New York, Boston, Dordrecht, Tokyo, Moscow, 220 p.
3. Dobrynin, A. V., Colby, R. H., & Rubinstein, M. (2004). Polyampholytes. *Journal of Polymer Science Part B: Polymer Physics*, 42(19), 3513–3538. doi:10.1002/polb.20207
4. Kudaibergenov S. E., Tatykhanova G. S., Klivenko A. N. Complexation of macroporous amphoteric cryogels based on N, N-dimethylaminoethyl methacrylate and methacrylic acid with dyes, surfactant, and protein // *Journal of Applied Polymer Science*. – 2016. – T. 133, № 32. – P. 9.
5. Dyakonova M. A., Berezkin A. V., Kyriakos K., Gkermpoura S., Popescu M. T., Filippov S. K., Stepanek P., Di Z. Y., Tsitsilianis C., Papadakis C. M. Salt-Induced Changes in Triblock Polyampholyte Hydrogels: Computer Simulations and Rheological, Structural, and Dynamic Characterization // *Macromolecules*. – 2015. – T. 48, № 22. – P. 8177-8189.
6. Alfrey T. Structure property relationships in polymers // *Acs Symposium Series*. – 1985. – T. 285. – P. 241-252.
7. Nair A. K. N., Jimenez A. M., Sun S. Y. Complexation Behavior of Polyelectrolytes and Polyampholytes // *Journal of Physical Chemistry B*. – 2017. – T. 121, № 33. – P. 7987-7998.
8. Batyrbekov A. A., Evdakov V. P., Kabanov V. A., Kozhinova E. V., Petrov R. V., Savinova I. V., Fedoseyeva N. A., Khaitov R. M., Khaustova L. I. Study of mechanism of polyelectrolyte and polyampholyte action on immune-response // *Tsitologiya*. – 1976. – T. 18, № 10. – P. 1259-1263.
9. Bekturov E. A., Kudaibergenov S. E., Zhaimina G. M. Reaction of synthetic styrene polyampholyte-copolymer and n, n-dimethylaminopropylmonoamide of maleic-acid, with Cu^{2+} and Fe^{3+} ions in aqueous-solution // *Koordinatsionnaya Khimiya*. – 1984. – T. 10, № 7. – P. 942-946.
10. Dobrynin A. V., Rubinstein M., Joanny J. F. Polyampholyte solutions between charged surfaces: Debye-Huckel theory // *Journal of Chemical Physics*. – 1998. – T. 109, № 20. – P. 9172-9176.
11. Kudaibergenov S., Jaeger W., Laschewsky A. Polymeric betaines: Synthesis, characterization, and application // *Supramolecular Polymers Polymeric Betains Oligomers / Donnio B. и др.* – Berlin: Springer-Verlag Berlin, 2006. – P. 157-224.
12. Baker J. P., Blanch H. W., Prausnitz J. M. Swelling properties of acrylamide-based ampholytic hydrogels - comparison of experiment with theory // *Polymer*. – 1995. – T. 36, № 5. – P. 1061-1069.

13. Ali S. A., Rasheed A. Synthesis and solution properties of a betaine-sulfur dioxide polyampholyte // *Polymer*. – 1999. – T. 40, № 24. – P. 6849-6857.
14. McCormick C. L., Salazar L. C. Water-soluble copolymers .46. Hydrophilic sulfobetaine copolymers of acrylamide and 3-(2-acrylamido-2-methylpropanedimethyl-ammonio)-1-propanesulphonate // *Polymer*. – 1992. – T. 33, № 21. – P. 4617-4624.
15. Ali M. M., Perzanowski H. P., Ali S. A. Polymerization of functionalized diallyl quaternary ammonium salt to poly (ampholyte-electrolyte) // *Polymer*. – 2000. – T. 41, № 15. – P. 5591-5600.
16. Sun, T. L., Kurokawa, T., Kuroda, S., Ihsan, A. B., Akasaki, T., Sato, K., ... & Gong, J. P. (2013). Physical hydrogels composed of polyampholytes demonstrate high toughness and viscoelasticity. *Nature materials*, 12(10), 932-937.
17. Patrickios, C. S., Hertler, W. R., Abbott, N. L., & Hatton, T. A. (1994). Diblock, ABC triblock, and random methacrylic polyampholytes: synthesis by group transfer polymerization and solution behavior. *Macromolecules*, 27(4), 930–937. Doi: 10.1021/ma00082a008
18. Sanjuan, S., & Tran, Y. (2008). Synthesis of random polyampholyte brushes by atom transfer radical polymerization. *Journal of Polymer Science Part A: Polymer Chemistry*, 46(13), 4305–4319. doi:10.1002/pola.22726
19. Kantor, Y., & Kardar, M. (1995). Instabilities of charged polyampholytes. *Physical Review E*, 51(2), 1299.
20. Kuznetsov, Y. A., Timoshenko, E. G., & Dawson, K. A. (1995). Kinetics at the collapse transition of homopolymers and random copolymers. *The Journal of chemical physics*, 103(11), 4807-4818.
21. Dobrynin, A. V., & Rubinstein, M. (1995). Flory Theory of a Polyampholyte Chain. *Journal de Physique II*, 5(5), 677–695. Doi: 10.1051/jp2:1995157
22. Salamone, J.C., Ahmed, I., Raheja, M.K, Elayaperumal, P., Watterson, A.C, Olson, A.P. (1988) Behavior of Polyampholytes in Aqueous Salt Solution. In: Stahl, G.A., Schulz, D.N.(eds) *Water-Soluble Polymers for Petroleum Recovery*. Springer, Boston, MA. https://doi.org/10.1007/978-1-4757-1985-7_11
23. Afolabi, F., Ojo, T., Udeagbara, S., Gbadamosi, A.: Bitumen extraction from tar sands using solvent techniques. *Int. J. Sci. Eng. Res.* 8, 783–790 (2017)
24. Giriki, S.O., Agunloye, M.A., Gbadamosi, A.O., Olafuyi, A.O.: Exploitation of Bitumen from Nigerian tar sand using hot-water/steam stimulation process. *Pet. Coal* 58, 407–413 (2016). <https://doi.org/10.1021/ac010415i>
25. Agi, A., Junin, R., Syamsul, M.F., Chong, A.S., Gbadamosi, A.: Intermittent and short duration ultrasound in a simulated porous medium. *Petroleum* (2018). <https://doi.org/10.1016/j.petlm.2018.03.012>
26. Gbadamosi, A.O., Junin, R., Manan, M.A., Yekeen, N., Augustine, A.: Hybrid suspension of polymer and nanoparticles for enhanced oil recovery. *Polym. Bull.* (2019). <https://doi.org/10.1007/s00289-019-02713-2>

27. Agi, A., Junin, R., Shirazi, R., Afeez, G., Yekeen, N.: Comparative study of ultrasound assisted water and surfactant flooding. *J. King Saud. Univ. Eng. Sci.* (2018). <https://doi.org/10.1016/j.jksues.2018.01.002>
28. Hanamertani, A.S., Pilus, R.M., Idris, A.K., Irawan, S., Tan, I.M.: Ionic liquids as a potential additive for reducing surfactant adsorption onto crushed Berea sandstone. *J. Pet. Sci. Eng.* 162, 480–490 (2018). <https://doi.org/10.1016/j.petro.2017.09.077>
29. Kamal, M.S., Hussein, I.A., Sultan, and A.S.: Review on surfactant flooding: phase behavior, retention, IFT, and field applications. *Energy Fuels* 31, 7701–7720 (2017). <https://doi.org/10.1021/acs.energyfuels.7b00353>
30. Olajire, A.A.: Review of ASP EOR (alkaline surfactant polymer enhanced oil recovery) technology in the petroleum industry: prospects and challenges. *Energy* 77, 963–982 (2014). <https://doi.org/10.1016/j.energy.2014.09.005>
31. Thomas, S.: Enhanced oil recovery—an overview. *Oil. Gas. Sci. Technol. Rev. L'IFP* 63, 9–19 (2007). <https://doi.org/10.2516/ogst:2007060>
32. Khalilinezhad, S.S., Cheraghian, G., Karambeigi, M.S., Tabatabaee, H., Roayaei, E.: Characterizing the role of clay and silica nanoparticles in enhanced heavy oil recovery during polymer flooding. *Arab. J. Sci. Eng.* 41, 2731–2750 (2016). <https://doi.org/10.1007/s13369-016-2183-6>
33. Levitt, D., Pope, G.A.: Selection and screening of polymers for enhanced-oil recovery. In: *Present. SPE Symp. Improv. Oil Recover.* 20–23 April. Tulsa, Oklahoma, USA, Society of Petroleum Engineers, pp. 1–18 (2008). <https://doi.org/10.2118/113845-ms>.
34. Sun, X., Zhang, Y., Chen, G., Gai, Z.: Application of nanoparticles in enhanced oil recovery: a critical review of recent progress. *Energies* 10, 345 (2017). <https://doi.org/10.3390/en10030345>
35. Liu, X., Jiang, W., Gou, S., Ye, Z., Feng, M., Lai, N., & Liang, L. (2013). Synthesis and evaluation of novel water-soluble copolymers based on acrylamide and modular β -cyclodextrin. *Carbohydrate polymers*, 96(1), 47-56.
36. Ohlemacher, A., Candau, F., Munch, J. P., & Candau, S. J. (1996). Aqueous solution properties of polyampholytes: Effect of the net charge distribution. *Journal of Polymer Science Part B: Polymer Physics*, 34(16), 2747-2757.
37. McCormick, C. L., & Johnson, C. B. (1988). Water-soluble copolymers. 29. Ampholytic copolymers of sodium 2-acrylamido-2-methylpropanesulfonate with (2-acrylamido-2-methylpropyl) dimethylammonium chloride: solution properties. *Macromolecules*, 21(3), 694–699. doi:10.1021/ma00181a026
38. McCormick C. L., Johnson C. B. Water-soluble polymers: 33. Ampholytic terpolymers of sodium 2-acrylamido-2-methylpropanesulphonate with 2-acrylamido-2-methylpropanedimethylammonium chloride and acrylamide: synthesis and aqueous-solution behaviour // *Polymer*. – 1990. – T. 31. – №. 6. – C. 1100-1107.
39. McCormick C. L., Salazar L. C. Water-soluble copolymers. XLV. Ampholytic terpolymers of acrylamide with sodium 3-acrylamido-3-methylbutanoate

and 2-acrylamido-2-methylpropanetrimethylammonium chloride //Journal of applied polymer science. – 1993. – T. 48. – №. 6. – C. 1115-1120.

40. Fevola, M. J., Ezell, R. G., Bridges, J. K., & McCormick, C. L. (2003). Ion-Containing Acrylamide Copolymers with PH-and Salt-Responsive Behavior. In Abstracts of Papers of the American Chemical Society (Vol. 225, p. U551).

41. Fevola, M. J., Kellum, M. G., Hester, R. D., & McCormick, C. L. (2004). PH-responsive ampholytic terpolymers of acrylamide, sodium 3-acrylamido-3-methylbutanoate, and (3-acrylamidopropyl) trimethylammonium chloride. II. Solution properties. *Journal of Polymer Science Part A: Polymer Chemistry*, 42(13), 3252-3270.

42. McCormick C. L., Salazar L. C. Water-soluble copolymers. 43. Ampholytic copolymers of sodium 2-(acrylamido)-2-methylpropanesulfonate with [2-(acrylamido)-2-methylpropyl] trimethylammonium chloride //Macromolecules. – 1992. – T. 25. – №. 7. – C. 1896-1900.

43. McCormick C. L., Blackmon K. P. Water-soluble copolymers. XII. Copolymers of acrylamide with sodium-3-acrylamido-3-methylbutanoate: Synthesis and characterization //Journal of Polymer Science Part A: Polymer Chemistry. – 1986. – T. 24. – №. 10. – C. 2635-2645.

44. Fevola M. J. Model polyzwitterions based on polyacrylamide: Synthesis, characterization, and stimuli-responsive solution behavior in aqueous media. – The University of Southern Mississippi, 2003.

45. Ezell, R. G., Gorman, I., Lokitz, B., Ayres, N., & McCormick, C. L. (2006). Stimuli-responsive ampholytic terpolymers of N-acryloyl-valine, acrylamide, and (3-acrylamidopropyl) trimethylammonium chloride: Synthesis, characterization, and solution properties. *Journal of Polymer Science Part A: Polymer Chemistry*, 44(9), 3125-3139.

46. Fevola, M. J., Bridges, J. K., Kellum, M. G., Hester, R. D., & McCormick, C. L. (2004). pH-Responsive ampholytic terpolymers of acrylamide, sodium 3-acrylamido-3-methylbutanoate, and (3-acrylamidopropyl)trimethylammonium chloride. I. Synthesis and characterization. *Journal of Polymer Science Part A: Polymer Chemistry*, 42(13), 3236–3251. doi:10.1002/pola.20173

47. McCormick C., Lowe A. "Smart" Multifunctional Polymers for Enhanced Oil Recovery. – University of Southern Mississippi, 2007.

48. Sorbie, K. S. *Polym Improved Oil Recovery* 1991, 1, 1. 40. Doe, P. H.; Needham, R. B. *Polym Flooding Rev* 1987, 1503.

49. Zhappasbaev, B., Gussenov, I., Shakhvorostov, A., Nuraje, N., & Kudaibergenov, S. (2016). Development of alkaline/surfactant/polymer (ASP) flooding technology for recovery of Karazhanbas oil. *Chemical Bulletin of Kazakh National University*, 81(1), 12-17. <https://doi.org/https://doi.org/10.15328/cb649>

50. Sorbie, K. S. *Polymer-Improved Oil Recovery*, CRC Press, Boca Raton, Florida (1991), 359p.

51. Bondino, I. Nguyen, R., Hamon, G., Ormehaug, P. A., Skauge, A., Jouenne, S. "Tertiary Polymer Flooding in Extra-Heavy Oil: An Investigation Using 1D and 2D Experiments, Core Scale Simulation and Pore-Scale Network Models",

International Symposium of the Society of Core Analysts, Austin, Texas, (2011), 12p.

52. Unsal, E., ten Berge, A. B. G. M., Wever, D. A. Z. "Low salinity polymer flooding: Lower polymer retention and improved injectivity", *J Pet Sci Eng*, (2018) 163:671–682. doi: 10.1016/j.petrol.2017.10.069

53. Dawson, R., Lantz, R. B. "Inaccessible Pore Volume in Polymer Flooding", *Soc Pet Eng J*, (1972) 12:448–452. doi: 10.2118/3522-PA

54. Moore, J. C. "Gel permeation chromatography. I. A new method for molecular weight distribution of high polymers", *J Polym Sci Part a Gen Pap*, (1964) 2:835–843. doi: 10.1002/pol.1964.100020220

55. Sorbie, K. S. "Depleted Layer Effects in Polymer Flow through Porous Media", *J Colloid Interface Sci*, (1990) 139:299–314. doi: 10.1016/0021-9797(90)90103-U

56. Omari, A., Moan, M., Chauveteau, G. "Wall effects in the flow of flexible polymer solutions through small pores". *Rheol Acta*, (1989) 28:520–526. doi: 10.1007/BF01332923

57. Stavland, A., Jonsbraten, H., Lohne, A., Moen, A., Giske, N. H. "Polymer Flooding - Flow Properties in Porous Media versus Rheological Parameters", *SPE EUROPEC/EAGE Annual Conference and Exhibition*, Barcelona, Spain, (2010), pp 14–17.

58. Chauveteau, G., Zaitoun, A. "Basic Rheological Behavior of Xanthan Polysaccharide Solutions in Porous Media: Effects of Pore Size and Polymer Concentration", *Proceedings to the European symposium on EOR*, (1981), pp 197–212.

59. API, "Recommended Practices for Evaluation of Polymers Used in Enhanced Oil Recovery Operations", (1990), 74p.

60. Wan, H., Seright, R. S. "Is Polymer Retention Different Under Anaerobic vs. Aerobic Conditions?", *SPE J*, (2017), 22:431–437. doi: 10.2118/179538-PA

61. Cardoso, O. R., Balaban, R. C. "Comparative study between Botucatu and Berea sandstone properties" *J South Am Earth Sci*, (2015), 62:58–69. doi: 10.1016/j.jsames.2015.04.004

62. Sandiford BB. Laboratory and field studies of water floods using polymer solution to increase oil recovery. *Journal of Petroleum Technology*. 1964; 16:917–922.

63. Szabo MT. Laboratory investigations of factors influencing polymer flood performance. *SPE Journal*. 1975; 15:338–346.

64. Dominguez JG, Willhite GP. Retention and flow characteristics of polymer solution in porous media. *SPE Journal*. 1977; 17:111–121.

65. Gleasure RW. An experimental study of non-Newtonian polymer rheology effects on oil recovery and injectivity. *SPE Reservoir Engineering*. 1990; 5:481–486.

66. Zaitoun, A., Makakou, P., Blin, N., Al-Maamari, R.S., Al-Hashmi, A.-A.R., Abdel-Goad, M.: Shear stability of EOR polymers. *SPE-141113-PA*. *SPE J*. 17, 335–339 (2012). <https://doi.org/10.2118/141113-pa>

67. Kumar, N., Gaur, T., Mandal, A.: Characterization of SPN pickering emulsions for application in enhanced oil recovery. *J. Ind. Eng. Chem.* 54, 304–315 (2017). <https://doi.org/10.1016/j.jiec.2017.06.005>
68. Bera, A., Kumar, T., Ojha, K., Mandal, A.: Adsorption of surfactants on sand surface in enhanced oil recovery: isotherms, kinetics and thermodynamic studies. *Appl. Surf. Sci.* 284, 87–99 (2013). <https://doi.org/10.1016/j.apsusc.2013.07.029>
69. Samin, A.M., Manan, M.A., Idris, A.K., Yekeen, N., Said, M., Alghol, A.: Protein foam application for enhanced oil recovery. *J. Dispers. Sci. Technol.* 38, 604–609 (2017). <https://doi.org/10.1080/01932691.2016.1185014>
70. Ko, S., Huh, C.: Use of nanoparticles for oil production applications. *J. Pet. Sci. Eng.* 172, 97–114 (2019). <https://doi.org/10.1016/j.petrol.2018.09.051>
71. Krishnamoorti, R.: Extracting the benefits of nanotechnology for the oil industry. *J. Pet. Technol.* 58, 24–25 (2006). <https://doi.org/10.2118/1106-0024-JPT>
72. Yousefvand, H., Jafari, A.: Enhanced oil recovery using polymer/nanosilica. *Proc. Mater. Sci.* 11, 565–570 (2015). <https://doi.org/10.1016/j.mspro.2015.11.068>
73. Khoja, A.H., Tahir, M., Amin, N.A.S.: Cold plasma dielectric barrier discharge reactor for dry reforming of methane over Ni/ γ -Al₂O₃-MgO nanocomposite. *Fuel Process. Technol.* 178, 166–179 (2018). <https://doi.org/10.1016/j.fuproc.2018.05.030>
74. Gbadamosi, A. O., Junin, R., Oseh, J. O., Agi, A., Yekeen, N., Abdalla, Y., ... Yusuff, A. S. (2018). Improving Hole Cleaning Efficiency using Nanosilica in Water-Based Drilling Mud. SPE Nigeria Annual International Conference and Exhibition. doi:10.2118/193401-ms
75. Gbadamosi, A.O., Junin, R., Abdalla, Y., Agi, A., Oseh, J.O.: Experimental investigation of the effects of silica nanoparticle on hole cleaning efficiency of water-based drilling mud. *J. Pet. Sci. Eng.* 172, 1226–1234 (2019). <https://doi.org/10.1016/j.petrol.2018.09.097>
76. Bera, A., Belhaj, H.: Application of nanotechnology by means of nanoparticles and nanodispersions in oil recovery—a comprehensive review. *J. Nat. Gas Sci. Eng.* 34, 1284–1309 (2016). <https://doi.org/10.1016/j.jngse.2016.08.023>
77. Agi, A., Junin, R., Gbadamosi, A.: Mechanism governing nanoparticle flow behaviour in porous media: insight for enhanced oil recovery applications. *Int. Nano Lett.* 8, 1–29 (2018). <https://doi.org/10.1007/s40089-018-0237-3>
78. Franco, C.A., Zabala, R., Cortés, F.B.: Nanotechnology applied to the enhancement of oil and gas productivity and recovery of Colombian fields. *J. Pet. Sci. Eng.* 157, 39–55 (2017). <https://doi.org/10.1016/j.petrol.2017.07.004>
79. Beg, M., Sharma, S., Ojha, U., Effect of cationic copolyelectrolyte additives on drilling fluids for shales, *Journal of Petroleum Science and Engineering* (2018), <https://doi.org/10.1016/j.petrol.2017.12.009>
80. Nikolov, A., Wu, P., Wasan, D.: Structure and stability of nanofluid films wetting solids: an overview. *Adv. Colloid Interface Sci.* 264, 1–10 (2019). <https://doi.org/10.1016/j.cis.2018.12.001>

81. Gbadamosi, A.O., Junin, R., Manan, M.A., Yekeen, N., Agi, A., Oseh, J.O.: Recent advances and prospects in polymeric nano- fluids application for enhanced oil recovery. *J. Ind. Eng. Chem.* (2018). <https://doi.org/10.1016/j.jiec.2018.05.020>
82. Yekeen, N., Manan, M.A., Idris, A.K., Padmanabhan, E., Junin, R., Samin, A.M., et al.: A comprehensive review of experimental studies of nanoparticles-stabilized foam for enhanced oil recovery. *J. Pet. Sci. Eng.* 164, 43–74 (2018). <https://doi.org/10.1016/j.petrol.2018.01.035>
83. Bera, A., Belhaj, H.: Application of nanotechnology by means of nanoparticles and nanodispersions in oil recovery—a comprehensive review. *J. Nat. Gas Sci. Eng.* 34, 1284–1309 (2016). <https://doi.org/10.1016/j.jngse.2016.08.023>
84. Raffa, P., Broekhuis, A.A., Picchioni, F.: Polymeric surfactants for enhanced oil recovery: a review. *J. Pet. Sci. Eng.* 145, 723– 733 (2016). <https://doi.org/10.1016/j.petrol.2016.07.007>
85. Cao, J., Meng, L., Yang, Y., Zhu, Y., Wang, X., Yao, C., Zhong, H. (2017). Novel Acrylamide/2-Acrylamide-2-methylpropanesulfonic Acid/4-Vinylpyridine Terpolymer as an Anti -calcium Contamination Fluid-Loss Additive for Water-Based Drilling Fluids. *Energy & Fuels*, 31(11), 11963–11970. doi:10.1021/acs.energyfuels.7b02354
86. Gbadamosi, A.O., Junin, R., Abdalla, Y., Agi, A., Oseh, J.O.: Experimental investigation of the effects of silica nanoparticle on hole cleaning efficiency of water-based drilling mud. *J. Pet. Sci. Eng.* 172, 1226–1234 (2019). <https://doi.org/10.1016/j.petrol.2018.09.097>
87. Cheraghian, G., Hendraningrat, L.: A review on applications of nanotechnology in the enhanced oil recovery part A: effects of nanoparticles on interfacial tension. *Int. Nano Lett.* 6, 129–138 (2016). <https://doi.org/10.1007/s40089-015-0173-4>
88. Mandal, A., Samanta, A., Ojha, K.: Mobility control and enhanced oil recovery using partially hydrolysed polyacrylamide (PHPA). *Int. J. Oil Gas Coal Technol.* 6, 245–258 (2013). <https://doi.org/10.1504/IJOGCT.2013.052236>
89. Wei, B.: Advances in polymer flooding. In: El-Amin, M.F. (ed.) *Viscoelastic and Viscoplastic Materials*. IntechOpen. <https://doi.org/10.5772/64069>. <https://www.intechopen.com/books/visco-elastic-and-viscoplastic-materials/advances-in-polymer-flooding>
90. Sheng, J.J.: Polymer flooding—fundamentals and field cases. *Enhanc. Oil Recover. F. Case Stud.* (2013). <https://doi.org/10.1016/b978-0-12-386545-8.00003-8>
91. Delshad, M., Kim, D.H., Magbagbeola, O.A., Huh, C., Pope, G.A., Tarahhom, F.: Mechanistic interpretation and utilization of viscoelastic behavior of polymer solutions for improved polymer- flood efficiency. In: *Present. SPE Symp. Improv. Oil Recover.* 20–23 April. Tulsa, Oklahoma, USA, Society of Petroleum Engineers, pp. 1–15 (2008). <https://doi.org/10.2118/113620-ms>

92. Pitts GN, Paul BC (1970) Low areal sweep efficiencies in flooding heterogeneous rock. Proceedings of SPE Production Techniques Symposium, Wichita Falls, Texas, United States. P.31.
93. Sydansk RD, Romero-Zeron L (2011) Reservoir conformance improvement. SPE, Richardson, United States. ISBN: 978-1-55563-302-8
94. Lowe A. B., McCormick C. L. Reversible addition–fragmentation chain transfer (RAFT) radical polymerization and the synthesis of water-soluble (co) polymers under homogeneous conditions in organic and aqueous media //Progress in Polymer Science. – 2007. – T. 32. – №. 3. – C. 283-351.
95. Mitsukami, Y., Donovan, M. S., Lowe, A. B., & McCormick, C. L. (2001). Water-soluble polymers. 81. Direct synthesis of hydrophilic styrenic-based homopolymers and block copolymers in aqueous solution via RAFT. *Macromolecules*, 34(7), 2248-2256.
96. Convertine, A. J., Sumerlin, B. S., Thomas, D. B., Lowe, A. B., & McCormick, C. L. (2003). Synthesis of block copolymers of 2- and 4-vinylpyridine by RAFT polymerization. *Macromolecules*, 36(13), 4679-4681.
97. Li, Z., Kang, W., Yang, H., Zhou, B., Jiang, H., Liu, D., and Wang, J. (2022). Advances of supramolecular interaction systems for improved oil recovery (IOR). *Advances in Colloid and Interface Science*, 301, 102617.
98. Xiong, Q., Ni, P., Zhang, F., & Yu, Z. (2004). Synthesis and characterization of 2-(dimethylamino) ethyl methacrylate homopolymers via aqueous RAFT polymerization and their application in miniemulsion polymerization. *Polymer bulletin*, 53, 1-8.
99. Lowe A. B., McCormick C. L. Synthesis, aqueous solution properties, and biomedical application of polymeric betaines // *Polyelectrolytes and Polyzwitterions: Synthesis, Properties, and Applications* / Lowe A. B., McCormick C. L., 2006. – P. 65-78.
100. Lowe A. B., McCormick C. L. Synthesis and solution properties of zwitterionic polymers // *Chemical Reviews*. – 2002. – T. 102, № 11. – P. 4177-4189.
101. Drozdov A. D., Christiansen J. D. The effects of pH and ionic strength on equilibrium swelling of polyampholyte gels // *International Journal of Solids and Structures*. – 2017. – T. 110. – P. 192-208.
102. Gao M., Gawel K., Stokke B. T. Polyelectrolyte and antipolyelectrolyte effects in swelling of polyampholyte and polyzwitterionic charge balanced and charge offset hydrogels // *European Polymer Journal*. – 2014. – T. 53. – P. 65-74.
103. Morishima Y., Lim H. S., Nozakura S., Sturtevant J. L. Effect of monomer sequence distribution in 2-vinylnaphthalene maleic-acid copolymers on energy migration and excimer formation in aqueous-solution // *Macromolecules*. – 1989. – T. 22, № 3. – P. 1148-1154.
104. Creutz S., Teyssie P., Jerome R. Living anionic homopolymerization and block copolymerization of 4-vinylpyridine at "elevated" temperature and its characterization by size exclusion chromatography // *Macromolecules*. – 1997. – T. 30, № 1. – P. 1-5.

105. Patrickios C. S., Hertler W. R., Abbott N. L., Hatton T. A. Diblock, triblock, and random methacrylic polyampholytes - synthesis by group-transfer polymerization and solution behavior (vol 27, PG 930, 1994) // *Macromolecules*. – 1994. – T. 27, № 8. – P. 2364-2364.

106. Webster O. W. Group-transfer polymerization and its relationship to other living systems // *Macromolecular Engineering: Recent Advances*. – 1995. – P. 1-9.

107. Lowe A. B., Billingham N. C., Armes S. P. Synthesis and characterization of zwitterionic block copolymers // *Macromolecules*. – 1998. – T. 31, № 18. – P. 5991-5998.

108. Georges M. K., Veregin R. P. N., Kazmaier P. M., Hamer G. K. Narrow molecular-weight resins by a free-radical polymerization process // *Macromolecules*. – 1993. – T. 26, № 11. – P. 2987-2988

109. Wang J. S., Matyjaszewski K. Controlled living radical polymerization - atom-transfer radical polymerization in the presence of transition-metal complexes // *Journal of the American Chemical Society*. – 1995. – T. 117, № 20. – P. 5614-5615.

110. Gussenov, I.S.; Mukhametgazy, N.; Shakhvorostov, A.V.; Kudaibergenov, S.E. Comparative Study of Oil Recovery Using Amphoteric Terpolymer and Hydrolyzed Polyacrylamide. *Polymers* 2022, 14,3095. <https://doi.org/10.3390/polym14153095>

111. Gussenov, I., Mukhametgazy, N., Shakhvorostov, A., & Kudaibergenov, S. (2021). Synthesis and characterization of novel acrylamide-based ternary polyampholyte as tracer agent. *Chemical Bulletin of Kazakh National University*, 100(1), 22-29. <https://doi.org/https://doi.org/10.15328/cb1183>

112. Ayazbayeva, A.Ye., Shakhvorostov, A.V., Seilkhanov, T.M., Aseyev, V.O., Kudaibergenov, S.E. (2021) Synthesis and characterization of novel thermo- and salt-sensitive amphoteric terpolymers based on acrylamide derivatives. *Bulletin of the University of Karaganda – Chemistry*, 104(4), 9-20. <https://doi.org/10.31489/2021Ch4/9-20>

113. You, Q.; Wang, K.; Tang, Y.; Zhao, G.; Liu, Y.; Zhao, M.; Li, Y.; Dai, C. Study of a novel self-thickening polymer for improved oil recovery. *Ind. Eng. Chem. Res.* 2015, 54, 9667–9674

114. Liu, F., Jiang, G., Peng, S., He, Y., & Wang, J. (2016). Amphoteric Polymer as an Anti -calcium Contamination Fluid-Loss Additive in Water-Based Drilling Fluids. *Energy & Fuels*, 30(9), 7221–7228. doi:10.1021/acs.energyfuels.6b01567

115. Alfrey T. Structure property relationships in polymers // *Acs Symposium Series*. – 1985. – T. 285. – P. 241-252.

116. Nair A. K. N., Jimenez A. M., Sun S. Y. Complexation Behavior of Polyelectrolytes and Polyampholytes // *Journal of Physical Chemistry B*. – 2017. – T. 121, № 33. – P. 7987-7998.

117. Batyrbekov A. A., Evdakov V. P., Kabanov V. A., Kozhinova E. V., Petrov

R. V., Savinova I. V., Fedoseyeva N. A., Khaitov R. M., Khaustova L. I. Study of mechanism of polyelectrolyte and polyampholyte action on immune-response //

Tsitologiya. – 1976. – T. 18, № 10. – P. 1259-1263.

118. Bekturov E. A., Kudaibergenov S. E., Zhaimina G. M. Reaction of synthetic styrene polyampholyte-copolymer and n, n-dimethylaminopropylmonoamide of maleic-acid, with Cu^{2+} and Fe^{3+} ions in aqueous-solution // *Koordinatsionnaya Khimiya*. – 1984. – T. 10, № 7. – P. 942-946.

119. Ali S. A., Rasheed A. Synthesis and solution properties of a betaine-sulfur dioxide polyampholyte // *Polymer*. – 1999. – T. 40, № 24. – P. 6849-6857.

120. McCormick C. L., Salazar L. C. Water-soluble copolymers .46. Hydrophilic sulfobetaine copolymers of acrylamide and 3-(2-acrylamido-2-methylpropanedimethyl-ammonio)-1-propanesulphonate // *Polymer*. – 1992. – T. 33, № 21. – P. 4617-4624.

121. Jaeger W., Wendler U., Lieske A., Bohrisch J. Novel modified polymers with permanent cationic groups // *Langmuir*. – 1999. – T. 15, № 12. – P. 4026-4032.

122. Wendler U., Bohrisch J., Jaeger W., Rother G., Dautzenberg H. Amphiphilic cationic block copolymers via controlled free radical polymerization // *Macromolecular Rapid Communications*. – 1998. – T. 19, № 4. – P. 185-190.

123. Kaladas J. J., Kastrup R., Schulz D. N. Poly(cyclosulfobetaines): Synthesis, characterization and solution properties // *Abstracts of Papers of the American Chemical Society*. – 1998. – T. 215. – P. 399-399.

124. Favresse P., Laschewsky A. New poly(carbobetaine)s made from zwitterionic diallylammonium monomers // *Macromolecular Chemistry and Physics*. – 1999. – T. 200, № 4. – P. 887-895.

125. Ali M. M., Perzanowski H. P., Ali S. A. Polymerization of functionalized diallyl quaternary ammonium salt to poly(ampholyte-electrolyte) // *Polymer*. – 2000. – T. 41, № 15. – P. 5591-5600.

126. McCormick C. L., Chen G. S. Water-soluble copolymers. IV. Random copolymers of acrylamide with sulfonated comonomers // *Journal of Polymer Science: Polymer Chemistry Edition*. – 1982. – T. 20. – №. 3. – C. 817-838.

127. Ezell R. G., Gorman I., Lokitz B., Ayres N., McCormick C. L. Stimuli-responsive ampholytic terpolymers of N-acryloyl-valine, acrylamide, and (3-acrylamidopropyl) trimethylammonium chloride: Synthesis, characterization, and solution properties // *Journal of Polymer Science Part a-Polymer Chemistry*. – 2006. – T. 44, № 9. – P. 3125-3139.

128. Toleutay G., Dauletbekova M., Shakhvorostov A., Kudaibergenov S. Quenched Polyampholyte Hydrogels Based on (3-Acrylamidopropyl) trimethyl Ammonium Chloride and Sodium Salt of 2-Acrylamido-2-methyl-1-Propanesulfonic Acid // *Macromolecular Symposia*. – 2019. – T. 385, № 1.

129. Lowe A. B., Billingham N. C., Armes S. P. Synthesis and characterization of zwitterionic block copolymers // *Macromolecules*. – 1998. – T. 31, № 18. – P. 5991-5998.

130. Kantor Y., Kardar M. Randomly charged polymers: An exact enumeration study // *Physical Review E*. – 1995. – T. 52. – №. 1. – C. 835.

131. Kudaibergenov S., Jaeger W., Laschewsky A. Polymeric betaines: Synthesis, characterization, and application // *Supramolecular Polymers Polymeric*

Betains Oligomers / Donnio B. и др. – Berlin: Springer-Verlag Berlin, 2006. – P. 157-224.

132. Ali S. A., Rasheed A. Synthesis and solution properties of a betaine-sulfur dioxide polyampholyte // *Polymer*. – 1999. – Т. 40, № 24. – P. 6849-6857.

133. McCormick C. L., Nonaka T., Johnson C. B. Water-soluble copolymers: 27. Synthesis and aqueous solution behaviour of associative acrylamide N-alkylacrylamide copolymers // *Polymer*. – 1988. – Т. 29. – №. 4. – С. 731-739.

134. Jaeger W., Wendler U., Lieske A., Bohrisch J. Novel modified polymers with permanent cationic groups // *Langmuir*. – 1999. – Т. 15, № 12. – P. 4026-4032.

135. Wendler U., Bohrisch J., Jaeger W., Rother G., Dautzenberg H. Amphiphilic cationic block copolymers via controlled free radical polymerization // *Macromolecular Rapid Communications*. – 1998. – Т. 19, № 4. – P. 185-190.

136. Favresse P., Laschewsky A. New poly(carbobetaine)s made from zwitterionic diallylammonium monomers // *Macromolecular Chemistry and Physics*. – 1999. – Т. 200, № 4. – P. 887-895.

137. Ali M. M., Perzanowski H. P., Ali S. A. Polymerization of functionalized diallyl quaternary ammonium salt to poly(ampholyte-electrolyte) // *Polymer*. – 2000. – Т. 41, № 15. – P. 5591-5600.

138. Harrison IM, Candau F, Zana R. Interactions between polyampholytes and ionic surfactants. *Colloid Polym Sci* 1999; 277: 48–57.

139. Ezell RG, McCormick CL. Electrolyte- and pH-responsive polyampholytes with potential as viscosity-control agents in enhanced petroleum recovery. *J Appl Polym Sci* 2007; 104: 2812–2821.

140. Chen, R. L., Kokta, B. V., Daneault, C., & Valade, J. L. (1986). Some water-soluble copolymers from lignin. *Journal of applied polymer science*, 32(5), 4815-4826.

141. Ezell RG, McCormick CL. Electrolyte- and pH-responsive polyampholytes with potential as viscosity-control agents in enhanced petroleum recovery. *J Appl Polym Sci* 2007; 104:).

142. Poole H. A., Gresser P. A. An annotated bibliography of greenhouse energy conservation and management. – 1980.

143. Taylor S. V. et al. Thiamin biosynthesis in *Escherichia coli*: identification of ThiSthiocarboxylate as the immediate sulfur donor in the thiazole formation // *Journal of Biological Chemistry*. – 1998. – Т. 273. – №. 26. – С. 16555-16560.

144. Tarannum N., Singh M. Advances in synthesis and applications of sulfo and carbo analogues of polybetaines: a review // *Reviews in Advanced Sciences and Engineering*. – 2013. – Т. 2. – №. 2. – С. 90-111.

145. Heininger K. Duality of stochasticity and natural selection: a cybernetic evolution theory. – 2015.

146. Lantman, C. W., MacKnight, W. J., Peiffer, D. G., Sinha, S. K., & Lundberg, R. D. (1987). Light scattering studies of ionomer solutions. *Macromolecules*, 20(5), 1096-1101.

147. Peiffer D. G., Lundberg R. D., Duvdevani I. Synthesis and rheological properties of low charge density polyampholytes in nonaqueous solvents //Polymer. – 1986. – T. 27. – №. 9. – C. 1453-1462.
148. Peiffer D. G., Lundberg R. D. Synthesis and viscometric properties of low charge density ampholytic ionomers //Polymer. – 1985. – T. 26. – №. 7. – C. 1058-1068.
149. Kudaibergenov S. E., Application of Polyampholytes //Polyampholytes: Synthesis, Characterization and Application. – 2002. – C. 189-203.
150. Lundberg R. D. Elastomers and fluid applications //Ionomers: Synthesis, structure, properties and applications. – Dordrecht : Springer Netherlands, 1997. – C. 477-501.
151. Waigh T. A. Microrheology of complex fluids //Reports on progress in physics. – 2005. – T. 68. – №. 3. – C. 685.
152. Higgs P. G., Joanny J. F. Theory of polyampholyte solutions //The Journal of chemical physics. – 1991. – T. 94. – №. 2. – C. 1543-1554.
153. Wittmer J., Johner A., Joanny J. F. Random and alternating polyampholytes //Europhysics Letters. – 1993. – T. 24. – №. 4. – C. 263.
154. Kujawa, P., Rosiak, J. M., Selb, J., & Candau, F. (2000). Synthesis and properties of hydrophobically modified polyampholytes. Molecular Crystals and Liquid Crystals Science and Technology. Section A. Molecular Crystals and Liquid Crystals, 354(1), 401-407.
155. Kantor Y., Kardar M. Polymers with random self-interactions //Europhysics Letters. – 1991. – T. 14. – №. 5. – C. 421.
156. Kantor Y., Kardar M. Collapse of randomly self-interacting polymers //Europhysics Letters. – 1994. – T. 28. – №. 3. – C. 169.
157. Kantor Y., Kardar M. Instabilities of charged polyampholytes //Physical Review E. – 1995. – T. 51. – №. 2. – C. 1299.
158. Artega G. A., Tapia O. Structural transitions in neutral and charged proteins in vacuo //Journal of Molecular Graphics and Modelling. – 2001. – T. 19. – №. 1. – C. 102-118.
159. Peiffer D. G., Lundberg R. D. Synthesis and viscometric properties of low charge density ampholytic ionomers //Polymer. – 1985. – T. 26. – №. 7. – C. 1058-1068.
160. Salamone, J. C., Ahmed, I., Rodriguez, E. L., Quach, L., & Watterson, A. C. (1988). Synthesis and solution properties of ampholytic acrylamide ionomers. Journal of Macromolecular Science—Chemistry, 25(5-7), 811-837.
161. Neyret S., Candau F., Selb J. Synthesis in microemulsion and characterization of low charge density ampholytic terpolymers //Acta polymerica. – 1996. – T. 47. – №. 8. – C. 323-332.
162. Ohlemacher, A., Candau, F., Munch, J. P., & Candau, S. J. (1996). Aqueous solution properties of polyampholytes: Effect of the net charge distribution. Journal of Polymer Science Part B: Polymer Physics, 34(16), 2747-2757.

163. Kadajji, V. G., & Betageri, G. V. (2011). Water Soluble Polymers for Pharmaceutical Applications. *Polymers*, 3(4), 1972–2009. doi:10.3390/polym3041972
164. McCormick C. L., Salazar L. C. Water-soluble copolymers. XLV. Ampholytic terpolymers of acrylamide with sodium 3-acrylamido-3-methylbutanoate and 2-acrylamido-2-methylpropanetrimethylammonium chloride // *Journal of applied polymer science*. – 1993. – T. 48. – №. 6. – C. 1115-1120.
165. Fevola M. J. et al. Ion-Containing Acrylamide Copolymers with PH-and Salt-Responsive Behavior // *Abstracts of Papers of the American Chemical Society*. – 2003. – T. 225. – C. U551.
166. Mahajan, S., Yadav, H., Rellegadla, S., & Agrawal, A. (2021). Polymers for enhanced oil recovery: Fundamentals and selection criteria revisited. *Applied Microbiology and Biotechnology*, 1-18.
167. Meng, X.; Zhang, Y.; Zhou, F.; Chu, P. K. Effects of carbon ash on rheological properties of water-based drilling fluids. *J. Pet. Sci. Eng.* 2012, 100, 1–8. (8) Hermoso, J.; Jofore, B. D.;
168. Meng, X.; Zhang, Y.; Zhou, F.; Chu, P. K. Effects of carbon ash on rheological properties of water-based drilling fluids. *J. Pet. Sci. Eng.* 2012, 100, 1–8. (8) Hermoso, J.; Jofore, B. D.; [2] Martínez-Boza, F. J.; Gallegos, C. High Pressure Mixing Rheology of Drilling Fluids. *Ind. Eng. Chem. Res.* 2012, 51, 14399–14407
169. Yang, P., Li, T.-B., Wu, M.-H., Zhu, X.-W., & Sun, X.-Q. (2015). Analysis of the effect of polyanionic cellulose on viscosity and filtrate volume in drilling fluid. *Materials Research Innovations*, 19(sup5), S5–12–S5 16. doi:10.1179/1432891715z.0000000001329
170. Navarrete, R. C.; Himes, R. E.; Seheult, J. M. Applications of Xanthan Gum in FluidLoss Control and Related Formation Damage. *SPE Permian Basin Oil and Gas Recovery Conference*, Midland, TX, March 23–26, 2000; Society of Petroleum Engineers: Richardson, TX, 2000; SPE Paper No. 59535.
171. Hui, L., Yan, W., Juan, W. et al. Development of a Drilling Fluid with High Calcium and Salt Tolerance. *Chem Technol Fuels Oils* 51, 61-65 (2015).
172. Jiang G, Wang K, He Y, Yang L, Li X, Deng Y. Synthesis of an amphoteric polymer as a high-temperature-resistant shale stabilizer in water-based drilling fluids. *J Appl Polym Sci.* 2020; e49016. <https://doi.org/10.1002/app.49016>
173. Mao, Hui; Wang, Weiji; Ma, Yongle; Huang, Yan (2020). Synthesis, characterization and properties of an anionic polymer for water-based drilling fluid as an anti-high temperature and anti-salt contamination fluid loss control additive. *Polymer Bulletin*, (), –. doi:10.1007/s00289-020-03227-y
174. N. Mukhametgazy, I. Sh. Gussenov, A.V. Shakhvorostov, S.E. Kudaibergenov. Salt tolerant acrylamide-based quenched polyampholytes for polymer flooding. // *Bulletin of Karaganda University, Chem. Ser.* 2020, No. 4(100), p.119-127.
175. Ahmad, H. M., Kamal, M. S., & Al-Harhi, M. A. (2018). High molecular weight copolymers as rheology modifier and fluid loss additive for water-based

drilling fluids. *Journal of Molecular Liquids*, 252, 133–143. doi:10.1016/j.molliq.2017.12.135

176. Kudaibergenov, S. E. (2020). Synthetic and natural polyampholytes: Structural and behavioral similarity. *Polymers for Advanced Technologies*. doi:10.1002/pat.5145

177. Thünemann, A. F., Sander, K., Jaeger, W., & Dimova, R. (2002). Polyampholyte-Dressed Micelles of Fluorinated and Hydrogenated Dodecanoic Acid. *Langmuir*, 18(13), 5099–5105. doi:10.1021/la020188v

178. Ibraeva, Z. E., Hahn, M., Jaeger, W., Bimendina, L. A., & Kudaibergenov, S. E. (2004). Solution Properties and Complexation of Polyampholytes based on N, N-Dimethyldiallylammonium Chloride and Maleic Acid or Alkyl (Aryl) Derivatives of Maleamic Acids. *Macromolecular Chemistry and Physics*, 205(18), 2464–2472. doi:10.1002/macp.200400242

179. Sun, J., Deng, C., Chen, X., Yu, H., Tian, H., Sun, J., & Jing, X. (2007). Self-assembly of polypeptide-containing ABC-type triblock copolymers in aqueous solution and its pH dependence. *Biomacromolecules*, 8(3), 1013–1017.

180. Chen L, Chen T, Fang W, et al. Synthesis and pH-responsive “schizophrenic” aggregation of a linear-dendron-like polyampholyte based on oppositely charged polypeptides. *Biomacromolecules*. 2013;14: 4320–4330.

181. Li, M.-C., Wu, Q., Song, K., De Hoop, C. F., Lee, S., Qing, Y., & Wu, Y. (2015). Cellulose Nanocrystals and Polyanionic Cellulose as Additives in Bentonite Water-Based Drilling Fluids: Rheological Modeling and Filtration Mechanisms. *Industrial & Engineering Chemistry Research*, 55(1), 133–143.

182. Reilly, S. I.; Vryzas, Z.; Kelessidis, V. C.; Gerogiorgis, D. I. First-Principles Rheological Modelling and Parameter Estimation for Nanoparticle-Based Smart Drilling Fluids. In *26th European Symposium on Computer Aided Process Engineering*; Elsevier Masson SAS, 2016; Vol. 38, pp 1039–1044. DOI: 10.1016/B978-0-444-63428-3.50178-8.

183. Amani, M.; Al-Jubouri, M. The Effect of High Pressures and High Temperatures on the Properties of Water Based Drilling Fluids. *Energy Sci. Technol.* 2012, 4, 27–33.

184. Kelessidis, V. C.; Maglione, R. Yield Stress of Water – Bentonite Dispersions. *Colloids Surf. A* 2008, 318, 217–226.

185. Dejtaradon, P.; Hamidi, H.; Chuks, M. H.; Wilkinson, D.; Rafati, R. Impact of ZnO and CuO Nanoparticles on the Rheological and Filtration Properties of Water-Based Drilling Fluid. *Colloids Surf. A* 2019, 570, 354–367.

186. Bondino, I. Nguyen, R., Hamon, G., Ormehaug, P. A., Skauge, A., Jouenne, S. "Tertiary Polymer Flooding in Extra-Heavy Oil: An Investigation Using 1D and 2D Experiments, Core Scale Simulation and Pore-Scale Network Models", *International Symposium of the Society of Core Analysts*, Austin, Texas, (2011), 12p.

187. Moore, J. C. "Gel permeation chromatography. I. A new method for molecular weight distribution of high polymers", *J Polym Sci Part a Gen Pap*, (1964) 2:835–843. doi: 10.1002/pol.1964.100020220

188. Stavland, A., Jonsbraten, H., Lohne, A., Moen, A., Giske, N. H. "Polymer Flooding - Flow Properties in Porous Media versus Rheological Parameters", SPE EUROPEC/EAGE Annual Conference and Exhibition, Barcelona, Spain, (2010), pp 14–17.
189. Dominguez JG, Willhite GP. Retention and flow characteristics of polymer solution in porous media. SPE Journal. 1977; 17:111–121.
190. Dai, C., Zhao, G., You, Q., & Zhao, M. (2014). The investigation of a new moderate water shutoff agent: Cationic polymer and anionic polymer. *Journal of Applied Polymer Science*, 131(3).
191. Yang, H., Kang, W., Yu, Y., Lu, Y., Li, Z., Wang, M., & Liu, T. (2015). Effects of surfactants on rheological properties of a dispersed viscoelastic microsphere. *Journal of Applied Polymer Science*, 132(30).
192. Yang, H., Kang, W., Yu, Y., Yin, X., Wang, P., & Zhang, X. (2017). A new approach to evaluate the particle growth and sedimentation of dispersed polymer microsphere profile control system based on multiple light scattering. *Powder technology*, 315, 477-485.
193. Hua, Z., Lin, M., Dong, Z., Li, M., Zhang, G., & Yang, J. (2014). Study of deep profile control and oil displacement technologies with nanoscale polymer microspheres. *Journal of colloid and interface science*, 424, 67-74.
194. Yang, H., Kang, W., Yin, X., Tang, X., Song, S., Lashari, Z. A., & Sarsenbekuly, B. (2017). Research on matching mechanism between polymer microspheres with different storage modulus and pore throats in the reservoir. *Powder Technology*, 313, 191-200.
195. Hamad, B. A., He, M., Xu, M., Liu, W., Mpelwa, M., Tang, S., Song, J. (2020). A Novel Amphoteric Polymer as a Rheology Enhancer and Fluid-Loss Control Agent for Water-Based Drilling Muds at Elevated Temperatures. *ACS Omega*. doi:10.1021/acsomega.9b03774
196. Liu, F.; Jiang, G.; Peng, S.; He, Y.; Wang, J. Amphoteric Polymer as an Anti-Calcium Contamination Fluid-Loss Additive in Water-Based Drilling Fluids. *Ener-gy Fuels* 2016, 30, 7221–7228.
197. Li, J., Sun, J., Lv, K., Ji, Y., Liu, J., Huang, X., & Shi, S. (2022). Temperature-and salt-resistant micro-crosslinked polyampholyte gel as fluid-loss additive for water-based drilling fluids. *Gels*, 8(5), 289. <https://doi.org/10.3390/gels8050289>
198. Aghdam, S. B., Moslemizadeh, A., Kowsari, E., & Asghari, N. (2020). Synthesis and performance evaluation of a novel polymeric fluid loss controller in water-based drilling fluids: High-temperature and high-salinity conditions. *Journal of Natural Gas Science and Engineering*, 103576. doi:10.1016/j.jngse.2020.103576
199. Beg, Mukarram; Singh, Priyanka; Sharma, Shivanjali; Ojha, Umapasana (2018). Shale inhibition by low-molecular-weight cationic polymer in water-based mud. *Journal of Petroleum Exploration and Production Technology*. <https://doi.org/10.1007/s13202-018-0592-7>.

200. Beg, Mukarram; Singh, Priyanka; Sharma, Shivanjali; Ojha, Umapasana (2018). Shale inhibition by low-molecular-weight cationic polymer in water-based 44y. <https://doi.org/10.1007/s13202-018-0592-7>.

201. V.C.Kelessidis, R. Maglione, C. Tsamantaki, Y. Aspirtakis, Optimal determination of rheological parameters for Herschel–Bulkley drilling fluids and impact on pressure drop, velocity profiles and penetration rates during drilling, *J. Pet. Sci. Eng.* 53 (2006) 203–224.

202. Pang, Boxue; Wang, Shuyan; Chen, Weiqi; Hassan, Muhammad; Lu, Huilin (2020). Effects of flow behavior index and consistency coefficient on hydrodynamics of power-law fluids and particles in fluidized beds. *Powder Technology*, S0032591020300735–. doi:10.1016/j. powtec.2020.01.061

203. Serres-Piole C., Preud’homme H., Moradi-Tehrani N., Allanic C., Jullia H., Lobinski R. Water tracers in oilfield applications: Guidelines // *Journal of Petroleum Science and Engineering*. – 2012. – Vol.98-99. – P.22-39.

204. Kang W.L., Hu L.L., Zhang X.F., Yang R.M., Fan H.M., Geng J. Preparation and performance of fluorescent polyacrylamide microspheres as a profile control and tracer agent // *Petroleum Science*. – 2015. – Vol.12. – P.483-491.

205. Yan L., Yin T., Yu W., Shen L., Lv M., Ye Z. A water-soluble oil-displacing agent with tracer properties for enhancing oil recovery // *RSC Advances*. – 2015. – Vol.5. – P.42843-42847.

206. Yang H., Hu L., Chen C., Gao Y., Tang X., Yin X., Kang W. Synthesis and plugging behavior of fluorescent polymer microspheres as a kind of conformance control agent in reservoirs // *RSC Advances*. – 2018. – Vol.8. – P.10478-10488.